NASA CONTRACTOR REPORT

NASA CR

NASA CR-610

SOLUBILITY STUDIES OF ULTRA PURE TRANSITION ELEMENTS IN ULTRA PURE ALKALI METALS

by R. L. McKisson, R. L. Eichelberger, R. C. Dahleen, J. M. Scarborough, and G. R. Argue

Prepared by
NORTH AMERICAN AVIATION, INC.
Canoga Park, Calif.
for Lewis Research Center

NATIONAL AERONAUTICS AND SPACE ADMINISTRATION • WASHINGTON, D. C. • OCTOBER 1966

NASA CR-610

SOLUBILITY STUDIES OF ULTRA PURE TRANSITION ELEMENTS IN ULTRA PURE ALKALI METALS

By R. L. McKisson, R. L. Eichelberger, R. C. Dahleen, J. M. Scarborough, and G. R. Argue

Prepared under Contract No. NAS 3-4163 by
NORTH AMERICAN AVIATION, INC.
Canoga Park, Calif.

for Lewis Research Center

NATIONAL AERONAUTICS AND SPACE ADMINISTRATION

For sale by the Clearinghouse for Federal Scientific and Technical Information
Springfield, Virginia 22151 – Price $3.25

TABLE OF CONTENTS

LIST OF FIGURES

LIST OF FIGURES (Cont'd)

LIST OF FIGURES (Cont'd)

LIST OF TABLES

ACKNOWLEDGEMENTS

The authors wish to acknowledge the contributions to this work of the following persons and to express their appreciation: to R. A. Lindberg, the NASA Technical Manager for the program, for the many useful suggestions made during the course of the work; to P. F. DeVries, J. W. Glass, H. L. Hoisch, R. G. Wilbourn, B. G. Johnson and N. M. Trahey for their assistance in performing the varied analytical chemistry support tasks; to W. A. McCullom for his contributions to the DLC studies; to L. O. Petersen and R. T. Albee, for their assistance in fabricating much of the test equipment; and to V. C. Davis, for his general assistance in performing the tests.

ABSTRACT

The solubilities of iron, molybdenum, niobium, and tantalum in liquid potassium were studied in the temperature range 800-1200°C, with emphasis on achieving a true two component experimental system. To this end, triple-pass electron beam zone-refined single crystals of Mo, Nb, and Ta, and triple-pass electron beam zone refined polycrystalline Fe were used as solute materials, and formed into crucibles. High purity potassium was additionally purified in a filtering, gettering, and distilling process. The still was designed with a fractionating column equivalent to 2-3 theoretical plates.

All operations in which there might be danger of contaminating the high purity materials were carried out under high vacuum (pressure $<10^{-6}$ torr) in a complex of interconnected vacuum chambers.

Least squares curves were fitted to the data, using six points for Fe at 800-1000°, six points for Mo at 1000-1200°, and twelve points for Ta at 800-1200°. The analytical expressions for the concentration of solute found are as follows:

$$\log (\text{wppm Fe}) = 3.4 - 1700/T°K$$
$$\log (\text{wppm Mo}) = 4.8 - 5600/T°K$$
$$\log (\text{wppm Ta}) = 5.2 - 2900/T°K$$

ΔH of solution from these curves is 7700 cal/mol, 25,500 cal/mol, and 13,200 cal/mol for Fe, Mo, and Ta, respectively. The high values for Mo and Ta suggest that there may be a reaction involved in the solution process. Twelve measurements for Nb at 1000-1200° showed a scatter between 15 and 171 wppm, and no curve was determined. Two experiments were completed with Nb-1% Zr alloy, at 1000° and 1200°. The niobium concentration found was <1 wppm (not detected) and 6 wppm, respectively.

It is apparent from the data that the solubility process for metals in liquid potassium is still not understood, although great care was taken to prepare and maintain high purity materials in this work.

SUMMARY

Information available in the literature on liquid metal-solid metal systems indicates substantial disagreement among various investigators with regard to the solubility of refractory metals in liquid alkali metals, and a disappointing degree of precision in data reported in individual studies. These problems are generally thought to arise from lack of control of the initial impurity levels in the solid and liquid metals, plus the fact that purity is greatly influenced by the handling procedures employed. The work described here was designed to minimize the uncertainties associated with the composition of the solid and liquid metals, and the introduction of impurities through handling techniques.

The experimental method employed emphasized the use of very highly purified sample materials and a high vacuum environment to prevent their contamination during the tests. The solute materials employed were triple pass electron beam zone refined single crystals of Mo, Nb, and Ta, and identically processed, but not single crystal, Fe, which were formed into crucibles. In each test, one of these crucibles was loaded with potassium, joined to a sample collector of a dissimilar metal, welded into a molybdenum pressure vessel, and then heated to the test temperature. At the end of each experiment the pressure vessel was swung out of the furnace through a 180° arc, causing the potassium to flow from the sample crucible into the collector. After the assembly was cool, the pressure capsule was cut open, and the sample collector removed for submission for analysis of the potassium.

High vacuum was chosen as the experimental "atmosphere," and an environmental test system was designed. This system consists of cylindrical vacuum chambers, 2 feet in diameter by two feet tall with domed ends. The chambers are interconnected by high vacuum gate valves to permit the transfer of materials through the system without exposing them to a gas atmosphere. Each chamber has its own pumping system consisting of mechanical pump, diffusion pump, water baffle, and liquid nitrogen baffle. High vacuum manipulators are installed in each chamber and permit operations to be carried out at pressures below 10^{-6} torr. A pressure below 1×10^{-7} torr is reached when no operations are being carried out in the system.

One vacuum chamber contains an outgassing furnace and the equipment necessary for loading the crucibles. The next chamber is equipped with an electron beam welding gun and a rotating chuck to permit welding of pressure capsules. A third chamber contains a high temperature furnace in which the test capsules are heated to 600-1200°C as required. This latter furnace is built in two parts, so that the front half may be swung away from the rest of the furnace. The test capsule can then be inverted by swinging it out of the furnace about a horizontal axis through the bottom of the furnace. Both the outgassing furnace and the test furnace use tantalum foil heating elements, and are powered by suitably controlled step-down transformers.

High purity potassium was purchased, and then additionally purified in a sequence of operations which includes filtering, gettering at 650°C with zirconium, and fractional distillation. The still column is packed with tantalum saddles, and is equivalent to 2 to 3 theoretical plates. The first 25% of each batch is discarded to remove impurities more volatile than potassium, and the final 25% containing the less volatile impurities is left in the still pot. The distilled product potassium is collected in the body of an extruder and allowed to solidify. The extruder outlet delivers inside the vacuum chamber which is used for loading capsules, thus insuring that the purified potassium does not contact any contaminating atmosphere. Extruded potassium is cut with a wire "cheese cutter" device, and adheres strongly to the wire. The cut sample is dropped off the cutter by heating the wire electrically.

Since it was hoped that useful kinetic data might be obtained from the solubility experiments, it was necessary to measure the internal surface area of the metal crucibles. This was done by measuring the double layer capacitance of each crucible surface, and comparing this value with that for standard metal specimens of very high polish. In all cases the surface roughness factor was found to be $1.1 \pm 10\%$.

The major experimental difficulty encountered was the unexpected transfer of solvent potassium from inside the crucible-collector assembly to the outer pressure capsule. Several mechanisms by which this transfer might occur were postulated, and attempts were made to prevent it by reducing the temperature gradient along the capsule, by providing a water-cooled device to quench the capsule rapidly at the end of a test, and by introducing various spring and spacer combinations inside the capsule to provide a tight seal between the crucible and the collector. When none of these measures was successful in preventing the potassium transfer, the decision was made to braze the crucible and collector together. Using nickel as the braze metal (except for tests with iron crucibles, in which copper was used) and a carefully machined tapered joint, positive sealing was obtained which prevented any transfer of the potassium. The complete retention of potassium then became a criterion for the acceptability of a solubility experiment.

More than twenty tests were made with iron crucibles, since they were used for many of the development tests of the crucible-collector seals. Of these, six met the criteria of experimental acceptability. These data, at 800-1000°C, yielded the least squares curve

$$\log (\text{wppm Fe}) = 3.4 - 1700/T°K.$$

The ΔH of solution (ΔH_s) derived from this curve is 7700 cal/mol, which is only somewhat higher than the value one would expect for a simple solution process. The concentration of iron in potassium at 1000°C is about 115 ppm from this curve.

Of about twenty tests made using molybdenum solute crucibles, six were made with non-leaking brazed joints. These data, at 1000-1200°C, yielded the least squares curve

$$\log (\text{wppm Mo}) = 4.8 - 5600/T°K.$$

The ΔH_S from this curve is 25,500 cal/mol, which suggests that there may be a reaction involved in the present solution process for molybdenum. The concentration at 1000°C is about 2.4 wppm.

Of seventeen experiments made with niobium solute crucibles, eleven showed full retention of the potassium. However, scatter of the data was too great to permit a curve to be derived. The measured niobium concentration in these tests at 1000-1200°C was 15 to 171 wppm. Two tests were completed with a niobium alloy containing 1% zirconium. At 1000°C no niobium was found in the potassium, indicating a concentration of less than 1 ppm. At 1200°C a concentration of 6 wppm was found. Since the role of zirconium in the alloy is to nullify the effect of interstitial impurities by reacting with them to form stable compounds, these results suggest that interstitial impurities in the niobium solute metal have a large effect on its apparent solubility.

Of fourteen tests made with tantalum solute crucibles, two were unusable because of operating difficulties. Data from the remaining twelve, at 800-1200°, define the following least squares curve,

$$\log (\text{wppm Ta}) = 5.2 - 2900/T°K.$$

The ΔH_S from this curve is 13,200 cal/mol, which suggests that there may be a reaction involved in the solution process for tantalum. The level of the data is quite high (about 800 wppm at 1000°C) compared with that obtained for molybdenum and niobium. One would expect the solubility of the more refractory tantalum to be in the same range as that of niobium, or possibly somewhat lower. The reason for the order-of-magnitude higher level is not at all clear.

INTRODUCTION

The need for the development of suitably refractory containers for alkali metals for high temperature service has engendered a substantial volume of engineering research on the corrosion behavior of refractory metals and alloys. Although the solution and subsequent diffusion processes affecting a given material of construction are fundamental to the understanding of corrosion processes, these phenomena are by no means the only types of interactions involved in corrosion. Thus, in addition to simple solution, there can be compound formation with the solvent, intergranular penetration by the liquid metal with subsequent deterioration of the solid material, reaction of the solvent or solute with impurities, selective leaching of constituents of an alloy with consequent catastrophic change of properties, and finally, transport of material under the influence of a temperature or concentration gradient.(7,8,25,37,75) While a detailed study of all these effects is not a part of this program, it is proper to point out that a recognition of the existence of such effects and of their importance is most relevant to the proper evaluation of past work, to the planning of a fundamental program, and to the interpretation of the experimental results. Such recognition applies particularly to the effect of impurities such as oxygen and carbon, which are especially difficult to control.(7,25) With these preliminary remarks in mind, it is pertinent to consider reported data for solubilities in potassium, and in other alkali metals.

The literature contains many references to compatibility and corrosion behavior of various metals and alloys in molten alkali metals, but there is a dearth of data on solubility, and particularly on solubility as a function of temperature. Tables I-V summarize the solubility data available in the literature. There is, in addition, a large amount of corrosion data available, but since it is not readily converted to solubility information, it has not been included in the tables.

It is interesting to note that although sodium, potassium, and NaK are currently being used as working coolants, there has been relatively little data developed for the solubility of containment alloy elements in these alkali metals. On the other hand, lithium in particular, and rubidium and cesium have been rather extensively studied as solvents.

Jesseman et al.(40) were the first experimenters to measure the solubilities of various construction elements and alloy constituents in liquid lithium. They investigated the solubilities of Be, Cr, Fe, Mo, Nb, Ni, Si, Ta, Ti, V, W, and Zr in the temperature range from 500° to about 1000°C. Sand(68) reported solubility data for iron in 1958. Then there was an upsurge in the amount of work undertaken using lithium as a solvent, and six reports(6,17, 18,45,52,55) were published in the 1960-62 period concerning the solubilities of some thirteen elements in molten lithium. It is difficult to compare in detail the data on Table I because of the differences in test procedures and conditions. However, it is of interest to prepare the plots shown in Figures 1-8 and to briefly examine the reported data. The points of interest are the degree of agreement among the various authors and the ΔH(solution) (or ΔH_s) exhibited by the data. The significance of the value ΔH_s is shown by the following discussion.

Table I

Solubility of Elements in Lithium

Solute	T °C	Solvent Oxygen Content ppm	Source Material*	Container Material**	Solubility ppm	Ref
Be	735	2400	Be	Fe	3000	40
	1000		Be		2500	18
	1000		Be		2500	17
	1000		Be	Fe	2100	19
Cr	500	2400	Cr	Fe	90	40
	600				1.5	45
	675		Cr		2	52
	715	2400	Cr	Fe	130	40
	800		Cr	Fe	1000	6
	800				6.7	45
	925		Cr		12	52
	990	2400	Cr	Fe	430	40
	1000		Cr	Fe	11000	6
	1000				18.7	45
	1200		Cr	Fe	40000	6
	1200				39.8	45
Fe	400		Fe	SSTL***	30	6
	440	2400	Fe	Fe	2700	40
	600		Fe	SSTL	40	6
	600		Fe		1.4	45
	660	2400	Fe		1030	40
	665		Fe		2	52
	760		Fe		85	55
	760		Fe		120	68
	800		Fe	SSTL	60	6
	800		Fe		6.5	45
	900		Fe		100	17
	900		Fe		100	18
	925		Fe		11	52
	930	2400	Fe	Fe	1100	40
	1000		Fe	SSTL	80	6
	1000		Fe		23	45

*Material from which the solute was dissolved.
**Material from which the solubility test container was made.
***Stainless steel.

Table I (continued)

Solute	T °C	Solvent Oxygen Content ppm	Source Material*	Container Material**	Solubility ppm	Ref
Fe (cont'd)	1000		Fe		200	17
	1000		Fe		200	18
	1200		Fe		350	18
	1200		Fe		350	17
Mo	550	2400	Mo	Fe	<15	40
	665		Mo		0.5	52
	800				0.7	45
	860	2400		Fe	<25	40
	870				0.9	13
	925		Mo		1.1	52
	985	2400	Mo	Fe	140	40
	1000		Mo		1	18,19
	1000				<1	17
	1000				1.4	45
	1200				30	18
	1200				6.5	45
Nb	500	2400	Nb	Fe	<30	40
	735	2400	Nb	Fe	80	40
	760		Nb	Mo	2	44
	800		Nb	Cb-1Zr	1.6	10
	975		Nb	Mo	3	44
	1000				<1	18
	1000				<1	17
	1000		Nb	Cb-1Zr	2.3	10
	1015	2400	Nb	Fe	900	40
	1200		Nb	Cb-1Zr	3.1	10
	1425		Nb	Mo	5	44
Ni	465	2400	Ni	Fe	4300	40
	600				76	45
	650		Ni		100	52
	675	2400	Ni	Fe	14000	40
	700				1500	17
	700				150	18,19
	750				5000	17
	750		Ni	Ni	5200	18,19
	800				370	45
	850				13600	17

*Material from which the solute was dissolved.
**Material from which the solubility test container was made.

Table I (continued)

Solute	T °C	Solvent Oxygen Content ppm	Source Material*	Container Material**	Solubility ppm	Ref
Ni (cont'd)	870		Ni		600	52
	950				32000	17
	950				32000	18
	1000				1100	45
Si	680	2400	Si	Fe	139200	40
Ta	725	2400	Ta	Fe	19	40
	1000	2400	Ta	Fe	1850	40
Ti	720				1.5	52
	730	2400	Ti	Fe	345	40
	800				1.2	45
	845		Ti		1.5	52
	900				140	17
	900				140	18
	1000				2.2	45
	1020	2400	Ti	Fe	3700	40
U	800		U	Mo	70	19
	800		U	Mo	70	18
	800		U	Mo	70	17
	1000		U	Mo	560	18
	1000		U	Mo	560	17
	1000		U	Mo	560	19
V	725	2400	V	Fe	150	40
	1010	2400	V	Fe	65	40
W	715	2400	W	Fe	1050	40
Zr	480		Zr		10	47
	700	2400	Zr	Fe	65	40
	760				1000	47
	965	2400	Zr	Fe	250	40
	1000				300	18
	1000				300	17
	1200				3000	18
	1200				3000	17

*Material from which the solute was dissolved.
**Material from which the solubility test container was made.

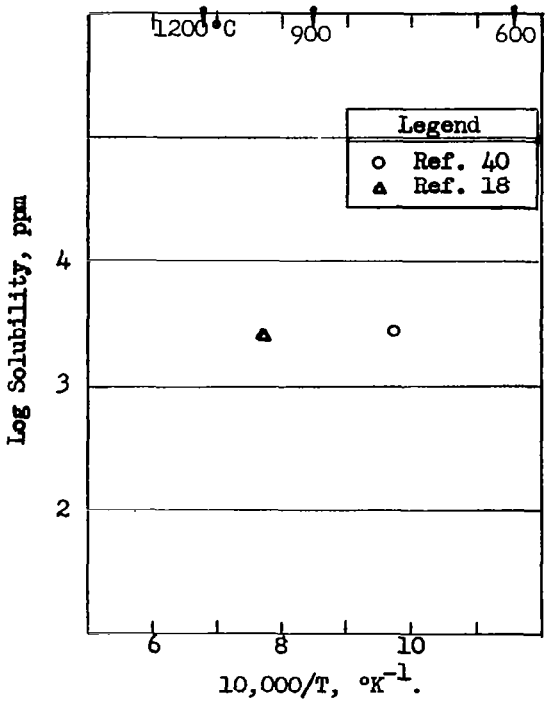

Figure 1. Solubility of Be in Li.

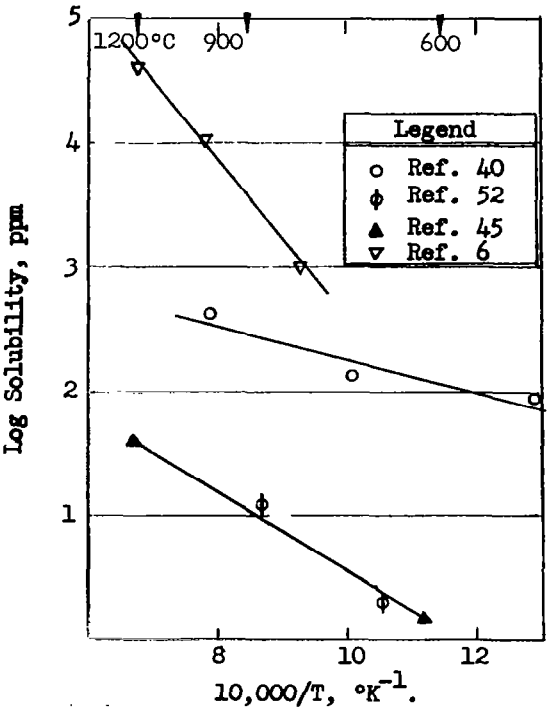

Figure 2. Solubility of Cr in Li.

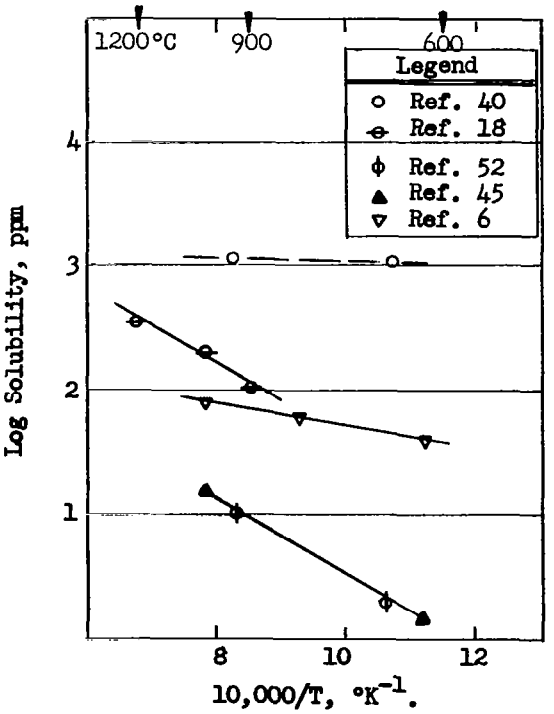

Figure 3. Solubility of Fe in Li.

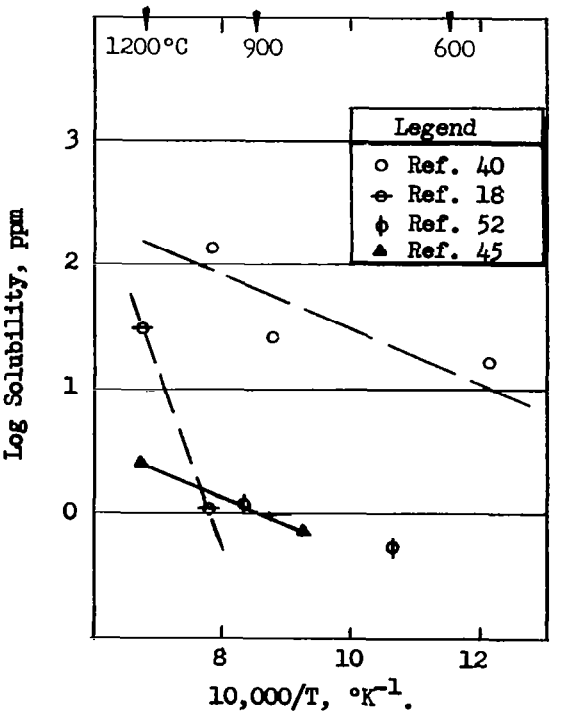

Figure 4. Solubility of Mo in Li.

The solubilities of interest here are a form of chemical equilibrium, for which a chemical reaction equation can be written,

$$M(s) \longrightarrow M\,[\text{solution in Li(l)}]$$

where M is the solute metal and lithium is the solvent alkali metal. For this reaction, one can write the usual equilibrium constant K, which is the solubility,

$$K_T = S_T = [\text{equilibrium concentration of M(s) in Li(l) at temperature T.}].$$

The temperature dependence of S_T is then given by the familiar thermodynamic expression,

$$\frac{d(\ln K)}{dT} = \frac{d(\ln S_T)}{dT} = \frac{\Delta H_s^\circ}{RT^2} \quad ,$$

or,

$$\frac{d(\ln S_T)}{d(1/T)} = -\frac{\Delta H_s}{R} \quad .$$

Thus, the slope of the $\ln S_T$ vs (1/T) line (curve) is equal to $-\Delta H_s/R$. This ΔH_S is the heat of reaction of the solution process, which can be thought of as the two sequential processes, fusion, plus mixing of the two liquids,

$$M(s) \longrightarrow M(l),$$

and

$$M(l) + Li(l) \longrightarrow M\,[\text{solution in Li(l)}]$$

For the first step, the ΔH is merely the heat of fusion of solute M, ΔH_f, at the temperature of interest. This quantity can be evaluated for temperatures below the melting point by the use of the expression,

$$\Delta H_{f,T} = \Delta H_{f,T_M} + \int_{T_M}^{T} \Delta Cp\, dT \quad .$$

For the second step, the ΔH is the integral heat of solution, ΔH_S, of the solute in the solution, so that the overall ΔH for the process becomes,

$$\Delta H_{s,T} = \Delta H_{f,T} + \Delta H_{S,T}.$$

The values of $\Delta H_{f,T}$ at 800°C range from about 1000 cal/mol for Be, which has a low melting point (1280°C) to about 5000 cal/mol for Ta, which has a high melting point (3000°C). $\Delta H_{S,T}$ can theoretically range from large negative values, which correspond to strong chemical interactions; to positive values,

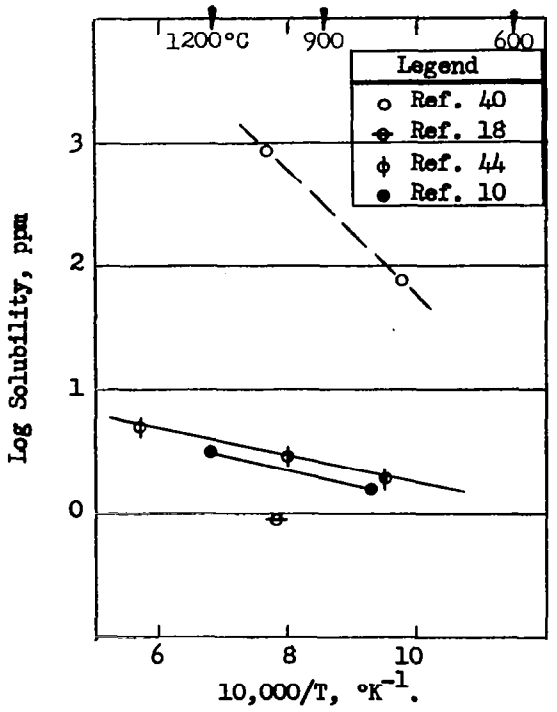

Figure 5. Solubility of Nb in Li.

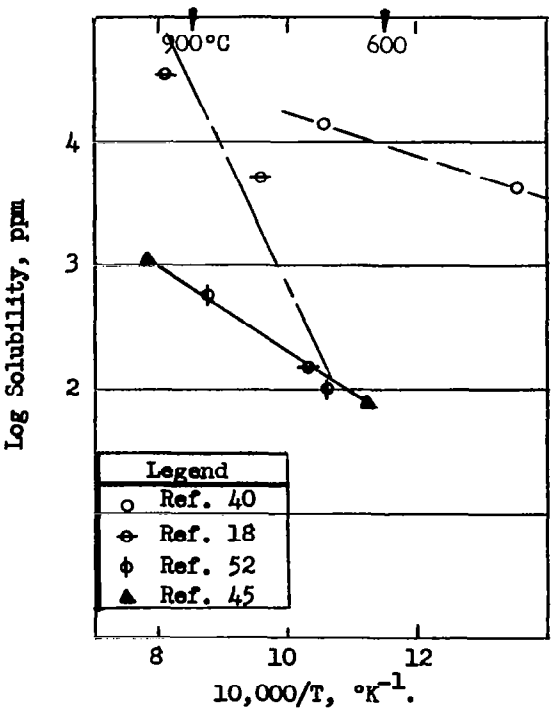

Figure 6. Solubility of Ni in Li.

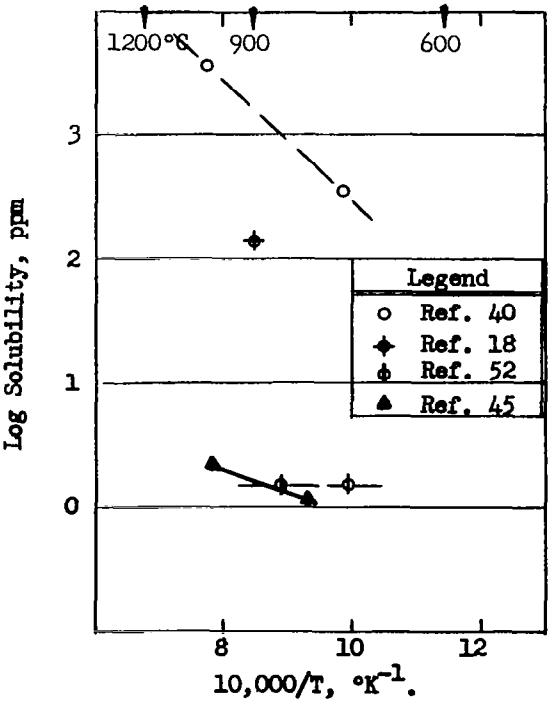

Figure 7. Solubility of Ti in Li.

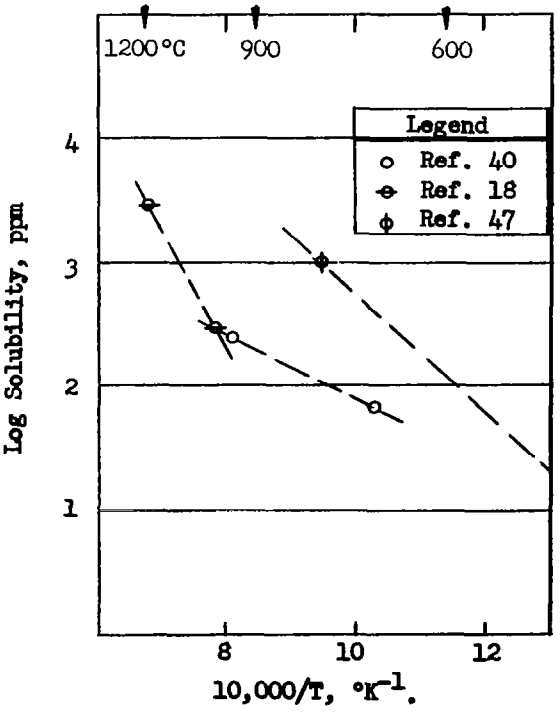

Figure 8. Solubility of Zr in Li.

which are indications of a large positive partial molal heat of mixing, i.e., a tendency to not mix; or the net value may represent a combination of these potential contributions. At the present state of knowledge about liquid alkali metal systems, one cannot separate these factors. About all that can be said is that if ΔH_S is not in the range of 1000 to 5000 cal/mol, some interaction is operating.

Figure 1 shows data of Bychkov, et al.(18) and of Jesseman, et al.(40) for the solubility of beryllium in lithium. Jesseman notes a high oxygen content (2400 ppm) of his lithium, which might tend to increase the Be solubility in his system.

Figure 2 shows the solubility data of Jesseman, et al.(40) Leavenworth and Cleary,(52) Kelley,(45) and Beskoravaynyy and Yakovlev(6) for chromium in lithium. The data reported by Kelly and that reported by Leavenworth and Cleary are from the same laboratory, and are expected to be the same data. Kelly's report gives equations, which presumably represent the best fit to the data which was available at the time. (The curves which are marked by solid points on the figures represent data evaluated from published equations.) The other authors' data lie two and three orders of magnitude above that of Kelly. Beskoravaynyy and Yakovlev's(6) data have a ΔH_S of 28,500 cal/mol which indicates the presence of some effect other than simple solution. Jesseman et al.(40) on the other hand give data whose ΔH_S is only 6300 cal/mol. Kelly's data(45) show a ΔH_S of 14,000 cal/mol, an intermediate value.

Figure 3 shows the data for the solubility of iron in lithium. Kelly(45) has again apparently reported data from the same source as that of Leavenworth and Cleary(52).

The indicated ΔH_S is 14,300 cal/mol. The data of Bychkov et al.(18) has about the same ΔH_S, but is a factor of ten or more higher in absolute value. Jesseman et al.(40) on the other hand, show even higher values, but the indicated ΔH_S is very small, so that the data can probably be discounted. The remaining report by Beskoravaynyy and Yakovlev(6) gives data having a ΔH_S of 4500 cal/mol and values of data near those of Bychkov. Because of these variations, one cannot readily fix the solubility of iron in lithium.

Figure 4 shows the data of four authors for the solubility of molybdenum in lithium. Kelly(45) and Leavenworth and Cleary(52) report similar data again, and show a ΔH_S of 7600 cal/mol. Jesseman, et al.(40) show a comparable ΔH_S, but their data lie almost two decades higher. Bychkov, et al.(18) show an extremely large ΔH_S, and should probably be discounted on this account. One is thus left with an unexplained large difference in the levels of the solubility of molybdenum in lithium.

Figure 5 shows the reported data for the solubility of niobium in lithium. Kelly(44) and Blecherman, et al.(10) show data which are from the same source, and have a ΔH_S of about 5000 cal/mol. Bychkov, et al.(18) to a degree, are in agreement, but the data of Jesseman, et al.(40) are two decades higher and show a ΔH_S of 22,000 cal/mol. Since they also report a 2400 ppm oxygen level in their solvent lithium, one might expect that oxygen is playing a role in the Jesseman, et al. niobium solubility processes.

Figure 6 shows the reported values for the solubility of nickel in lithium. The data of Kelly(45) and of Leavenworth and Cleary(52) have a ΔH_S of 15,000 cal/mol. Jesseman, et al.(40) show much higher solubility values with a ΔH_S of 8000 cal/mol. Bychkov, et al.(18) give data whose ΔH_S is 51,000 cal/mol, and must be the result of a chemical reaction.

Figure 7 shows the data for the solubility of titanium in lithium. The data are badly scattered with a three-decade range of values. Jesseman, et al.(40) show a ΔH_S of 21,000 cal/mol, while Kelly's(45) ΔH_S is 10,000 cal/mol. Leavenworth and Cleary(50) show values similar to Kelly's, but with a very small ΔH_S.

Figure 8 shows data for the solubility of zirconium in lithium. Jesseman, et al.(40) report data having a ΔH_S of 13,000 cal/mol. Koenig(47) reports data whose ΔH_S is 26,000 cal/mol, while the ΔH_S of the data of Bychkov, et al.(18) is larger, at 45,000 cal/mol, which suggests an interaction other than simple solution must have been operating in his tests.

In summary, the metal solubility data in lithium are quite varied, both with respect to the magnitude of the solubilities reported from one worker to another, and also with respect to the values of ΔH_S, which range from essentially zero to 50,000 cal/mol. Although one cannot be certain, it seems very likely that oxygen and perhaps nitrogen have been contributing factors to the metal solution processes in liquid lithium.

Table II summarizes the data reported for the solubility of various elements in liquid sodium. Again, the test procedures and conditions are varied, so that a detailed evaluation of the data is not warranted. It is, however, informative to compare the data of the various authors.

Figure 9 shows the data reported for the solubility of carbon in sodium. Although carbon is not a metal, it was included in the present tabulation because of the great interest in its solubility in connection with the concern about the carburization of stainless steels. The earliest data was published by Gratton(31) of KAPL, who investigated the solubility at two oxygen levels, 40 and 260 ppm O. His data are quite consistent and show an increased solubility of carbon in the higher oxygen-level sodium. The data of Adams(1) lie about 60% above those of Gratton, but have the same slope, ΔH_S = 5000 cal/mol. Vogel(83) reports data which are in nominal agreement with those of Gratton and Adams, but which have a lower ΔH_S (3500 cal/mol). Thus, the three experimenters are in nominal agreement, and indicate solubilities in the several tens of ppm C. However, all also agree that it is a very difficult experimental problem to ensure that particulate carbon is not present in the samples analyzed, and apparently have reservations about their data on this account. This is of particular interest in that a theoretical analysis of the solution process for carbon indicates that its solubility is expected to be very low,(9) perhaps below 1 ppm.

Figure 10 shows the data reported for the solubility of iron in sodium. There is a wide variation in the magnitudes of the data reported. Bogard(11) carried out a study of the solubility of iron in sodium using a radioactive tracer technique and found solubilities to be in the ppb range. The iron used

Table II

Solubility of Elements in Sodium

Solute	T °C	Solvent Oxygen Content ppm	Source Material*	Container Material**	Solubility ppm	Ref
C	158		Graphite		73	1
	158		Graphite		76	83
	250	100			33	2
	291		Graphite		63	83
	300		Graphite		58	1
	307		Graphite		53	83
	375		Graphite		91	83
	400	40	Graphite	SSTL***	56	31
	400	260	Graphite	SSTL	73	31
	445		Graphite		110	1
	455		Graphite		108	83
	700	40	Graphite	SSTL	155	31
	700	260	Graphite	SSTL	184	31
Co	365	10-20			0.028	30
	425				0.021	30
	525				1.00	30
Fe	200		Fe	SSTL-304	0.0013	11
	225				5	38
	300		Fe	SSTL-304	0.0024	11
	300	50	SSTL	SSTL	7.5	67
	400		Fe	SSTL-304	0.0047	11
	500				13	38
	500	50	SSTL	SSTL	12	67
	500		Fe	SSTL-304	0.0084	11
Nb	800		Nb-1Zr		15	51
	800		Nb-1Zr	Mo	178	24
	800		Nb-1Zr	Mo	18	24
	1000		Nb-1Zr		7	51
	1010		Nb-1Zr	Mo	7.5	24
	1180		Nb-1Zr	Mo	35	24

*Material from which the solute was dissolved.
**Material from which the solubility test container was made.
***SSTL, stainless steel.

Table II (continued)

Solute	T °C	Solvent Oxygen Content ppm	Source Material*	Container Material**	Solubility ppm	Ref
Nb (cont'd)	1185		Nb-1Zr	Mo	12	24
	1200		Nb-1Zr		30	51
	1380		Nb-1Zr	Mo	243	24
	1500		Nb-1Zr		500	51
Ni	200		Ni	Ni	6.5	67
	300		Ni	Ni	10	67
	400		Ni	Ni	14	67
	500		Ni	Ni	17	67
Ta	325	10-20			0.032	30
	425				0.19	30
	525				2.9	30
Zr	800		Nb-1Zr	Mo	1.7	24
	800		Nb-1Zr	Mo	0.8	24
	800		Nb-1Zr		<1	51
	1000		Nb-1Zr		<1	51
	1010		Nb-1Zr	Mo	0.6	24
	1180		Nb-1Zr	Mo	1.0	24
	1185		Nb-1Zr	Mo	2.4	25
	1200		Nb-1Zr		<1	51
	1380		Nb-1Zr	Mo	3.6	24
	1500		Nb-1Zr		4	51

*Material from which solute was dissolved.
**Material from which the solubility test container was made.

in this study was a very highly purified material prepared by H. E. Cleaves and R. A. Lindberg(53). The ΔH_S as shown is 4200 cal/mol. Jackson(38) reports values which are about 1000 times higher than those of Bogard, and with a ΔH_S of 2600 cal/mol. Finally, Rodgers, et al.(67) report data which are about 10 times greater than those of Jackson and with a similar ΔH_S value. There is no obvious way of reconciling these data.

Figure 11 shows the solubility data for niobium in sodium. All the data reported appear to have been developed at the same laboratory. Ewing, et al. (24) and Kovacina, et al.(51) are authors of different progress reports of a series. If one neglects the data reported for 800°C, a curve can be drawn through the remaining points. Its ΔH_S is 36,600 cal/mol.

Figure 12 shows the data reported for the solubility of zirconium in sodium. Since all the data originated with Ewing, et al.(24) and Kovacina, et al.(51) at NRL, a single curve has been drawn through all the data points. The ΔH_S is seen to be 5300 cal/mol.

As was noted above, there is a dearth of data on the solubilities of metals in sodium. Further, the data which are available are not as consistent as would be desired to provide support for the systems using sodium coolant.

Table III lists the data reported in the literature for the solubilities of metals in potassium. Up to the time of the initiation of this present program, there had been practically no data developed for the solubilities of construction metals in potassium. Since the initiation of the program Swisher(77) and Ginell and Teitel(29) have reported the additional data shown in the table.

Swisher used a large block of molybdenum held in a vacuum furnace as a means of maintaining temperature uniformity. Samples were placed in holes in the block which was mounted in a furnace which could be rotated to invert the samples. The samples were contained in a capsule made of the collector material. The solute sample was a crucible which fitted into a recess in the capsule so that when the capsule was inverted at the end of a test the potassium would pour into the collector to be separated from the solute metal. The capsule was welded closed and a minimum of two of these were installed in the molybdenum block for each test made at a single temperature.

Ginell and Teitel have developed a novel test device consisting of an L-shaped test capsule mounted on a centrifuge, which operates in an ion pumped high vacuum system. The test capsule consists of a sample leg which is horizontal during the initial test period. This is welded to a second leg at a right angle. This second leg contains the collector which is a vapor deposited (and quite pure) tungsten thimble. The upper end of the sample leg has a small dam positioned to regulate the amount of the potassium which can flow into the collector.

The test is conducted by raising the temperature of the centrifuge furnace to about 100°C above the nominal test temperature while the centrifuge is rotating at a rate sufficient to prevent the potassium from flowing over the dam. This temperature is maintained for several hours, during which time the potassium is expected to dissolve more solute than the saturation amount at the test temperature. Then the furnace is allowed to cool to the test temperature and the centrifuge is operated to produce a gravitational field of 50-70 g in the capsule. The purpose of this is to allow the solution to come to equilibrium with the solid solute and to force any tiny particles of solute precipitate to the bottom of the sample crucible. At the end of the test the rate of centrifuge rotation is slowly reduced to allow the upper layers of the potassium to decant over the dam and to drop into the collector. This is a novel device and was designed to allow solubility equilibrium to be approached from a condition of supersaturation.

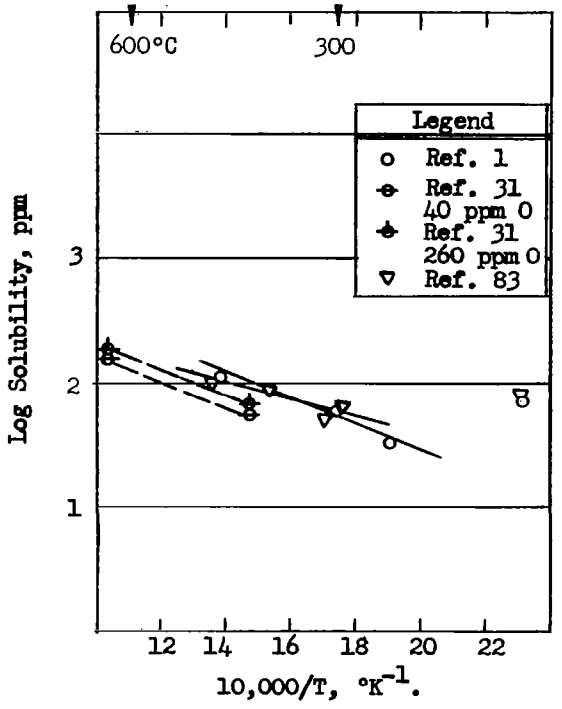

Figure 9. Solubility of C in Na.

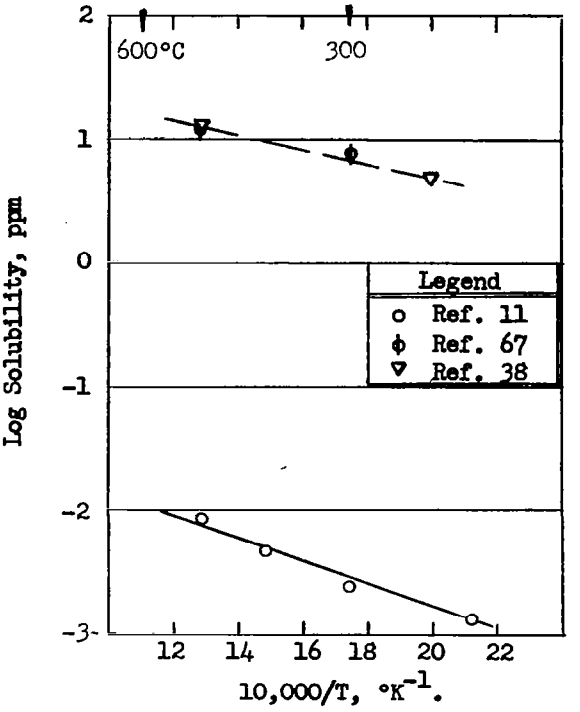

Figure 10. Solubility of Fe in Na.

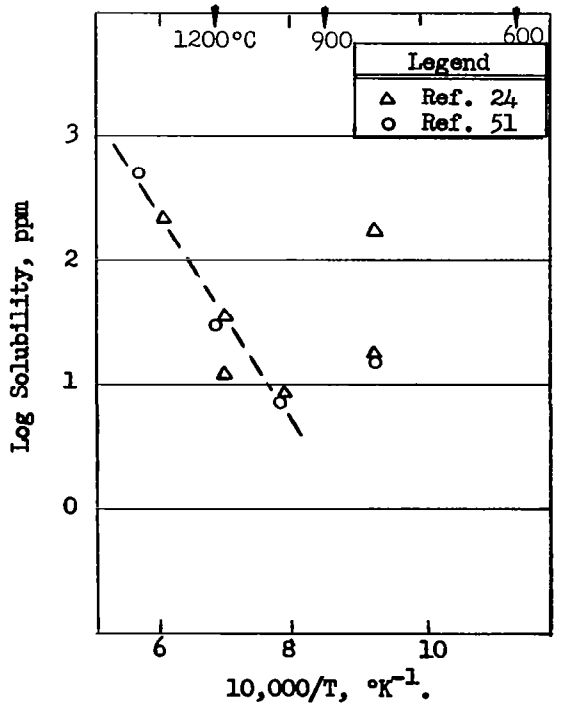

Figure 11. Solubility of Nb in Na.

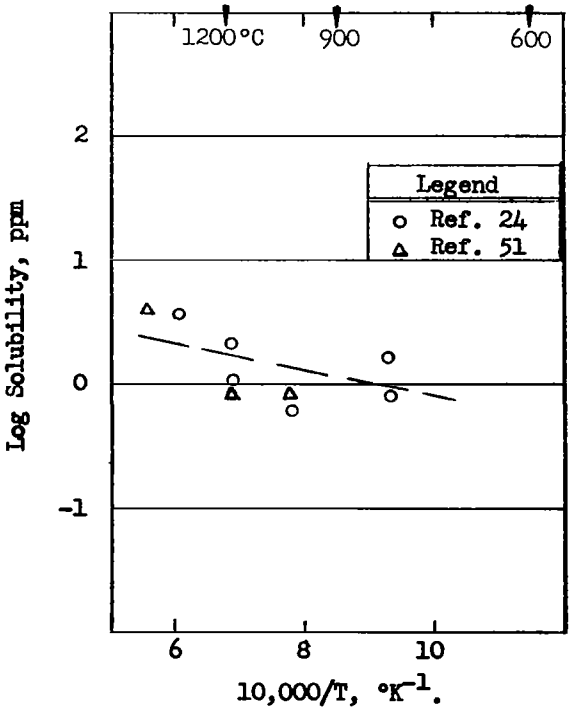

Figure 12. Solubility of Zr in Na.

Table III

Solubility of Elements in Potassium

Solute	T °C	Solvent Oxygen Content ppm	Source Material*	Container Material**	Solubility ppm	Ref
Co	870		Co	Nb	<5	77
	1060		Co	Nb	<5	77
Fe	670	20	Fe	Fe	43	77
	760	20	Fe	Fe	250	77
	870	20	Fe	Fe	650	77
	925		Fe	Nb-1Zr	447-457	91
	930	20	Fe	Fe	1300	77
	1000	20	Fe	Fe	1000	77
	1000	10	Fe	Nb-1Zr	500	29
	1000		Fe	Nb-1Zr	555	91
	1000		Fe	Nb-1Zr	444	91
	1060	20	Fe	Fe	1000	77
Nb	1095	500	Nb	Nb-1Zr	3-20	10
	1095	1000	Nb	Nb-1Zr	5-30	10
	1095	3000	Nb	Nb-1Zr	6-30	10
	1095	5000	Nb	Nb-1Zr	1000-3000	10
	1130	23	Nb	Nb-1Zr	10	29,91
	1225	23	Nb	Nb-1Zr	9-28	29,91
	1245	10	Nb	Nb-1Zr	7-14	29,91
	1330	23	Nb	Nb-1Zr	31	29
Ni	670		Ni	Ni	6	77
	760		Ni	Ni	6	77
	870		Ni	Ni	18	77
	925		Ni	Nb-1Zr	3	29
	925		Ni	Nb-1Zr	2-4	91
	1000		Ni	Nb-1Zr	4	91
	1000		Ni	Nb-1Zr	25	77
	1000		Ni	Nb-1Zr	4-115	29
	1060		Ni	Ni	58	77
Ta	1130	23	Ta	Nb-1Zr	17	29,91
	1225		Ta	Nb-1Zr	15	91
	1245		Ta	Nb-1Zr	126-151	91
	1245	10	Ta	Nb-1Zr	138	29
	1330	23	Ta	Nb-1Zr	6-114	29
	1330		Ta	Nb-1Zr	6-15	91
Ti	1000		Ti	Nb-1Zr	68-100	91
Zr	1000		Zr	Nb-1Zr	58-156	91

*Material from which the solute was dissolved.
**Material from which the solubility test container was made.

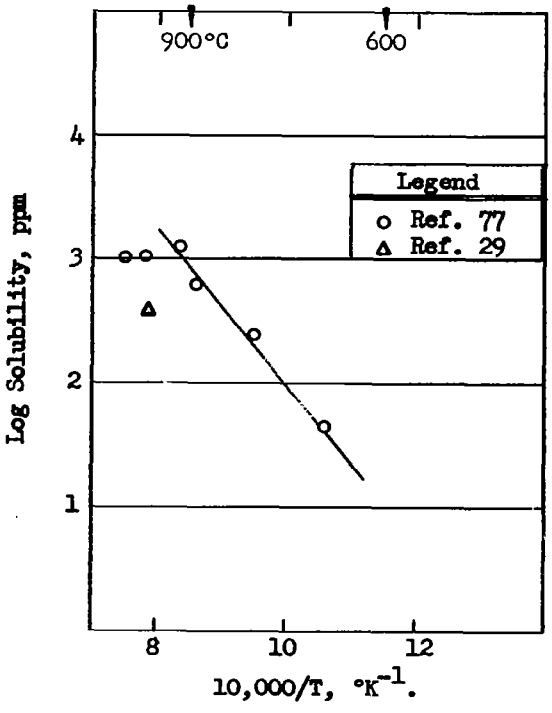

Figure 13. Solubility of Fe in K.

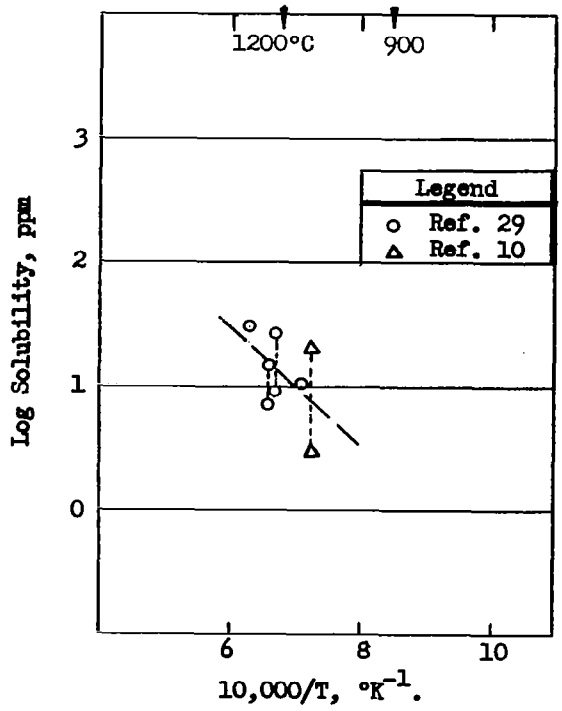

Figure 14. Solubility of Nb in K.

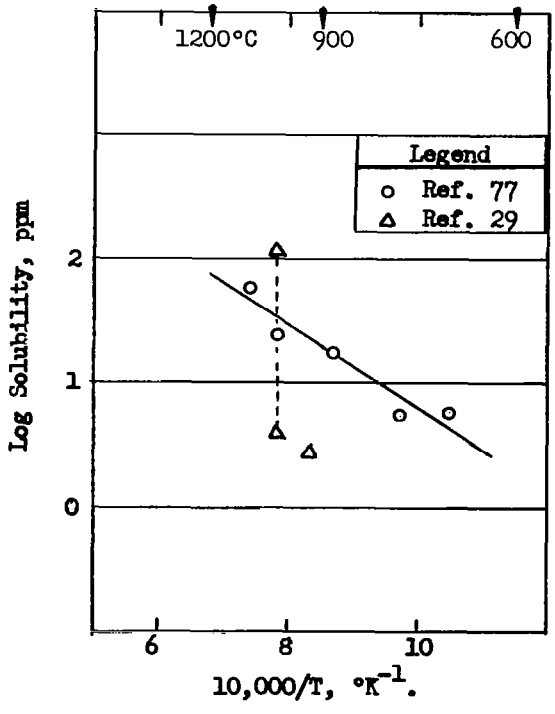

Figure 15. Solubility of Ni in K.

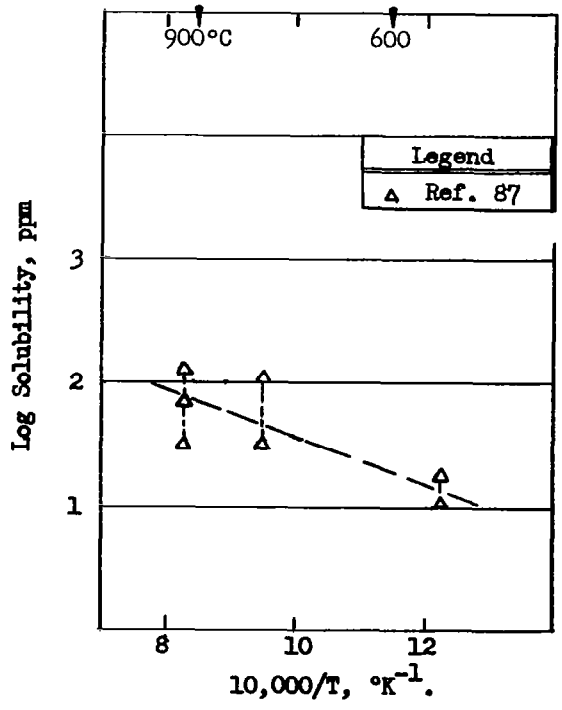

Figure 16. Solubility of Fe in Rb.

Figure 13 shows the solubility data for iron in potassium. The curve of Swisher(77) is characterized by ΔH_S of 28,200 cal/mol. Swisher's data show a definite break at about 950°C. At lower temperature the data show the expected kind of temperature dependence; but at higher temperatures, the solubility data tend to be constant at about 1000 ppm. Ginell and Teitel(29) report 500 ppm as the solubility of iron at 1000°C in potassium having 10 ppm oxygen. Swisher's source potassium contained about 20 ppm oxygen.

Figure 14 shows the data reported for the solubility of niobium in potassium. Neither of the experimenters report well-defined values for solubility, but there is an indication of a trend with temperature as indicated by the tentative curve sketched through all the data in the figure. The ΔH_S defined by this line is about 23,000 cal/mol. However, it should be emphasized that little significance can be assigned to this curve.

Figure 15 summarizes the solubility data for nickel in potassium. Swisher(77) reports data which define a curve having a ΔH_S of 13,900 cal/mol. Ginell and Teitel's data(29) scatter about this line.

In addition to the solubility data in potassium solvent shown in Figures 13, 14, and 15, Ginell and Teitel(29) report data for tantalum, and Swisher(77) reports data for cobalt. No other solubility data for metals in potassium was found.

Table IV lists the data reported in the literature for the solubilities of metals in rubidium. The data were obtained by exposing construction alloys to rubidium and analyzing for the various major constituents. This technique should yield solute concentrations which are below the true solubility values because of the lowered activity of the metals in the alloys. However, the quoted values do give an indication of the expected solubility values.

Figure 16 shows the solubility data of Young and Arabian(87) for iron in rubidium obtained from the solution of Haynes-25. The curve drawn through the points has a ΔH_S of 9000 cal/mol.

Figure 17 shows the data reported for the solubility of molybdenum in rubidium. All of the data shown were obtained from the report of Young and Arabian(87), who exposed Mo-0.5% Ti alloy to liquid rubidium metal. A tentative line has been drawn through their data. and its slope corresponds to a ΔH_S of 14,800 cal/mol.

Figure 18 shows the solubility data for niobium in rubidium. All of the data were obtained from the exposure of Cb-1% Zr alloy by Young and Arabian(87). The reported points fall on the well-defined curve shown. The ΔH_S of this curve is 7000 cal/mol.

Figure 19 shows the Young and Arabian(87) data reported for the solubility of titanium from Mo-0.5% Ti alloy in rubidium, and for the solubility of zirconium from Cb-1% Zr alloys in rubidium. All of the titanium data reported are below 5 ppm, but because of the low activity of Ti in the alloys, one would expect

Table IV						
Solubility of Elements in Rubidium						
Solute	T °C	Solvent Oxygen Content ppm	Source Material*	Container Material**	Solubility ppm	Ref
Be	540		Be	Ta	<1	87
	760	9	Be	Ta	<1	87
Co	760	92	Haynes 25	Haynes 25	<1	87
	930		Haynes 25	Haynes 25	<1-18	87
Cr	760	92	Haynes 25	Haynes 25	13	87
	930		Haynes 25	Haynes 25	<1-35	87
Fe	540		Haynes 25	Haynes 25	18	87
	760		Haynes 25	Haynes 25	33-115	87
	930		Haynes 25	Haynes 25	33-70	87
Mn	760	92	Haynes 25	Haynes 25	1	87
	930		Haynes 25	Haynes 25	<1-6	87
Mo	760	53	Mo-0.5Ti	Ta	2-7	87
	930	49	Mo-0.5Ti	Ta	1-4	87
	1090	5	Mo-0.5Ti	Ta	3-10	87
Nb	760	19	Nb-1Zr	Ta	<15	87
	930	55	Nb-1Zr	Ta	<15-26	87
	1090	11	Nb-1Zr	Ta	30	87
Ni	760	92	Haynes 25	Haynes 25	<1	87
	930		Haynes 25	Haynes 25	<1-17	87
Ta	540		Ta	Ta	105-13,000	87
	760	92	Ta	Ta	350-11,000	87
	930		Ta	Ta	200-26,000	87
	1090		Ta	Ta	12-50,000	87
Ti	760	53	Mo-0.5Ti	Ta	2-3	87
	930	49	Mo-0.5Ti	Ta	1-2	87
	1090	5	Mo-0.5Ti	Ta	3-4	87
V	540	54	V	Ta	<1	87
	760	74	V	Ta	<1	87

Table IV (continued)

Solute	T °C	Solvent Oxygen Content ppm	Source Material*	Container Material**	Solubility ppm	Ref
W	760	92	Haynes 25	Haynes 25	<15	87
	930		Haynes 25	Haynes 25	<15	87
Zr	760	19	Nb-1Zr	Ta	7	87
	930	55	Nb-1Zr	Ta	7-100	87
	1090	11	Nb-1Zr	Ta	70-100	87

*Material from which the solute was dissolved.
**Material from which the solubility test container was made.

the true solubility of pure Ti to be higher. However, the data reported define a tentative solubility curve whose ΔH_S is 8600 cal/mol. The zirconium data range up to 100 ppm, even though the source zirconium is present at only one per cent in the Cb-1%Zr alloy. Again, the data define a tentative curve and its slope corresponds to a ΔH_S of 23,000 cal/mol.

In addition to the data plotted in Figures 16 through 19, there are "solubility" data in rubidium for cobalt, chromium, manganese, nickel, and tungsten from Haynes-25.(87) While the data are of interest as qualitative indications of the solubility of these alloying elements, their true solubilities should properly be determined using samples of the pure elements as sources.

Table V summarizes the data reported for the solubilities of metals in cesium. All of the data have been reported over a period of several years by Tepper, et al., (78,79) of MSA, who used carbon, and Haynes-25, Mo-0.5% Ti, and Cb-1%Zr alloys as solute sources. The metal solubility data are sparse and appear to show lower 'solubilities' at the higher temperatures. As was noted above in the case of the rubidium solvent, the data are perhaps useful in defining the nominal levels of solubility to be expected for metals in cesium, but if accurate values are desired, they should be obtained by using pure metals as solute sources.

Figure 20 shows the data reported by Tepper, et al.,(78) for the solubility of carbon in cesium. Because only two points were given, the curve between them is shown as a dashed line. The corresponding ΔH_S is 5300 cal/mol which is comparable with the value for the solubility curves for carbon in sodium.

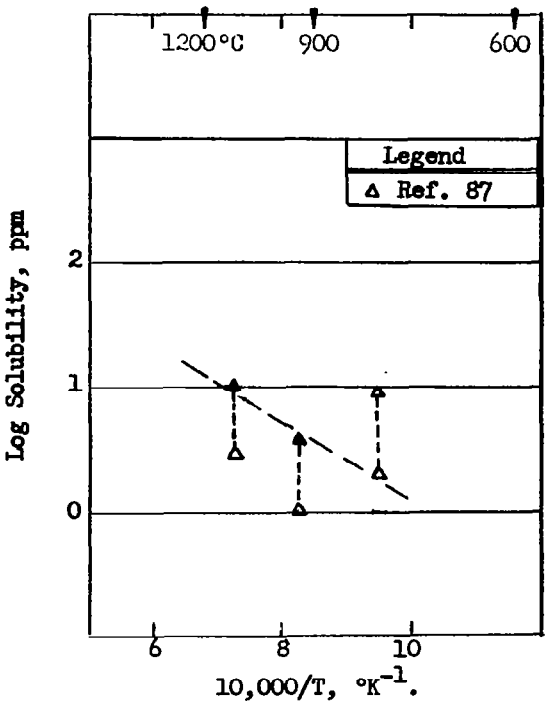

Figure 17. Solubility of Mo in Rb.

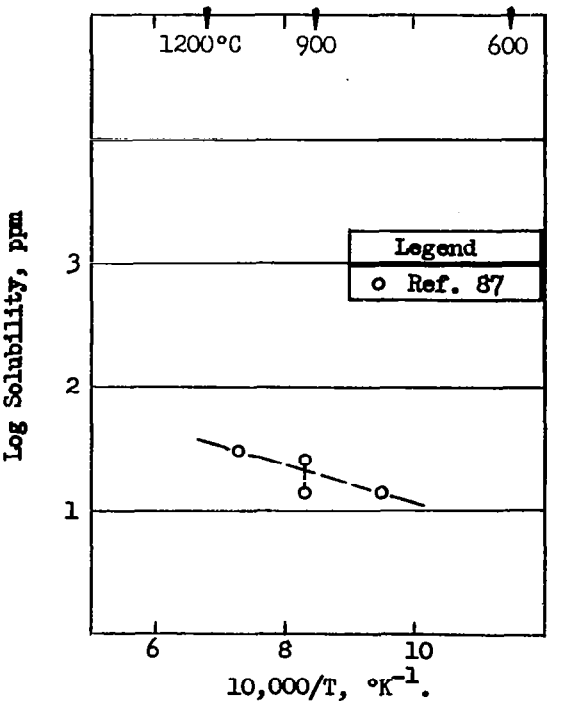

Figure 18. Solubility of Nb in Rb.

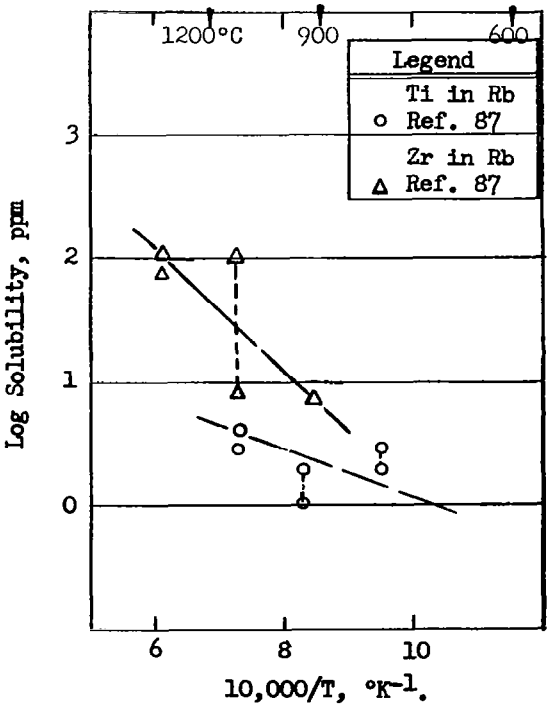

Figure 19. Solubility of Ti and Zr in Rb.

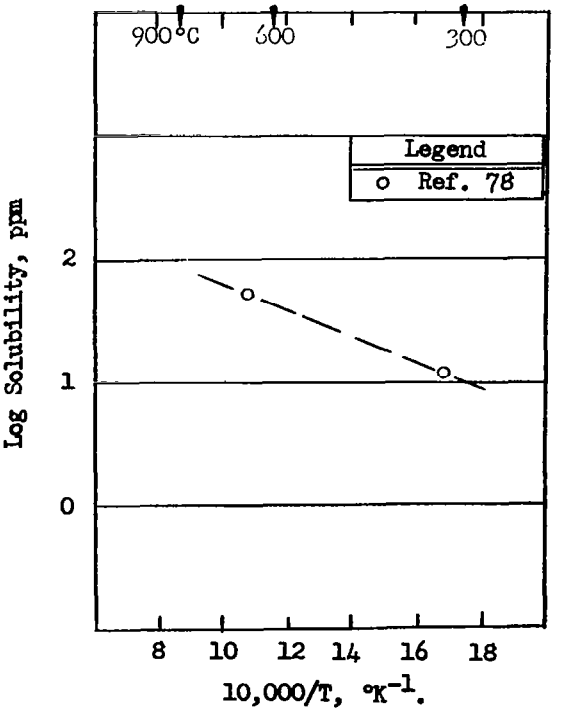

Figure 20. Solubility of C in Cs.

Table V						
Solubility of Elements in Cesium						
Solute	T °C	Solvent Oxygen ppm ppm	Source Material*	Container Material**	Solubility ppm	Ref
C	315 650		Graphite Graphite		12 53	78 78
Co	980	12	Haynes 25	Haynes 25	<6-125	79
Cr	980	12	Haynes 25	Haynes 25	<6-18	79
Fe	980	12	Haynes 25	Haynes 25	<1-9	79
Mo	1370 1370	12	Mo-0.5Ti Mo-0.5Ti	Mo-0.5Ti Nb-1Zr	12-110 10-25	79 78
Nb	1260 1370	12	Nb-1Zr Nb-1Zr	Nb-1Zr Mo-0.5Ti	125 10-30	79 78
Ni	980	12	Haynes 25	Haynes 25	<6-18	79
Ti	1370 1370	12	Mo-0.5Ti Mo-0.5Ti	Mo-0.5Ti Nb-1Zr	<6-90 <5-150	79 78
Zr	1260 1370	12	Nb-1Zr Nb-1Zr	Nb-1Zr Mo-0.5Ti	125 10	79 78

*Material from which solute was dissolved.
**Material from which solubility test container was made.

Table VI lists the ΔH_S values of the various solutes in the alkali metals. As was noted in the text above, there is a wide range in ΔH_S reported by various workers for most elements. However, one might consider only the lowest value of ΔH_S reported (which might be considered to represent the closest approach to a simple solution process) and seek a trend in the sequence from Li to Rb. No universal trend is found for any of the elements for which data is reported for three or more of the alkali metals. For iron, the ΔH_S(Na)(min) is the smallest, and ΔH_S(K) is the largest. For niobium solute, rather large ΔH_S-values are found for sodium and for potassium solvent. For nickel solute, ΔH_S(Na) is the lowest, as is ΔH_S(Na) for zirconium solute, also.

Table VI							
Heats of Solution of Elements in the Alkali Metals							
Solute	Solvent	ΔH_s cal/mol	Ref.	Solute	Solvent	ΔH_s Cal/mol	Ref.
C	Na	3500 5000 5000	(83) (1) (31)	Nb	Li	5000 22,000	(44)(10) (40)
	Cs	5300	(78)		Na	36,600	(24)(51)
Co	Na	30,000	(30)		K	23,000	(29)
Cr	Li	6300 28,500 14,000	(40) (6) (45)		Rb	7000	(87)
Fe	Li	4500 14,000 14,300	(6) (18) (45)	Ni	Li	8000 15,000 51,000	(40) (45)(52) (18)
	Na	2600 2600 4200	(38) (67) (11)		Na	2400	(67)
	K	28,200	(77)		K	13,900	(77)
	Rb	9000	(87)	Ta	Na	25,000	(30)
Mo	Li	7500 7600 65,300	(40) (45)(52) (18)		K	51,000	(29)
	Rb	14,800	(87)	Ti	Li	10,000 21,000	(45) (40)
					Rb	8600	(87)
				U	Li	17,000	(17)(18)
				Zr	Li	13,000 26,000 45,000	(40) (47) (18)
					Na	5300	(24)(51)
					Rb	23,000	(87)

In the general overview of the status of the existing solubility data, it is obvious that reproducibility of data is very difficult to attain. This is undoubtedly due in part to the interactions of impurities in the solvent with the solute. Further, the impurities in the solute materials are almost equally as likely to introduce uncontrolled perturbations on the solubility. It therefore seems virtually impossible to obtain reproducible true solubility data using commercial metals or alloys as solutes, and commercial grade alkali metals as solvents. However, measurements using such materials are useful in defining the degree of interaction to be expected in coolant loop or test systems which must employ commercial-grade materials. In one sense, it is this sort of analysis that leads to the operation of corrosion loop tests in order to obtain performance data for a given system.

Such performance data are of unquestioned value. However, in the interest of understanding the mechanisms of corrosion in practical systems, it is also necessary to know the fundamental solubilities of the metals which are used as construction materials or as components of construction materials. The essential parts of such a basic study are the use of very highly purified sample materials, and the employment of an experimental technique which ensures that the sample purity is maintained during the test period. This is the goal of the study described herein.

EXPERIMENTAL METHOD

An experimental test procedure designed to meet the various requirements of the experimental study was set early in the program and the design of the apparatus and its auxiliaries was defined by this procedure. The constraints were that the high purity solute crucibles would be re-usable for ten or more tests and that the crucibles would not be contaminated during the test sequence. Further, it was required that the test solvent be separated from the solute at the end of the test period to minimize the uncertainty in the test exposure period. Because of the high vapor pressure of potassium at 1200°C (150 psia), it is necessary to use a sealed capsule for the tests to prevent loss of potassium. Therefore, for reasons of economy, it is essential that the pressure vessel or capsule be re-usable. Finally, all parts of the test capsule should be as free of surface contamination oxygen and nitrogen as possible, especially during the sample loading procedure, to minimize contamination of the sample.

In order to satisfy the requirement that the samples not be contaminated, the decision was made to employ a test system comprising a minimum of two high vacuum chambers as the test system. One of these (Chamber #1) was designated as the sample loading chamber. The second was designated to be the sample closing or welding chamber. The remaining chamber(s) then house test furnaces as required. The details of the design and construction of this test system are given in the following section.

In order to minimize the problems associated with the handling and loading of potassium, the purification system was designed to deliver its product directly into Chamber #1. In this way, this very reactive metal cannot be contaminated during storage or transport to the loading station. The design and construction of the potassium purification unit are described below.

The test assembly designed to meet the above criteria is described below and is shown in Figure 51 (page 91). The solute crucible was to be formed so that its single crystallinity would not be compromised, and to have a shoulder at its open end. The collector is made of a material different from that of the crucible and originally had a square open end which seated into the shoulder or lip of the crucible. The capsule and cap are made of arc-melted molybdenum, and the closure is an electron beam weld at the bevelled edge of the cap.

In practice, the solute crucibles and the capsule parts are cleaned and rinsed with acetone. They are then given a high temperature, high vacuum outgassing, and when cool they are let down to a purified argon atmosphere. By this procedure the materials are freed of much of their volatile impurity content and are left with an adsorbed argon gas layer on their surfaces. These cleaned parts are then placed in Chamber #1 for a final outgassing at 350 $\pm$ 25°C to remove the argon gas before being used in the experiments. After the argon is removed from the parts, the purified potassium, which is delivered into Chamber #1, is loaded into the crucible. Then the collector is put in place and the sub-assembly slipped into the capsule body. Finally, the cap is put in place and the capsule sealed under high vacuum by electron beam welding.

Once the capsule is welded closed the sample is well protected. The test exposure is carried out in the test furnace in the cap-up position. The capsule is swung out of the furnace through an 180° arc at the end of the test so that the cap is then at the bottom. During this operation, the potassium in the capsule is transferred to the collector. After the capsule has cooled, it is cracked open by using a pipe-cutter blade bearing in the notch of the cap. When the molybdenum cap breaks it exposes the end of the collector. The collector is then separated from the crucible and is sent with its contents for chemical analysis. The crucible, the collector, and the capsule are then cleaned and reworked for re-use in later tests. This sequence is shown in flow-sheet form in Figure 21.

Figure 21. Solubility Test Flow Sheet

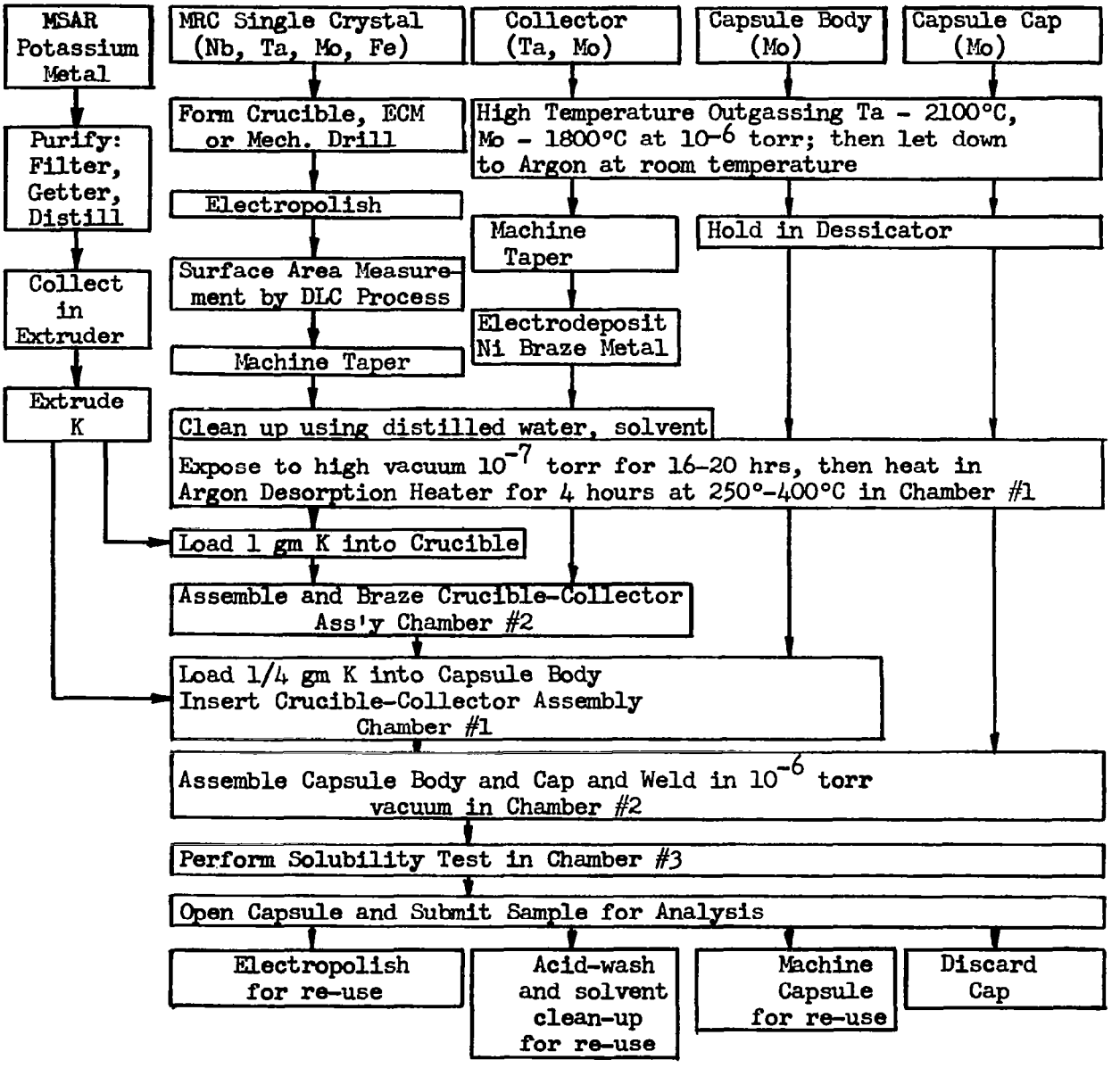

ENVIRONMENTAL TEST SYSTEM

General:

The experimental program involves solubility testing at temperatures up to 1200°C, at which temperature the potassium vapor pressure is about 150 psia. Because of this rather high vapor pressure it is necessary to conduct the solubility tests within a sealed capsule which can withstand the internal pressure. Because of the temperature, stress, and time considerations, the only suitable capsule materials were the commercially available refractory metals and their alloys. Of these, pure molybdenum was the least expensive one having suitable strength properties at 1200°C. However, it must be used in a neutral or reducing atmosphere in order to avoid catastrophic oxidation. A second restriction which is imposed on this system is that hot molybdenum is somewhat permeable to hydrogen gas (the most convenient reducing agent). Because of this permeability, hydrogen might pass into the interior of the capsule and interfere with the tests by reacting with the solute or solvent. Therefore, one must restrict the test chamber atmosphere to an inert gas such as argon or to a vacuum. The choice between these two protective atmospheres depends upon the concentrations of oxygen and water vapor which can be maintained in the argon as compared to the partial pressures of oxygen and of water vapor in the "vacuum". One important factor in the argon box system is the permeability of the gloves to reactive gases. Because of this, one must continuously circulate the argon through a water vapor and oxygen scavenger system to maintain a low partial pressure of these contaminants. In a 10^{-6} torr vacuum, the nominal oxygen concentration is about 3×10^{-10} atm. Argon box manufacturers guarantee a level of one ppm (10^{-6} atm) oxygen in the argon, a 3000-fold greater pressure. However, the effect of this greater pressure is not directly proportional to the pressure because of the strong inhibitory effect of the argon gas on the diffusion of the oxygen (and water vapor) to a reactive surface. An estimate is reported in the literature by Bromley, et al. (15) which indicates that a very good argon box atmosphere (10^{-6} atm O_2) is equivalent to a vacuum of about 10^{-7} torr, i.e., the arrival rate of oxygen at a surface is the same in both systems. However, the effective sticking coefficient under the argon atmosphere was expected to be higher than that in vacuum because of the blanketing effect of the gas. Therefore, the estimate as quoted by Bromley et al. should be modified to account for this effect. That this is an important consideration is shown in a recent study by Pasternak(60), who measured the sticking probability of nitrogen on niobium as a function of temperature and pressure. He reports values ranging from a probability of 0.01 to 0.1 in the temperature range 400-1800°C and in the pressure range 6×10^{-6} torr to 6×10^{-9} torr. Therefore, one must conclude that a vacuum environment of 10^{-7} torr is somewhat superior to a well-scavenged argon gas atmosphere.

Fabrication of the Environmental Test System:

Even though the vacuum system was expected to be the better choice, environmental test systems based on both the vacuum chamber and the argon atmosphere concepts were examined. However, both systems considered employed vacuum environments for handling and loading the potassium, and differed in that the

test chambers of the one system had vacuum atmospheres, while the second system employed an argon atmosphere in a single large test chamber. The all-vacuum system was made up of five interconnected vacuum chambers, each with its own pumping system, and separated by vacuum valves. The first chamber was 24 inches in diameter and 22 inches high and was to be used to outgas and to store clean samples and parts, and to contain the potassium-fill apparatus. The second chamber was 24 inches in diameter and 18 inches high and was to contain the electron beam welding assembly and a cutter for opening the test capsules. The remaining three chambers were 24 inches in diameter and 22 inches high and were to be used for separate test stations. Each chamber was to be fitted with two manipulators capable of operating in the 10^{-7} torr vacuum range. All metal parts exposed to the vacuum were to be polished stainless steel.

The second system which was examined used the same first and second chambers described above. The third chamber in this system was an argon-filled glove box, sized to provide space for three experimental test stations. This chamber was to communicate with the second vacuum chamber through an evacuable port. The argon atmosphere was to be continuously scavenged to maintain the oxygen and water vapor levels at less than 1 ppm.

Bids were obtained and evaluated for both systems. One important aspect of the comparison was the question of being able to maintain a vacuum in the 10^{-7} torr range while the various handling and manipulating operations were carried out. Fortunately, a vacuum system manipulator was found whose operating characteristics met our requirements. Therefore, the system chosen for use was the all-vacuum system offered by the D. L. Herring Corp. which is now called the Vacuum/Atmospheres Corporation (VAC), North Hollywood, Calif. The construction and performance specifications for the system are presented in Appendix I. Figure 22 shows an overall plan drawing of the system, and Figures 23 and 24 show details of a chamber cover and chamber wall layout, respectively.

The progress of the fabrication is shown in Figures 25 through 28. The system is shown undergoing preliminary testing in the D. L. Herring shop in Figure 29, and the system as presently installed at Atomics International is shown in Figure 30.

Acceptance Testing of the System:

The environmental test system was delivered on April 21, 1964, and was tested to certify that it did indeed meet the required performance specifications. Prior to delivery, all components had met the vacuum specifications when tested in the VAC shop. A summary of these specifications and the corresponding observed data are shown in Table VII for the acceptance tests performed at Atomics International. Following the vacuum-level checkout, the chambers were opened and the various accessories described below were installed in Chambers 1, 2, and 3. A re-check of the vacuum performance was made with very satisfactory results. Vacuum levels in the middle 10^{-7} torr range were obtained using only the water-baffles.

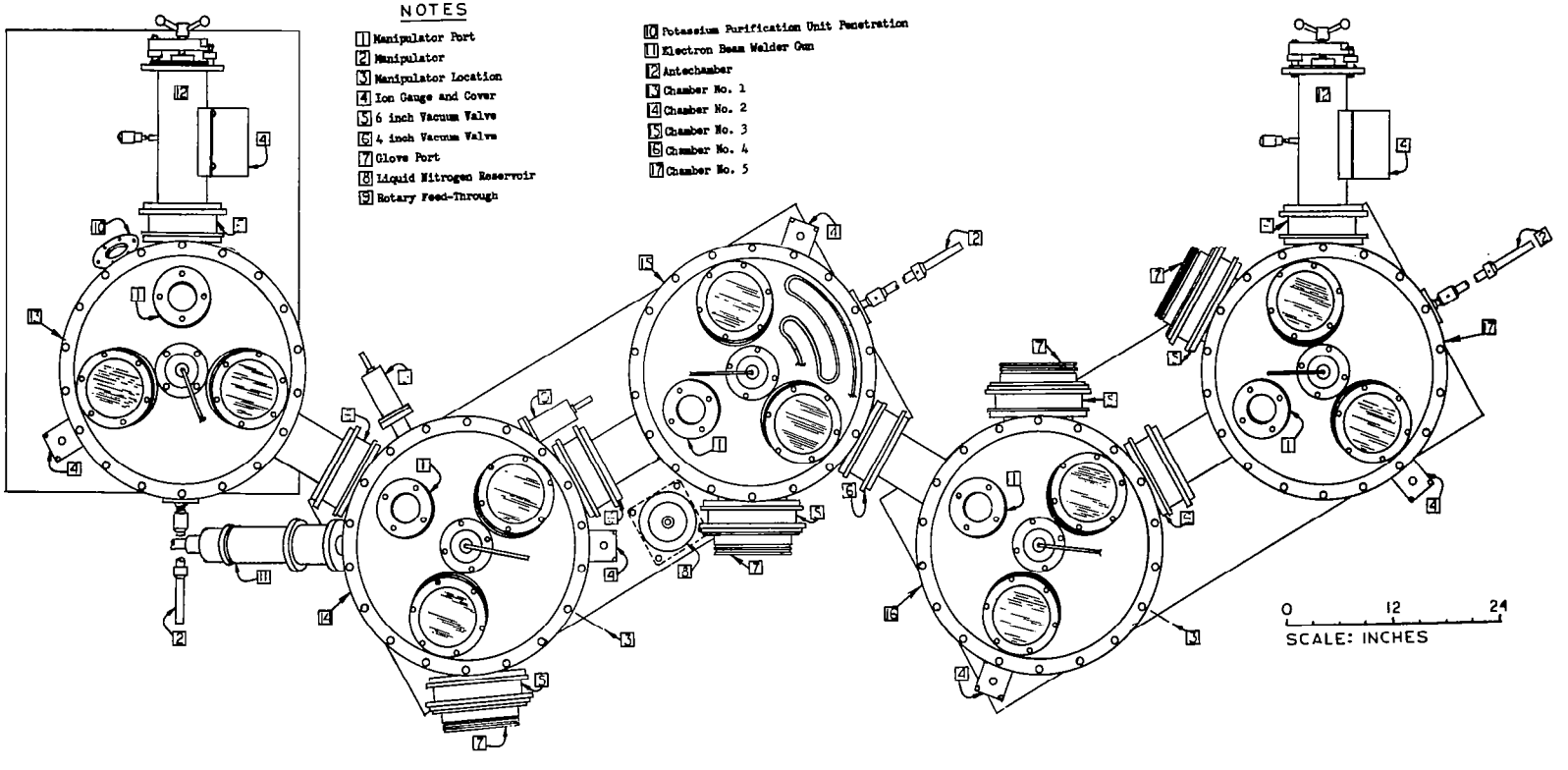

Figure 22. Environmental Test System.

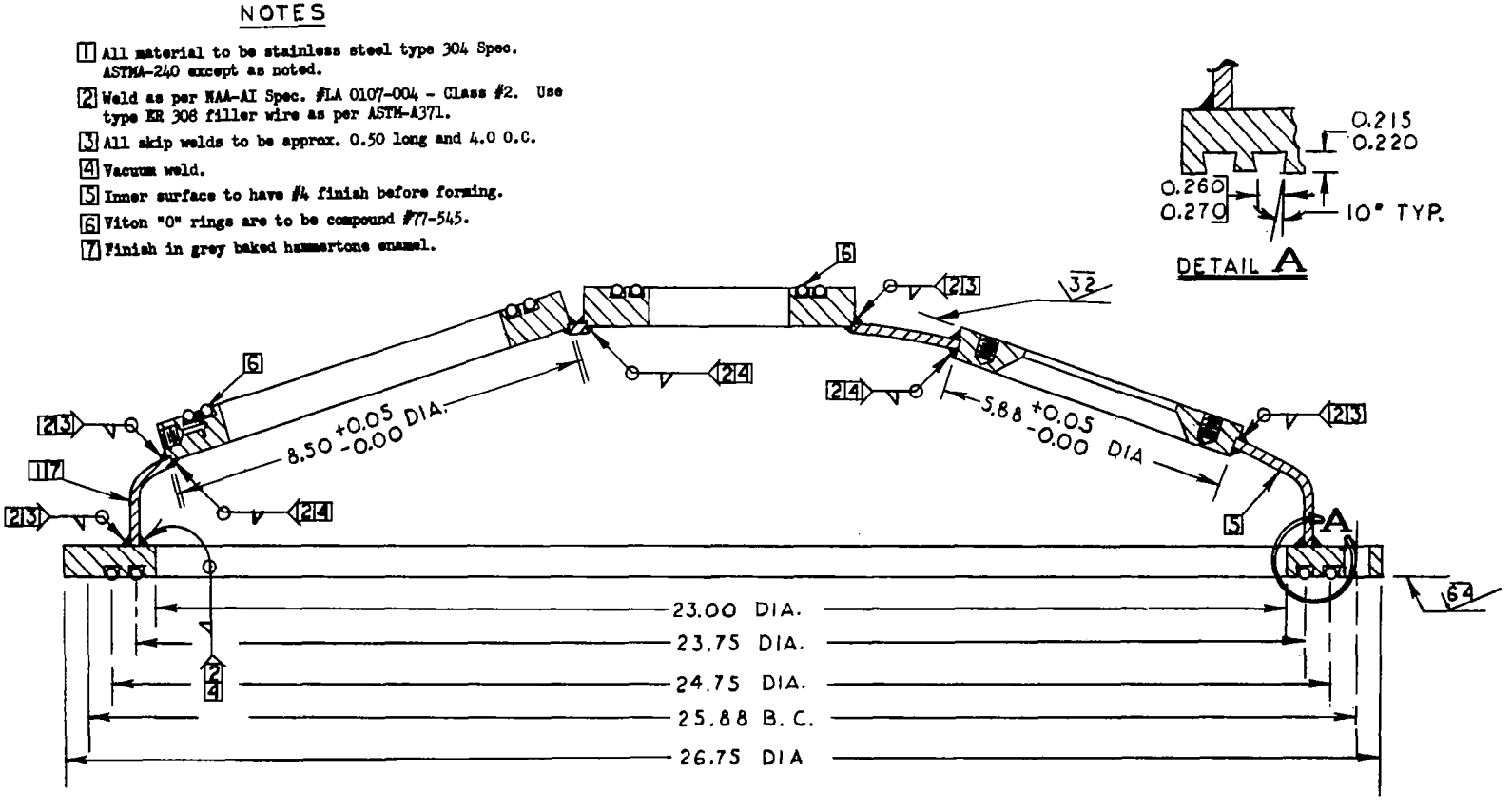

Figure 23. Chamber Cover Details.

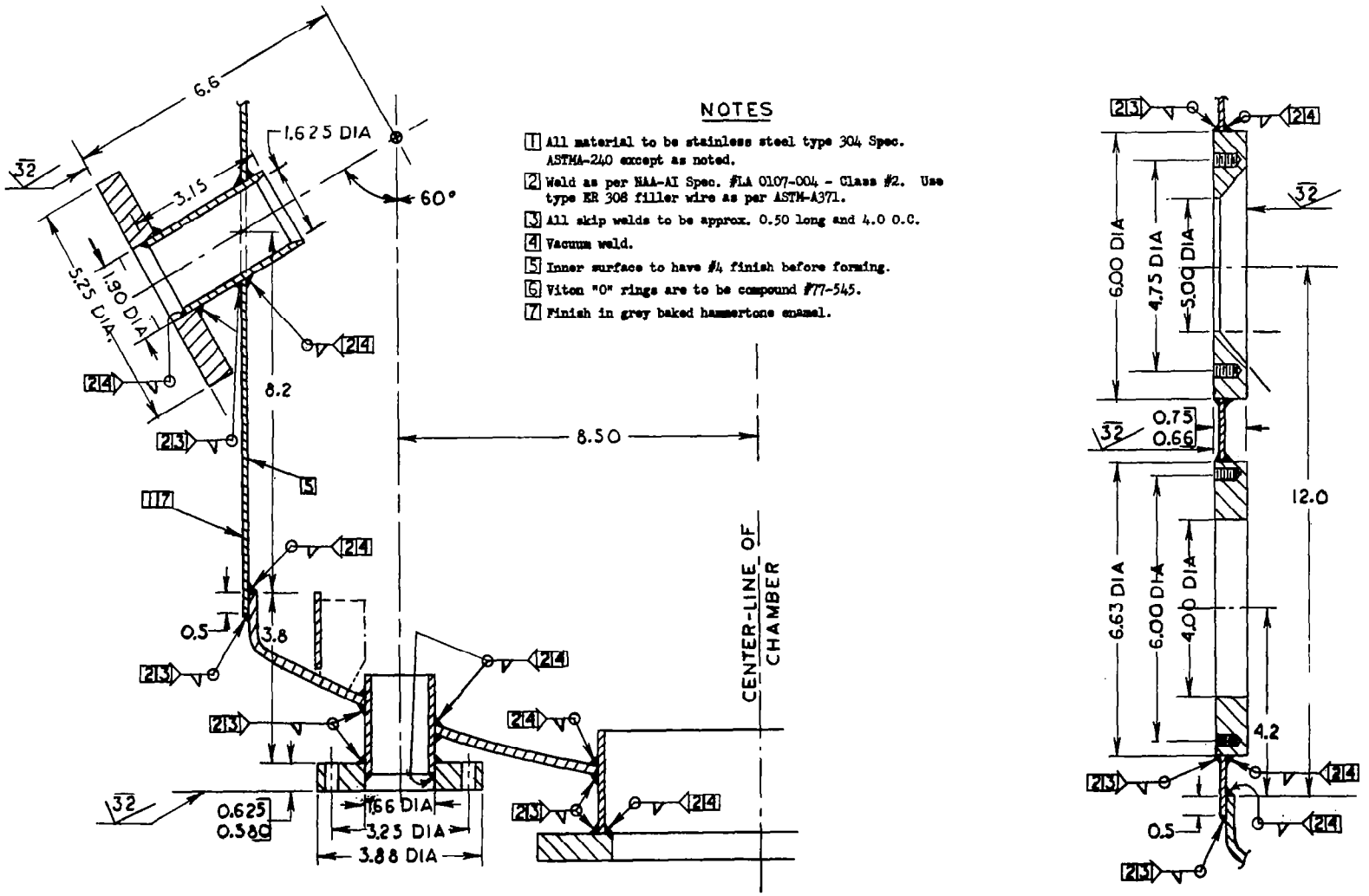

Figure 24. Chamber Wall Layout, Typical Details.

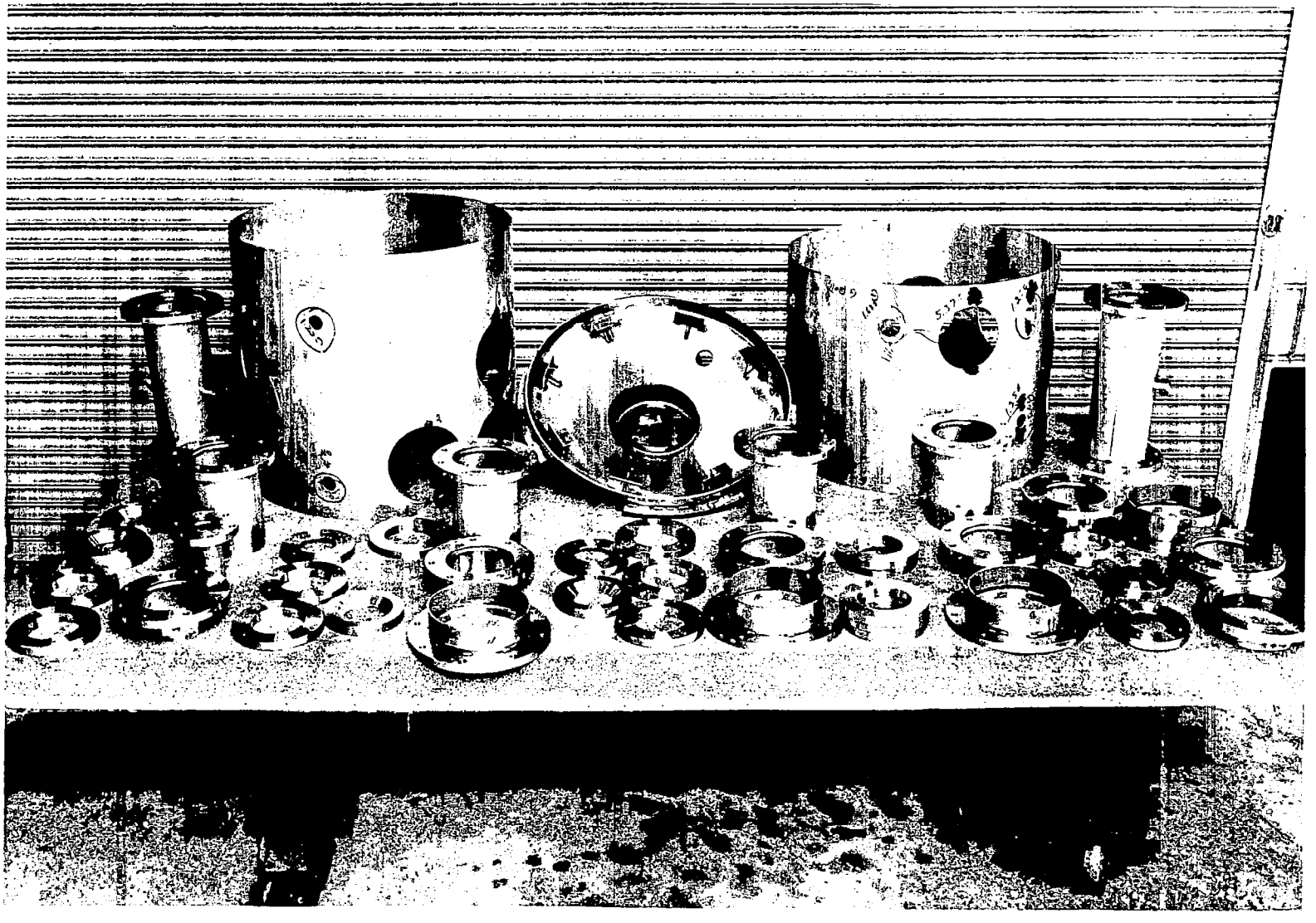

Figure 25. Parts for Environmental Test System.

Figure 26. Partially Assembled Chambers for Environmental Test System.

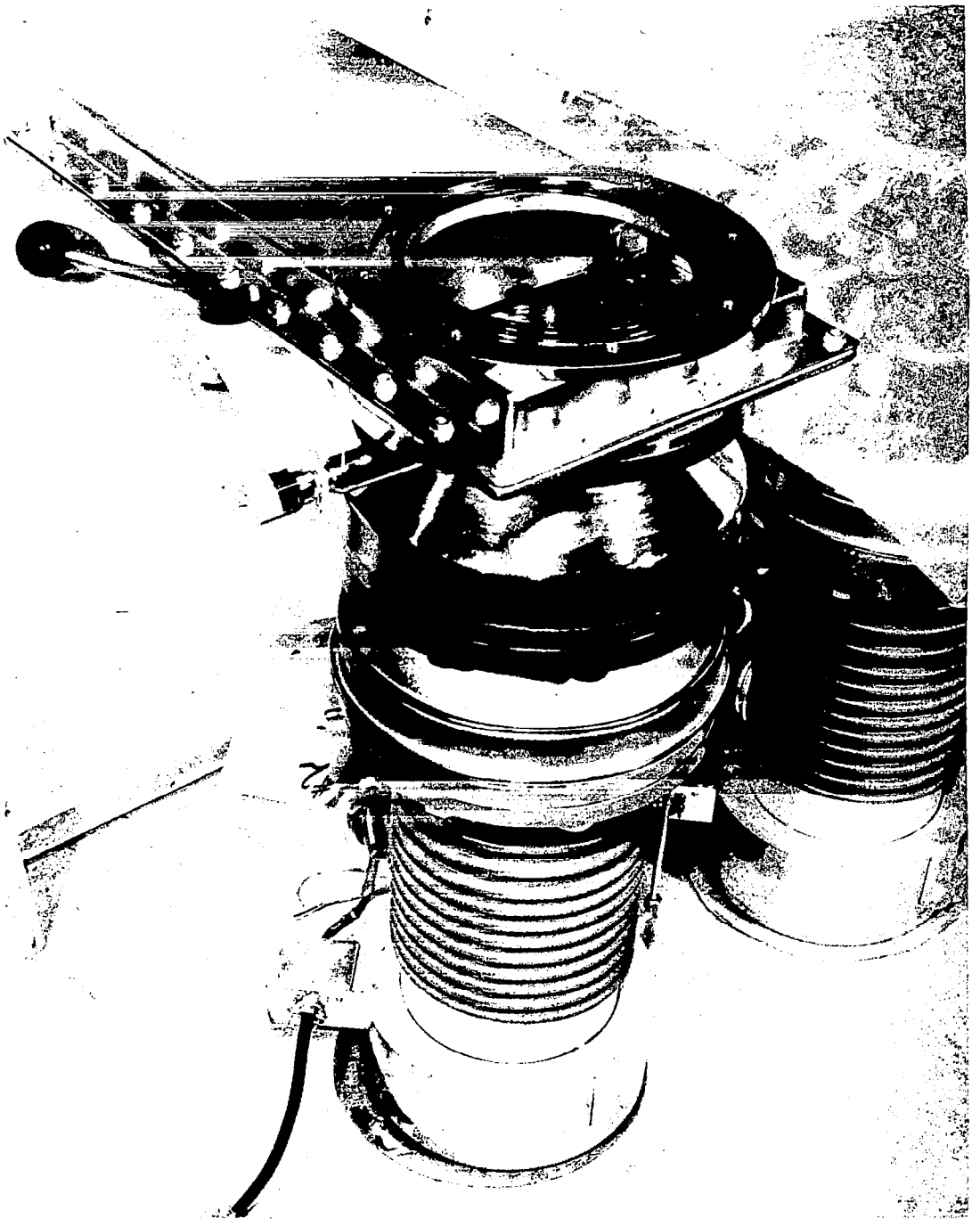

Figure 27. Vacuum Pump Sub-Assembly.

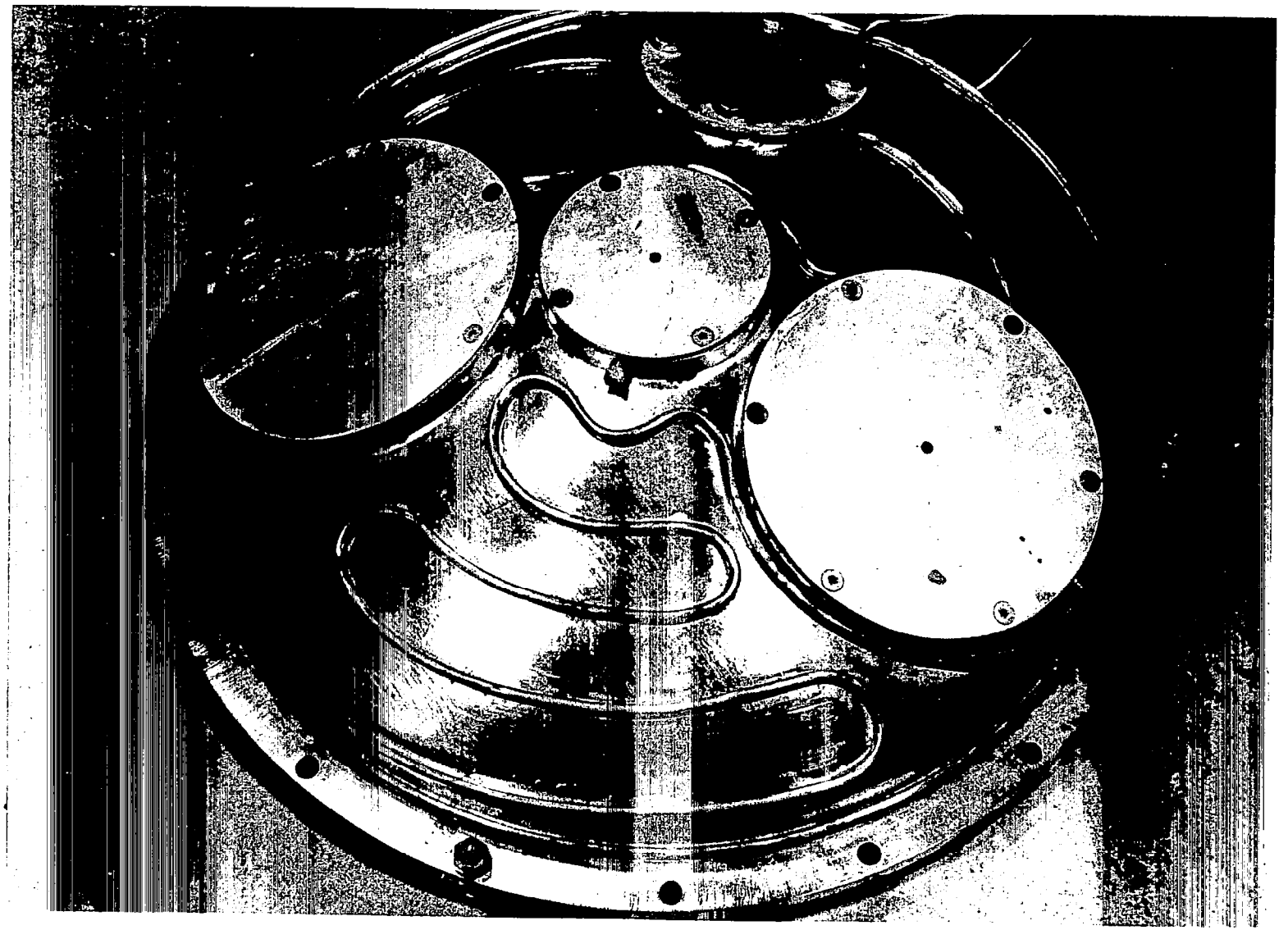

Figure 28. Chamber Cover.

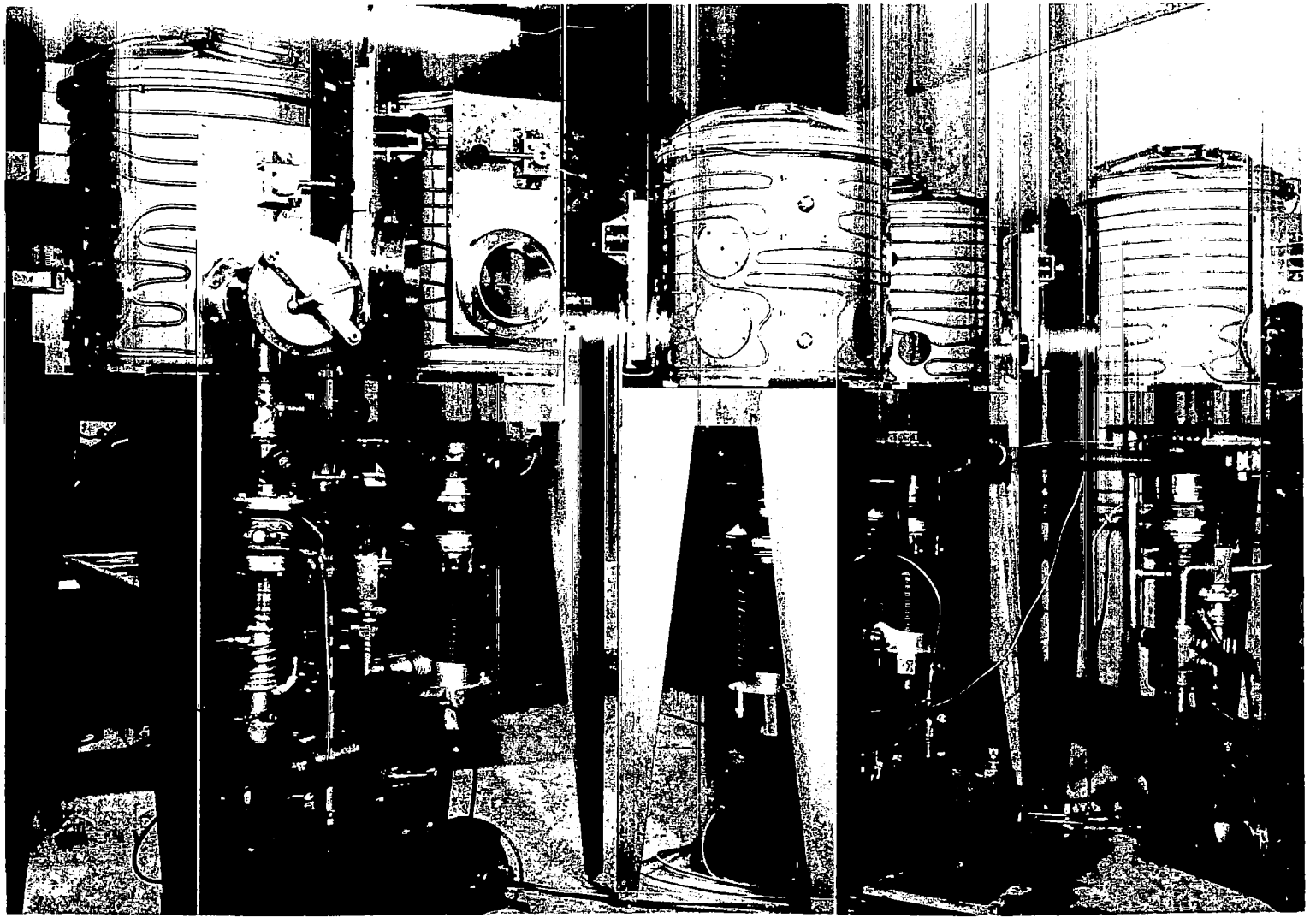

Figure 29. Chambers Undergoing Final Vacuum Checking.

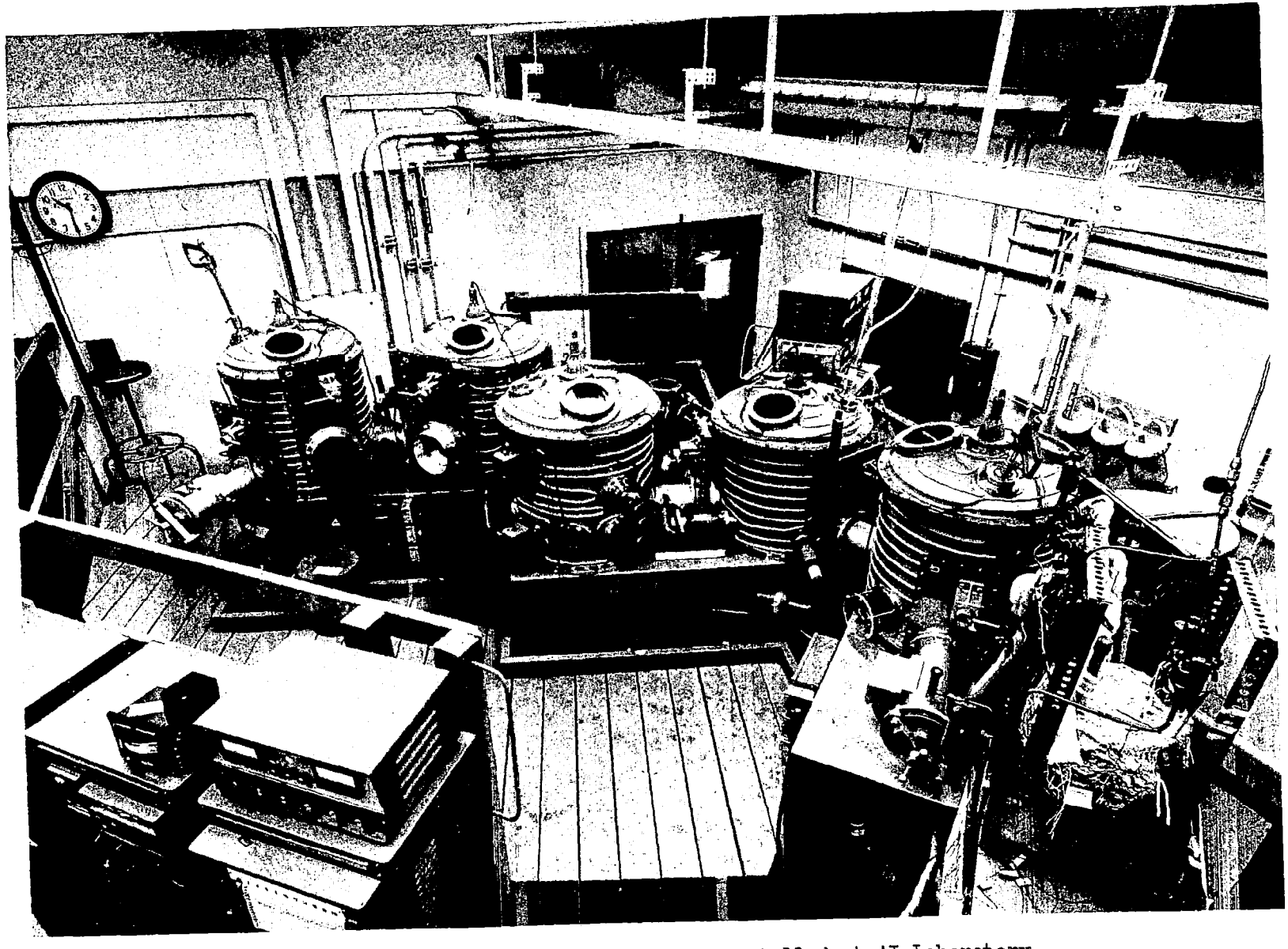

Figure 30. Environmental Test System Installed at AI Laboratory.

Table VII

Environmental Test System Acceptance Test Results

Chambers, Ante-chambers*	Specification "Ultimate" Vacuum**	Specification Pump-down time***	Observed Best Vacuum****	Observed Pump-down time
C-1	$1x10^{-7}$ Torr	1 hr.	$8x10^{-8}$ Torr	15 min.
C-2	"	"	$9x10^{-8}$ Torr	12 min.
C-3	"	"	$7x10^{-8}$ Torr	15 min.
C-4	"	"	$5.5x10^{-8}$ Torr	16 min.
C-5*****	$5x10^{-6}$ Torr	-	$2x10^{-7}$ Torr	-
AC-1	$1x10^{-6}$ Torr	-	$1x10^{-6}$ Torr	-
AC-5	"	-	$6x10^{-7}$ Torr	-

*These chambers are identified on Figure 21, page 29.

**The vacuum level to be reached after normal outgassing and pumping using the liquid nitrogen cold trap, in a clean, dry, and empty chamber.

***Maximum time to pump from 1 atm to $1x10^{-6}$ Torr (using a hot diffusion pump).

****These figures are not "ultimate" vacuum levels, but are those read for each chamber during the acceptance tests. All chambers in which pumping was continued after completion of the acceptance tests achieved lower vacuum levels.

*****C-5 is the mercury diffusion pumped chamber. Its vacuum level specification was based upon manufacturer's data, but the system performs significantly better than their expectations.

As a result of the marginal performance of the AC-1 system (the ante-chamber to Chamber #1), and its relatively long pump-down time, the two-inch diffusion pump was replaced by a four-inch diffusion pump to increase the overall pumping speed of the assembly. The system as presently operating is satisfactory, but if a further reduction in pump-down time is desired, it will be necessary to re-work the piping system to increase the vacuum line conductance.

Environment Purity Verification:

In order to verify that the vacuum chamber was not a source of contamination, an experiment was designed to evaluate the rate of contamination of an exposed surface of potassium by the nominal (1-3)x10^{-7} Torr atmosphere in the vacuum system. Four weighing bottles were loaded with solid potassium and were placed on the floor plate of Chamber #1 near the discharge port of the potassium extruder to be exposed to the vacuum atmosphere for two days. After the exposure, the potassium was analyzed for the oxygen absorbed. The results of this study are summarized in Table VIII, which indicates the average oxygen contamination rate to be 0.1135 μgm/cm^2/hr.

Table VIII

Summary of Oxygen Contamination Rate Experiments*

Effective Area cm^2	Net Oxygen Absorbed μgm	Absorption Rate μgm/cm^2/hr (48 hr test)
3.47	27.9	0.168
4.92	32.1	0.132
4.92	25.8	0.109
5.66	12.3	0.045
	Avg	0.1135
	Avg Dev	0.0365

*P = 3x10^{-7} Torr - without liquid nitrogen trapping.

Thus, the estimated amount of oxygen contamination of a standard 1.5-2.0 gm sample having about eight cm^2 of exposed area is less than 0.5 μgm during normal crucible loading. Normally, the time of exposure to the liquid nitrogen trapped atmosphere at (1-3)x10-7 Torr is less than 30 minutes.

System Auxiliaries:

Manipulators: The need for being able to prepare and manipulate samples in the environmental test system was very well met by the use of the RYE manipulators, model MLHT*. These units are made of stainless steel and have parallel movement jaws. The manipulator is fitted with a teflon chevron sealed ball joint which

*Obtained from the RYE Manufacturing Co., El Cerritto, Calif., but now available through the Vacuum/Atmospheres Corp., 7356 Greenbush Avenue, North Hollywood, California.

allows a 90° cone of action, a double O-ring sealed sliding shaft 30 inches long which allows the operator to reach the far side of the vacuum chamber, and a pistol-type grip whose trigger actuates the jaws through a double O-ring sealed sliding push rod. The basic unit is shown in Figure 31.

Each of the manipulators was given a vacuum performance test prior to acceptance. Eleven of the first twelve units were acceptable in that they would hold a vacuum level of $1\text{-}2\times10^{-7}$ torr when they were at rest, and could be operated, i.e., moved in and out, rotated in the ball joint, and the jaws opened and closed, without causing the vacuum level to exceed 2×10^{-6} torr during the operation. The twelfth manipulator was replaced with one which also met the performance requirements. As one would expect, the degradation of the vacuum was a strong function of the rapidity of the movement, but a careful operator can perform useful operations with the vacuum remaining on the 10^{-7} torr scale. Vacuum recovery to the low 10^{-7} torr level is observed within 30 seconds after the manipulators are placed at rest.

Three problems were encountered in the use of these manipulators. The first was that when the shaft is moved into the vacuum system after having been exposed to air, it would apparently physically carry adsorbed air and moisture on its surface. Then, under the influence of the high vacuum, the air and moisture would desorb from the shaft and at least momentarily contaminate the vacuum atmosphere. This phenomenon cannot be prevented, but its effect is neutralized by the use of the plastic sleeve cover shown installed on a manipulator in Figure 32. In operation the sleeve is filled with dry argon gas so that argon is the only gas that can be transported into the vacuum system on the moving shaft.

The second problem was associated with the seals on the ball joint and on the shaft. During the course of operations, it was found that the manipulators develop leaks in the ball joints, and sometimes in the sliding shaft-seal as well. The problem with the ball joint appears to be that the original teflon chevron-type seal did not have any provision for adjusting the seal pressure. In order to allow the use of the clamping ring to adjust the sealing pressure, the teflon chevron seal is separated into a 'front' half and a 'back' half as shown in the sketch in Figure 33. Then, a spacer is inserted under the clamping ring so that the tightening of the ring now applies a sealing force directly to the teflon lips. A marked reduction of the leak rate caused by the movement of the ball is achieved with the modified manipulators. However, one must be very careful not to use the teflon seal as a fulcrum, because the seal will deform (elastically) and a large leak will be developed momentarily.

In the manipulators which get the most use, the shaft-seal was modified so that more pressure can be applied to the double O-ring seal. In the original design a force of approximately 3 pounds is applied by a spring to deform the O-ring to form the seal, but the springs were too weak and did not continue to maintain a tight seal for an extended period. The springs have been replaced in some of the manipulators by a sleeve which compresses the O-rings directly. Clamping pressure is developed by using screws which can be tightened as required to effect the desired seal pressure. These changes are shown in Figure 33.

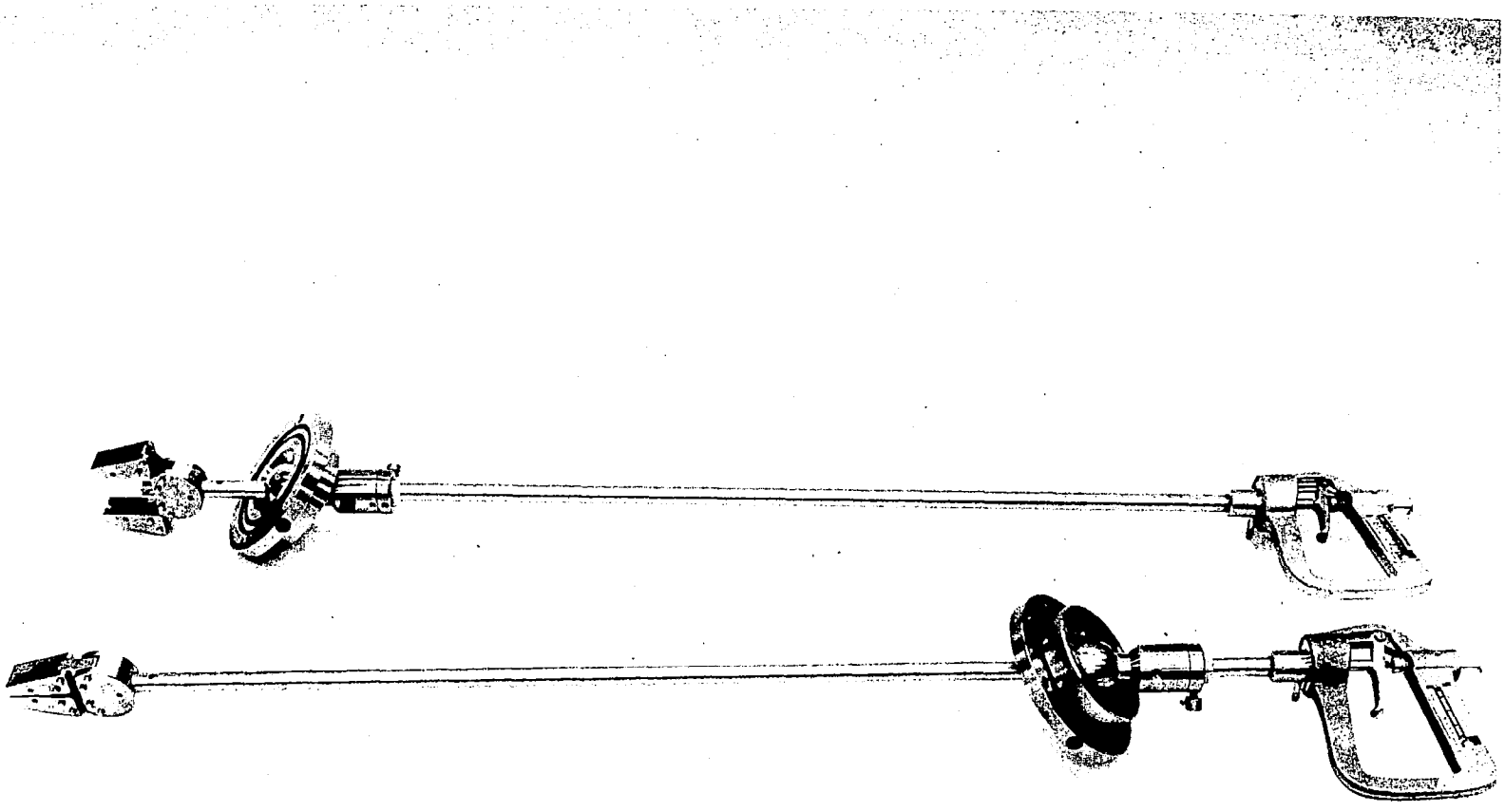

Figure 31. Vacuum Manipulators.

Figure 32. Manipulator with Plastic Bag.

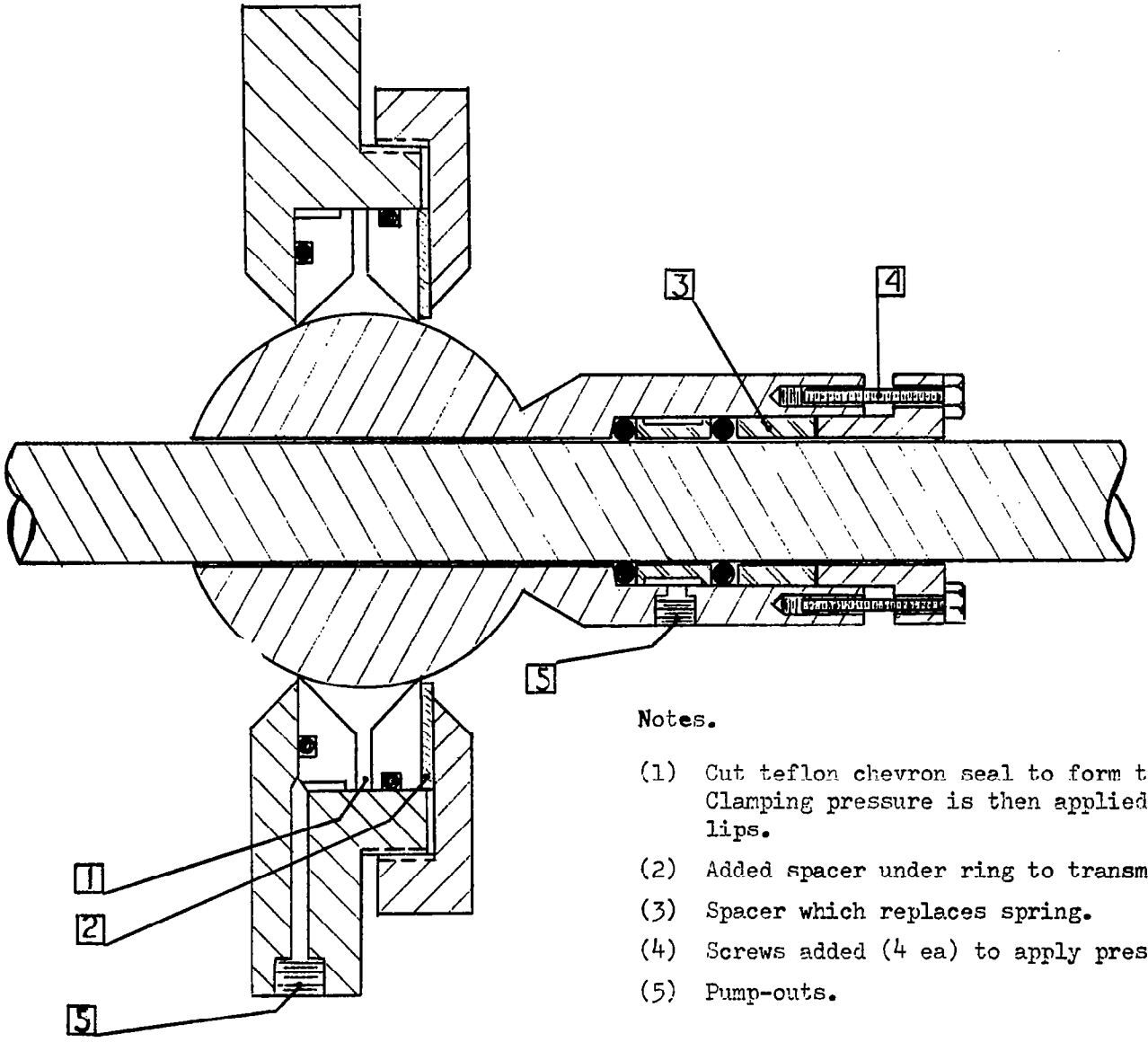

Notes.

(1) Cut teflon chevron seal to form two separate parts. Clamping pressure is then applied directly to teflon lips.

(2) Added spacer under ring to transmit clamping pressure.

(3) Spacer which replaces spring.

(4) Screws added (4 ea) to apply pressure to O-rings.

(5) Pump-outs.

Figure 33. Manipulator Modifications.

A third operating problem was found in that the manipulator jaw mechanisms began to show signs of wear. These mechanisms operate very satisfactorily when they are properly adjusted and are clean. The problem is that the jaw action becomes hard to control after they have been in heavy service for a few days. The jaw operates through a cam action, and the cam and cam follower were originally made of type 304 stainless steel. During the gripping action, there is a substantial force at the cam surface and the parts tend to wear and to gall. Therefore, it is necessary to remove each manipulator periodically and resurface the cam parts.

Electron Beam Welder:

It was required that the sealing of the test capsule be performed under high vacuum. The electron beam welding technique was therefore the method of choice, and a suitable 30 KV, 6 KW unit was commercially available*. The electron beam gun is mounted on a flange on Chamber #2 and the beam is directed upward at an inclination of 30° to the horizontal as is shown in Figure 34. The welding station consists of the power supply console, the electron beam gun, and a welding view port as shown in Figure 34. The capsule and cap are held in a quench block in a chuck as shown in Figure 35. The beam enters through the port immediately to the left of the cap. The chuck is driven by an externally-mounted, reversible, variable speed motor through a rotary seal**. The manufacturer guarantees the performance of the seal to 10^{-6} torr, but it was expected that when the oil originally supplied with the seal was replaced with a high vacuum oil***, the seal would operate satisfactorily at lower pressure. It was found that the modified seals are capable of retaining pressures in the high 10^{-8} torr range while they are at rest, and allow the pressure to rise to about $2\text{-}3 \times 10^{-7}$ torr during rotation at the normal welding speed.

The nature of the welds achieved by this unit is shown in Figure 36. In making the welds it is necessary to preheat the capsule by directing the beam to strike it just below the edge of the cap until it gets to, say, 1600°C. Then the beam is raised to strike the bevelled region of the cap. The weld is complete when the molybdenum puddle moves around the cap during 1-1/2 to 2 revolutions of the chuck. This technique produces a uniform, 1/8" wide weld with good penetration and strength. If the capsule is not preheated, however, the puddled molybdenum of the cap tends to ball up and does not produce a smooth weld area. Furthermore, such welds frequently leak.

---

*Manufactured by the Brad Thompson Industries, 83-810 Tamarisk St., Indio, California; Model 1615.10.

**Manufactured by the Consolidated Vacuum Corporation, 1775 Mt. Read Blvd., Rochester, New York; Type SR-75.

***Dow Corning 705.

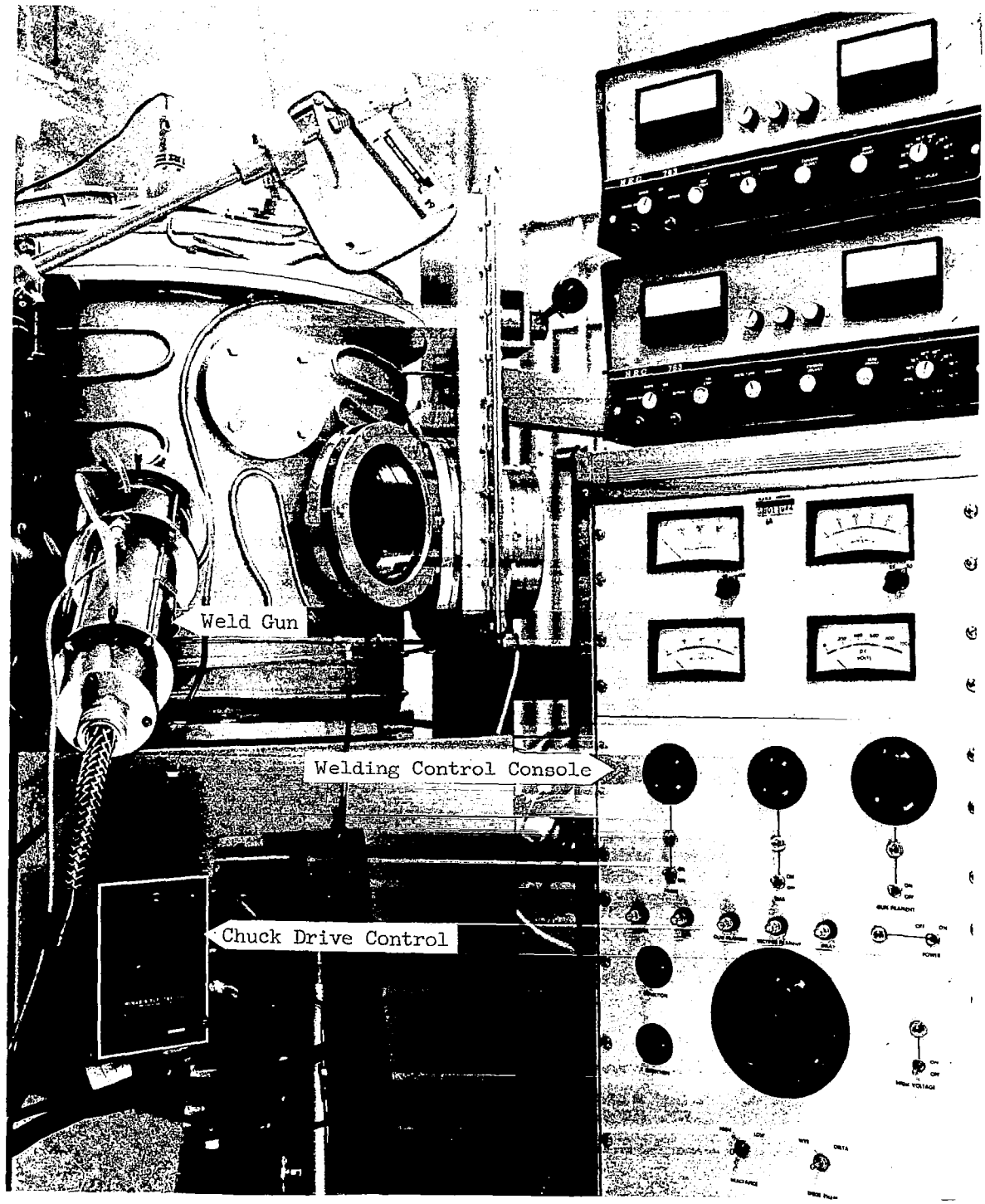

Figure 34. Welding Station.

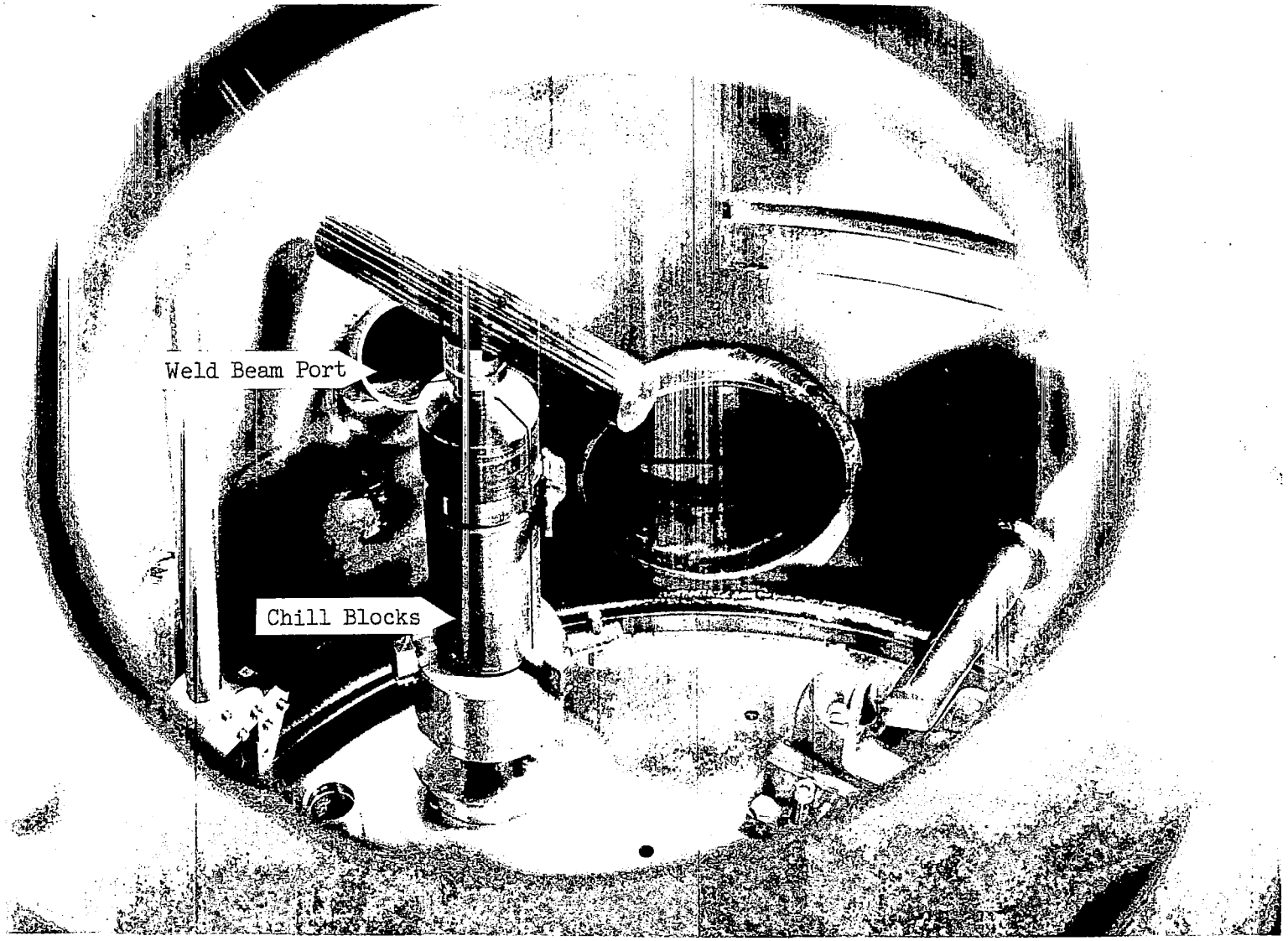

Figure 35. Capsule Welding Set-up.

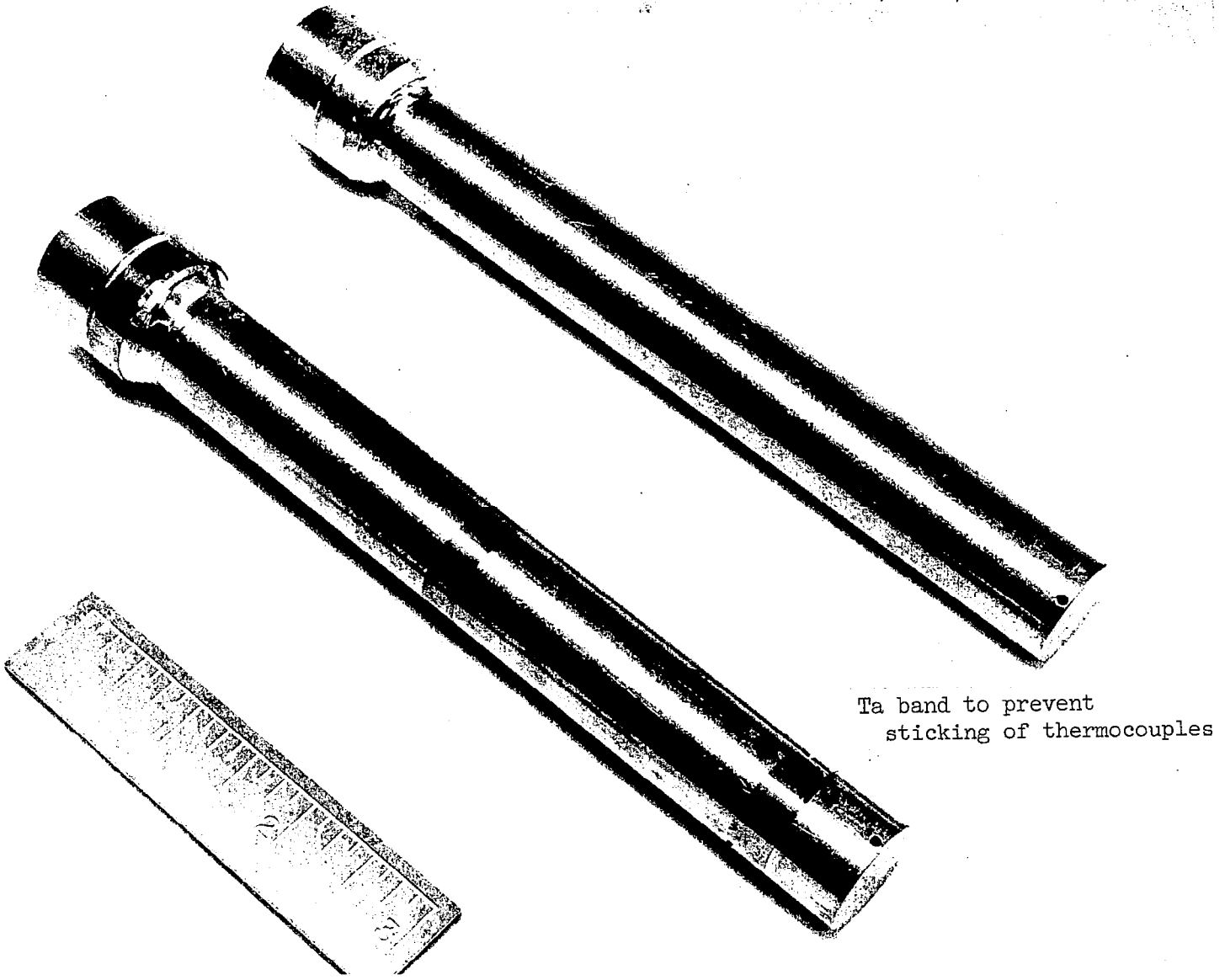

Figure 36. Loaded Capsules, Showing Closure Weld.

Argon Desorption Heater:

The argon desorption heater is used in Chamber #1 to desorb argon from the surfaces of the test capsule parts and the single crystal crucibles prior to their use in the experiments. The parts have argon adsorbed on their surfaces rather than air as a result of the "hard" outgassing and clean-up treatment which precedes their introduction into the environmental test system. The clean-up operation consists of heating to, say, 1800-2100°C in a vacuum of 10^{-6} torr to remove oxygen as volatile sub-oxides from the refractory metals. This heating is begun when the vacuum level has reached about 3×10^{-6} torr, and continued until it drops to 1×10^{-6} torr. This usually takes three to four hours. (It should be noted that if the system were to be re-vamped, this operation would be carried out in Chamber #1.) At the close of the clean-up heating, the samples and parts are cooled in vacuum and flooded with purified argon. The parts are then transferred into and stored in a vacuum dessicator so that the time during which air can displace the adsorbed argon is minimized. Prior to using the outgassed parts, the layer of adsorbed argon is "removed" by heating to about 350°C in the desorption heater in the vacuum of Chamber #1. (See Figure 23.) The service of this heater is therefore not severe and a long service life is expected. The design concept is shown in Figure 37. The heater is mounted on a base plate with legs which slip into brackets affixed to the floor plate. Polished stainless steel radiation shields are attached to the heater shell with bolt-and-metal-washer supports. The heater is supported from the top ring and is held in place by screws along the top rim of the shell. The heating element is made in two sections which are supported by the power leads as shown. A 1/4-inch tube is supported in the base plate on the axis of the furnace and extends to the top of the furnace. The nominal furnace temperature is read on a chromel-alumel thermocouple inserted half way up the tube. The tube is also used as a guide along which the mounting rod assembly (with the parts to be outgassed) is slipped to prevent accidental contact with the heating elements.

Figure 38 shows the partially assembled heater parts, and Figure 39 shows the assembled unit.

Test Furnace:

The test capsule furnace is used to carry out the sample exposures. The design concept is shown in Figure 40. This furnace has a clam-shell design and is mounted on a base plate which is supported just above the test capsule quench assembly. The furnace sections consist of a heavy base-plate and half-shell as the structural supports. Radiation shields are supported by these parts as shown and are permanently fixed in place. The two heating elements are identical and are supported by their electrical leads through the heavy top plate.

The movable half of the furnace is mounted on a cam-type hinge which can hold the furnace in either the open or the closed position. The fixed half of the furnace is permanently attached to its support and is fitted with the thermocouple assemblies and the test capsule inverting mechanism. The thermocouple assemblies are designed so that the thermocouples themselves can be adjusted

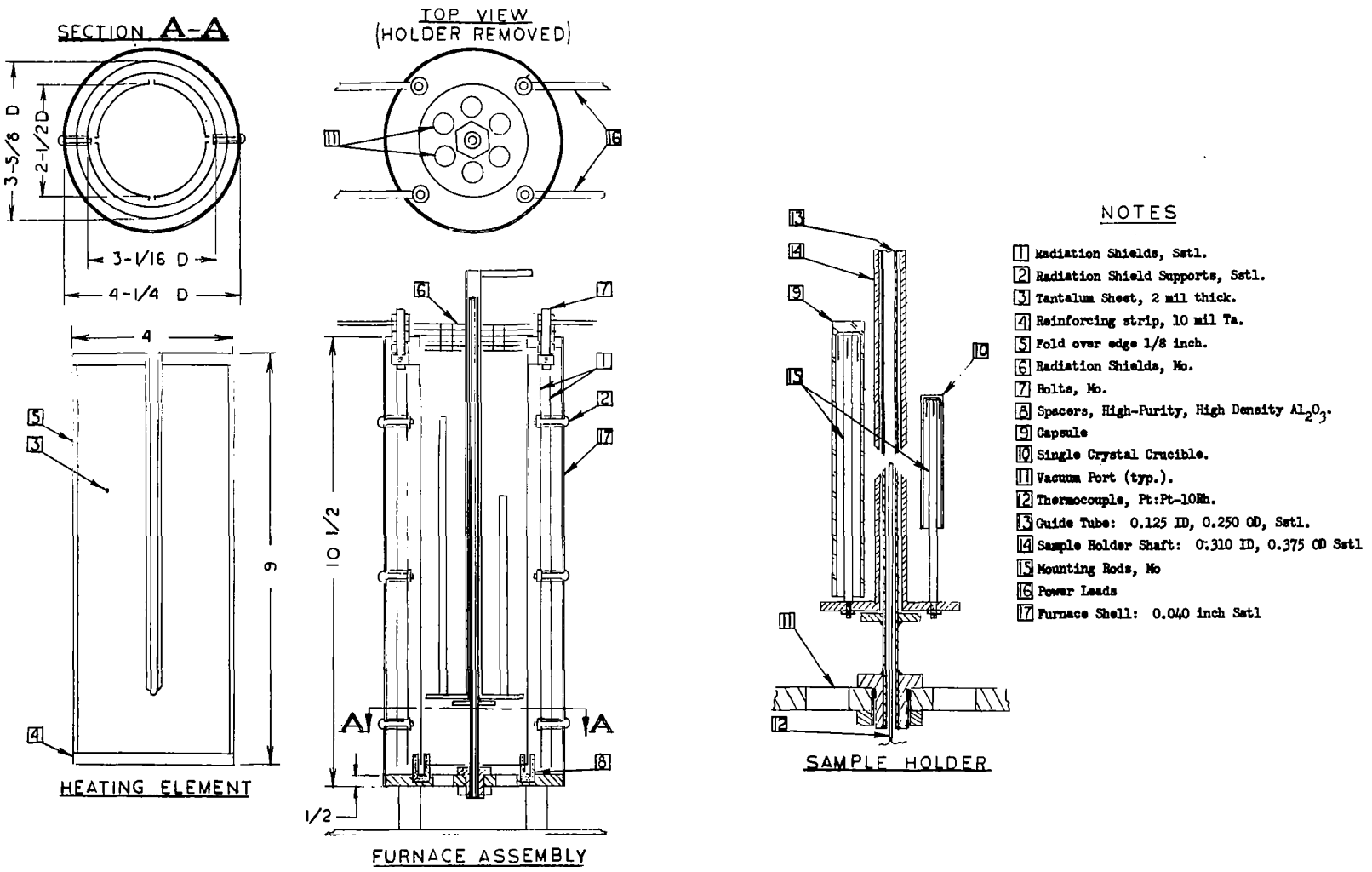

Figure 37. Argon Desorption Heater Assembly.

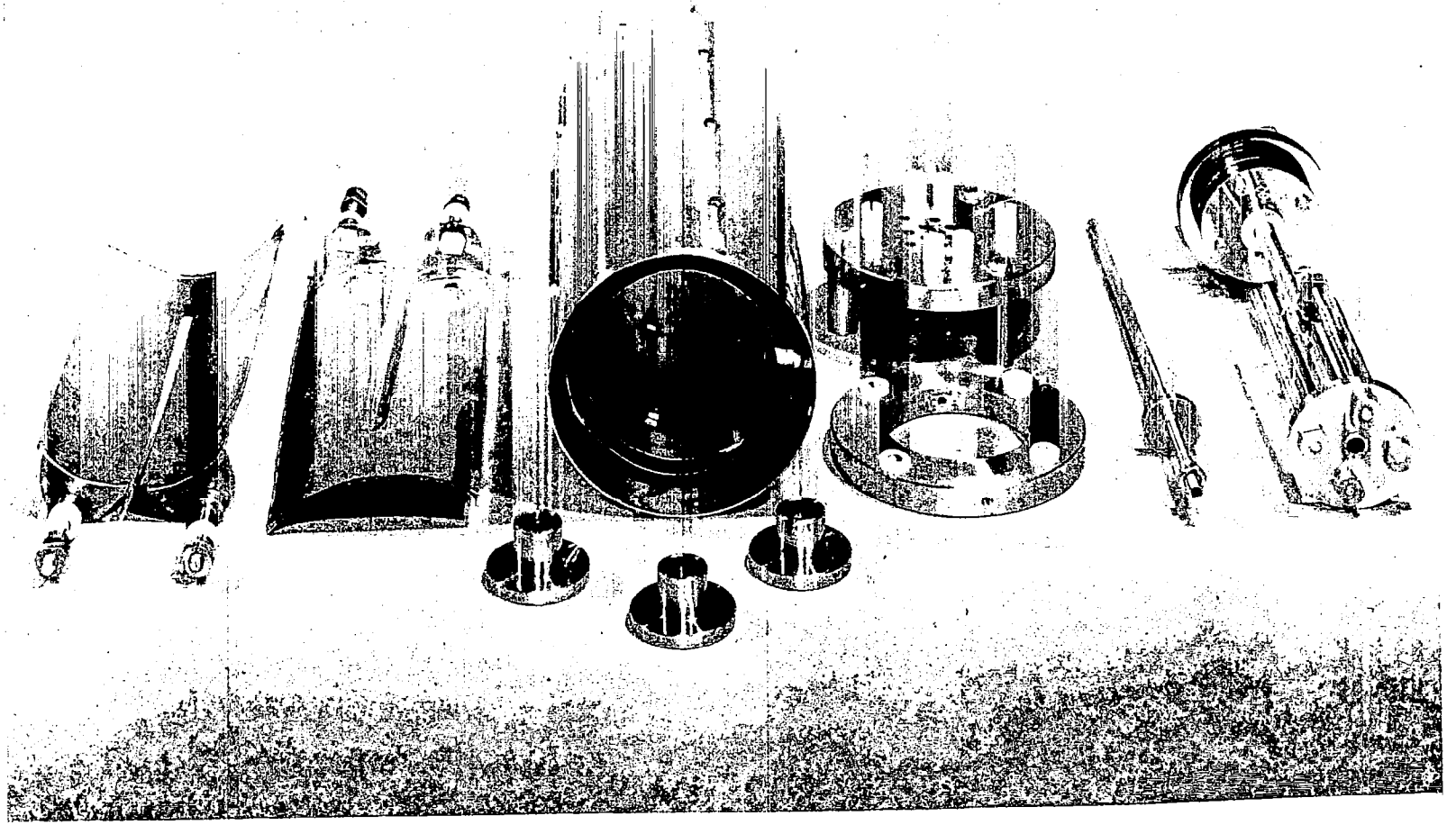

Figure 38. Argon Desorption Heater Parts.

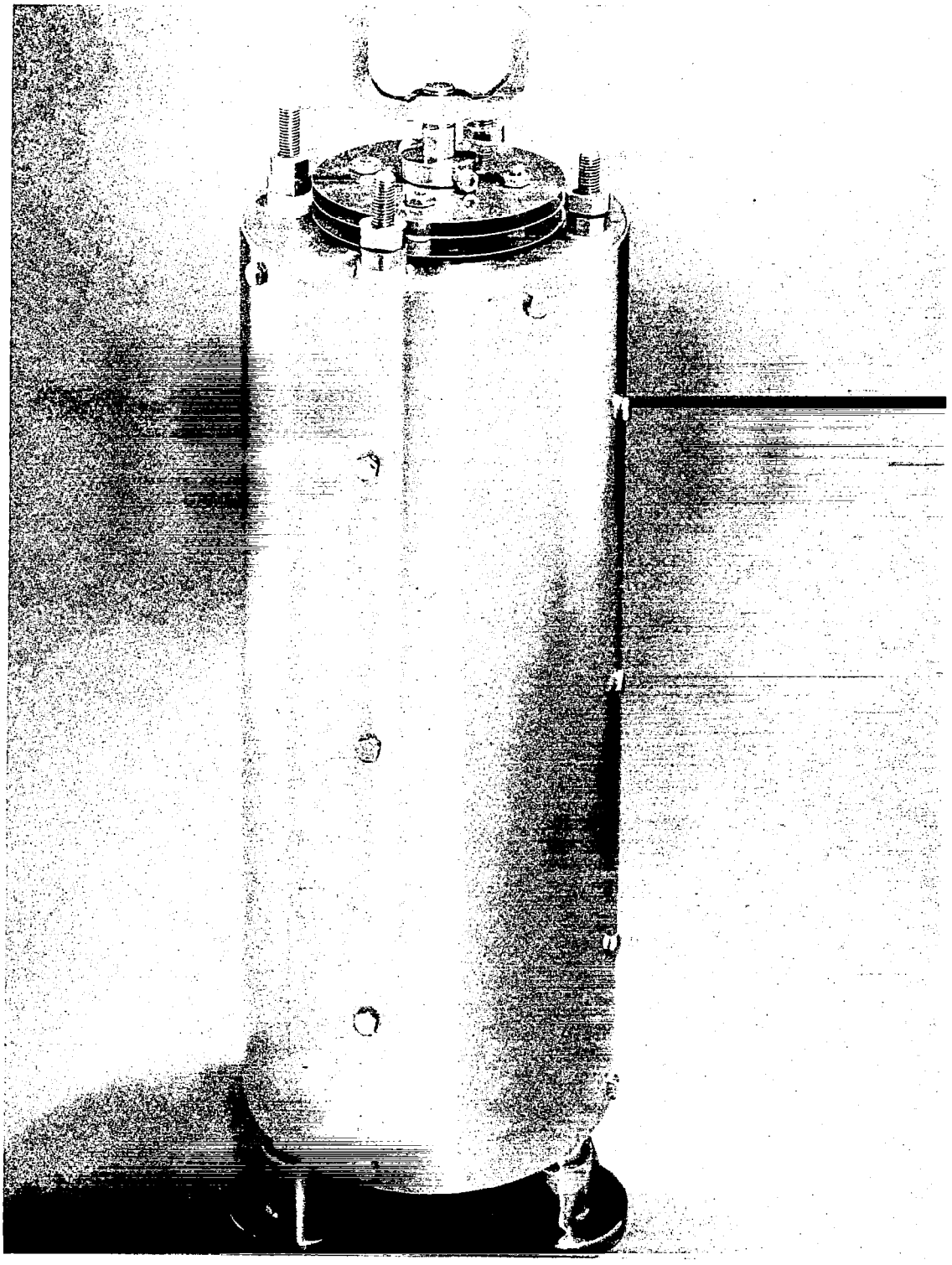

Figure 39. Argon Desorption Heater.

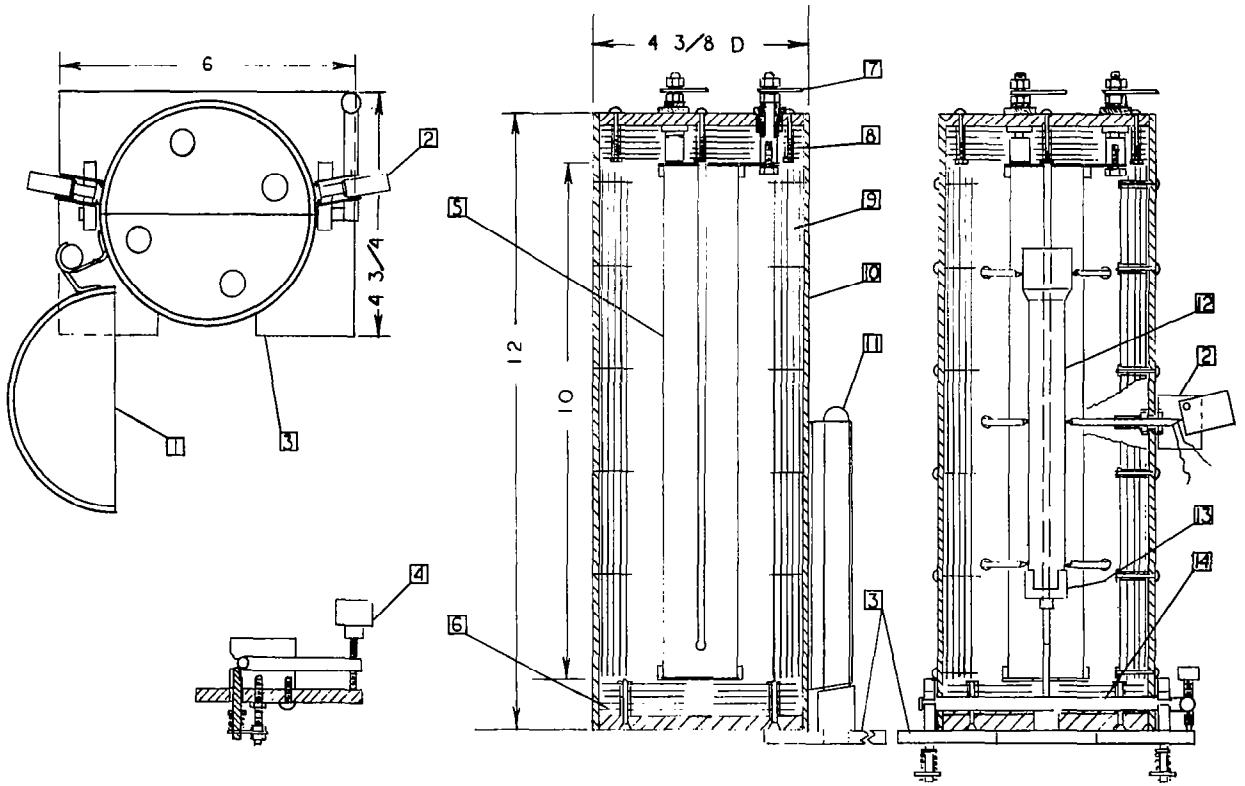

Figure 40. Solubility Test Furnace Assembly.

using the manipulators. Normally, one of the center thermocouples is used for temperature control, and the others are monitored on a multipoint recorder.

The test capsule inverting mechanism consists of a TZM shaft to which an arm ending in a cup is affixed. The cup has a hole drilled through it to accept a pin which also passes through the hole in the end of the test capsule. The outer end of the shaft has another arm whose end is fitted with a screw. This screw acts as the test capsule positioning adjustment and is adjusted so that the capsule is stable just off-center in the furnace, but does not touch the furnace heating element. The inverting lever is held in place by spring-loaded pins which apply continuous pressure against the shaft to keep it firmly seated in its bearing block. If necessary, however, the shaft can be removed by springing each end out of the block. The assembled furnace is shown in place with the original chill block in Figure 41.

Each furnace is powered by a separate step-down transformer, delivering a maximum of about 40 volts at 100 amperes. Temperature control is effected by a Minneapolis-Honeywell control complex which uses a thermocouple-activated precision set-point unit. The emf from the control thermocouple is opposed by the emf from an internal Zener diode regulated supply which is adjusted to the desired set point. The difference signal is amplified and used to operate a controller unit which has a variable current output. This variable output is in turn used to control a silicon-controlled rectifier unit which then regulates the duty cycle of the furnace power transformer.

During the testing program it became obvious that the chill block provided by the first design did not quench the test capsule effectively at the end of the experiment. The first unit was a clam-shell block with one movable half which was closed over the capsule to effect the quenching. Because of the variation in the way in which the various capsules seated themselves in the block, there was a variation in the quenching rate. Furthermore, the blocks were not cooled so that their temperatures rose slowly during the test periods. Because these factors produced wide variations in the efficacy of the quenching operation, a means of obtaining a more uniform and more rapid quenching operation was sought.

The result is the cooling device shown in Figure 42. This rather simple device consists of a 1/4-inch copper tubing cooling water loop to which a loop of braided copper strap is hard-soldered. The capsule cap seats into the strap loop and the copper provides a good heat conduction path to the cooling water line. Typical cooling curves of each of the quench devices are shown in Figure 43. The improved performance of the water-cooled device is shown very clearly in that the entire capsule is cooled from 1000°C to the melting point of potassium (62°C) in less than 20 minutes.

Timer:

The timing device used for this program is electrically driven and is capable of recording times to 0.2 sec*. It is started when the test capsule reaches the test temperature. Just prior to inverting the capsule at the conclusion of the test, a switch (located at the test chamber) is opened to stop the clock.

*Manufactured by the Standard Electric Time Co., 89 Logan St., Springfield, Mass.

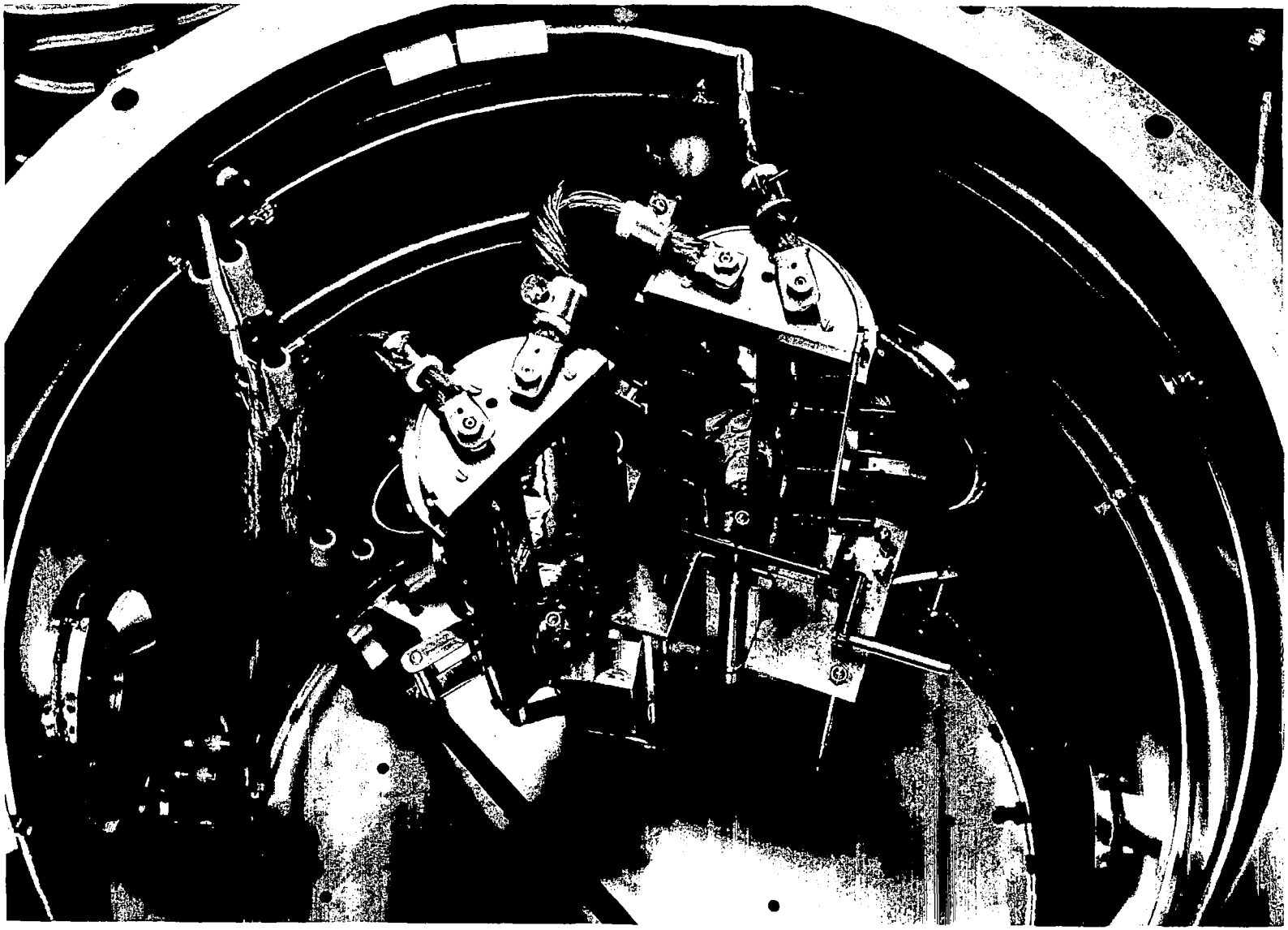

Figure 41. Solubility Test Furnace and Chill Blocks.

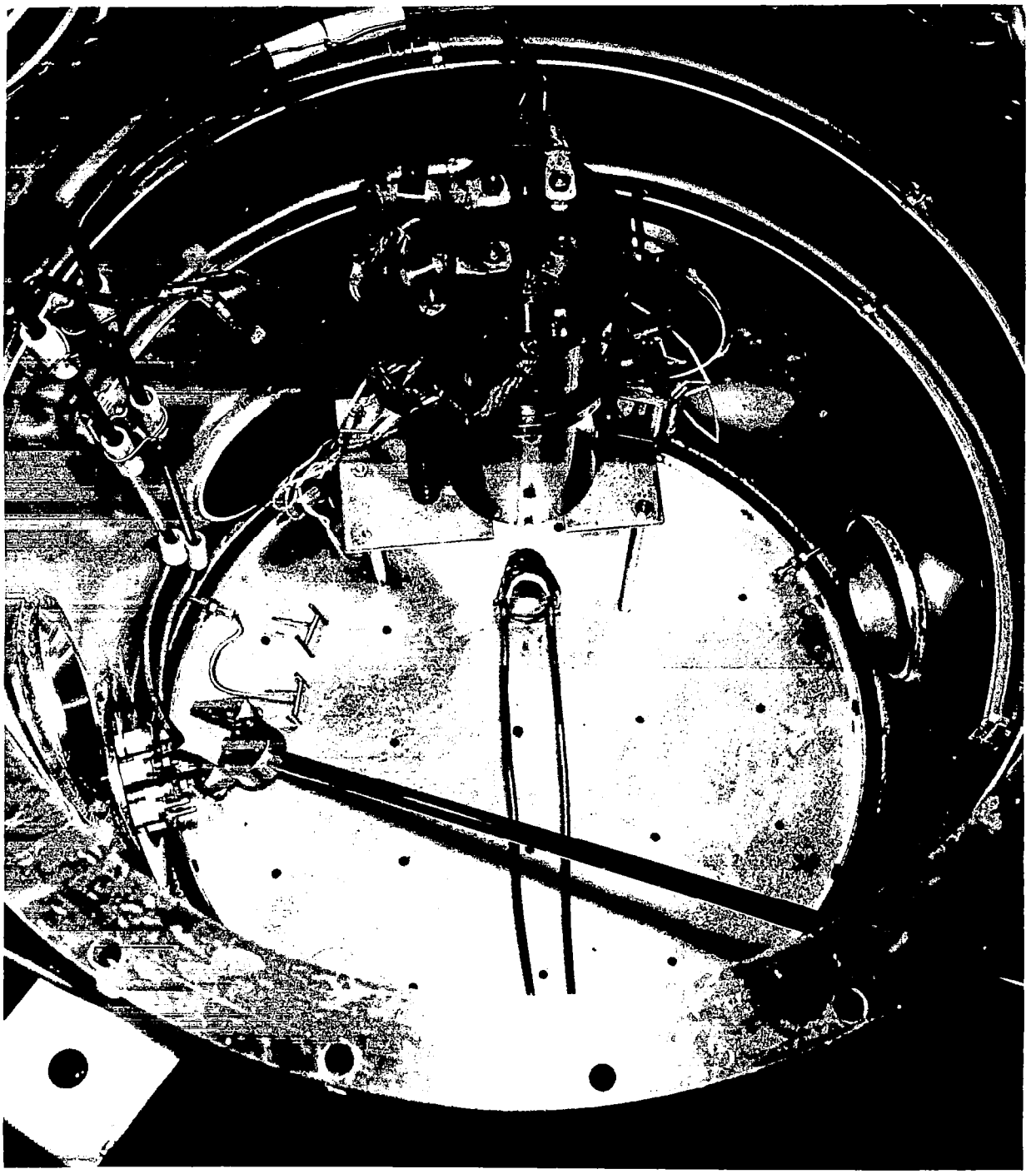

Figure 42. Furnace and Water-Cooled Quench Device.

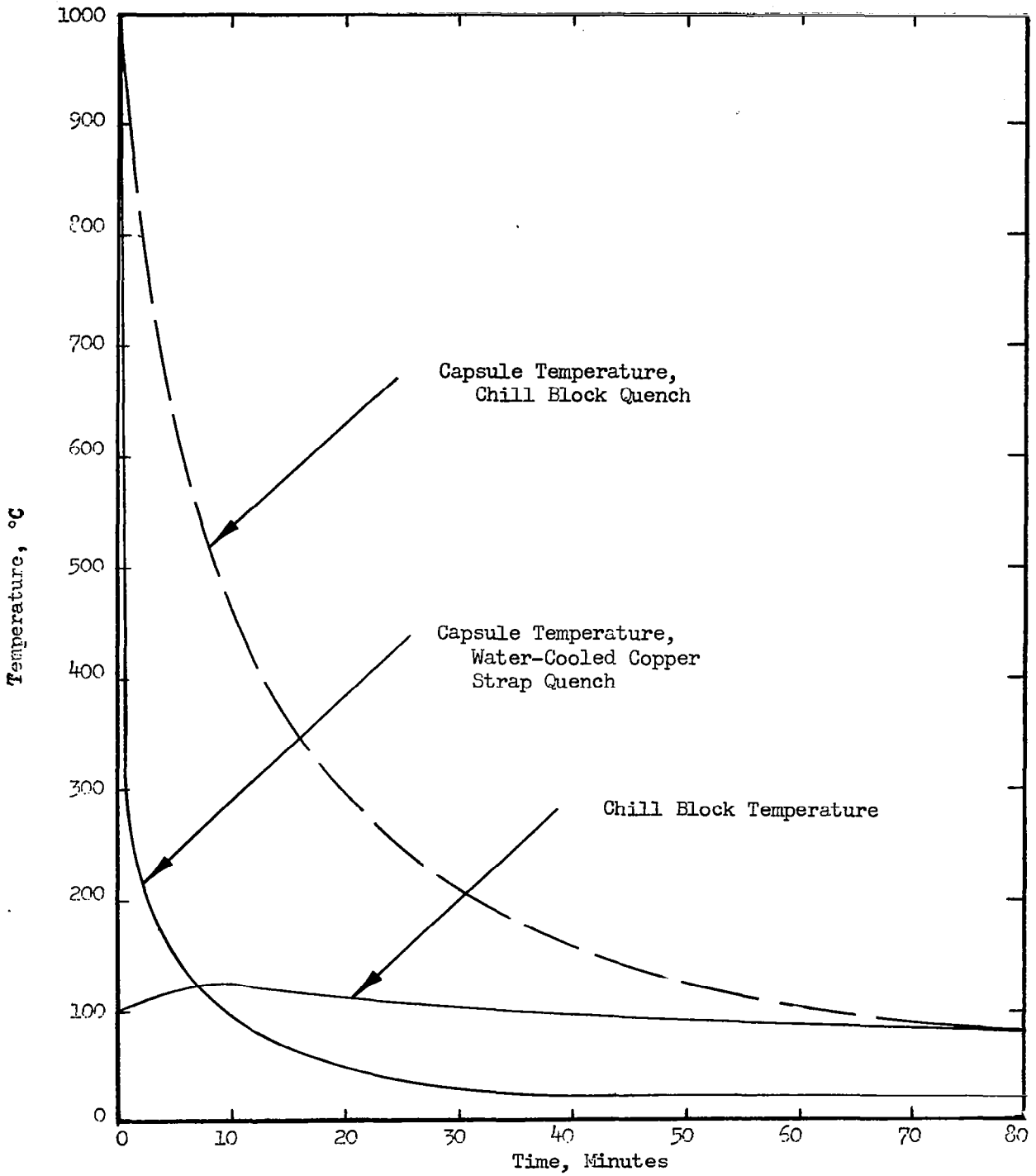

Figure 43. Quench Curves for Chill Block and Water-Cooled Quench Device.

MATERIAL PROCUREMENT

The procurement of solute materials suitable for this program involved a survey of suppliers offering single crystals one-half inch in diameter. About forty companies were contacted, and five of these appeared to be potential sources. These were: Linde, Materials Research Corporation, Metals Research, Ltd., Semi-Elements, and Westinghouse. Of the materials of particular interest, single crystal niobium and molybdenum were available in 0.45-0.50 inch diameter, tantalum was available as 0.45 inch diameter single crystal, and iron was available in 0.50-inch diameter, but only in zone-refined high-purity polycrystalline rod. Table IX is a summary of the responses obtained to our inquiries.

Three triple-pass zone refined single crystals each of niobium, tantalum, and molybdenum were ordered from Metals Research, Ltd., and two single crystals each of triple-pass zone-refined tantalum and molybdenum were ordered from the Materials Research Corporation (MRC). In addition, three triple-pass zone refined polycrystalline iron rods and three triple-pass zone refined single crystals of niobium were ordered from MRC. The MRC products were all delivered on time and were quite usable, although the tantalum crystals had a marked bow, and were about 0.42 inch in diameter rather than 0.45. A telephone inquiry was made of the supplier and we were informed that the delivered tantalum crystals were typical products of present-day technology, and an exchange of crystals would not solve the problem of the bowing in the 3-inch lengths.

In order to compensate for this crystal condition, it was necessary to reduce the crucible I.D. dimension specifications for the tantalum crucibles.

The supplier's analyses of the refractory crystals are given in Table X, together with the data determined at AI to check the supplier. Since the analytical results of the elements tested at AI agreed well with the quoted results, no further analyses were deemed necessary.

The materials received from Metals Research, Ltd., did not meet specifications and could not be used on the program. The principal difficulty was that the diameters of the molybdenum and the niobium crystals were altogether too small. No tantalum crystals were received.

Techniques of producing cavities in the single crystals to form sample crucibles were investigated. At the outset of the program the Elox technique was thought to be satisfactory if the "machined" surface were electropolished prior to use. The two stage process is necessary because the Elox technique removes metal by a local melting during which only a part of the molten metal is swept away by the carrier fluid. The remainder of this heat-affected metal remains on the surface to a depth of 2-3 mils. Electropolishing should remove this material and leave an undisturbed single crystal surface. However, a new process called electrochemical machining (ECM) was reported by which one might be able to do all the "machining" using an electrochemical method. Recent developments using this technique indicated that the surface produced was superior to that directly produced by any other machining technique, in that the surface metal was the least disturbed. Furthermore, the metal

Table IX

Availability of Single Crystal Solute Metals in 1963

Supplier		Fe	Nb	Ta	Mo	W	Re	Zr	Hf	V
Materials Research Corporation (MRC)	Purity, % Diam., in. Cost, $*	99.992** 0.50 450	99.992 0.50 450	99.995 0.45 450	99.999 0.45 450	99.999 0.31 375	99.997 0.31 450	high** 0.50 225	high** 0.50 225	99.95 0.50 450
Metals Research, Ltd.	Purity, % Diam., in. Cost, $*		(99.98) 0.50 308	(99.99) 0.375 308	(99.99) 0.50 224	(99.99) 0.375 308	(99.99)**** (3.75) 2436			(99.9) 0.50 308
Semi-Elements	Purity, % Diam., in. Cost, $*	- 0.375*** 600	- 0.50 450	- 0.50 450	- 0.50 210	- 0.50 375	- 0.25*** 975	- 0.25*** 750	- 0.25*** -	- 0.50 600
Westinghouse	Purity, % Diam., in. Cost, $*		- 0.275 450	- 0.275 480	- 0.275 480	- 0.275 450	- 0.275 600			
Linde	Purity, % Diam., in. Cost, $*		(99.9+) 0.50 225	(99.9+) 0.50 291	(99.9+) 0.50 165	(99.9+) 0.50 150	****	****	****	(99.9+) 0.50 375

*Cost for a three-inch length.
**Polycrystalline material.
***One-inch length, three-inch length not available.
****Supplier will attempt a preparation if stock material is supplied.

Values in parentheses are estimated.

Table X

Analyses of Solute Material, ppm

Solute and Anal. Source	Impurity Element: Interstitials O	N	H	C	Total	Metals Fe	Mo	Nb	Ta	Si
Nb, MRC*	10	10	0	8	28	<10	20	-	20	<5
Nb, AI						11.5		-		
Ta, MRC*	2.5	2.5	0.3	6	11.3	<10	<10	<20	-	
Ta, AI						8	8.5	15	-	
Mo, MRC*	1	0.5	0.3	5	6.8	5	-			
Mo, AI						5.5	-			<10
Fe, MRC*	<8	0.1	0.1	10	18	-	1.0			1.0
Fe, AI						-				

*Analyses of single crystals supplied by Materials Research Corporation. For each material, MRC states, "this is a typical analysis obtained on similar material electron beam zone refined in an identical manner".

removal rate was reported to be a factor of ten greater than that for the Elox process. Although the process was still in the development stage, it seemed capable of providing good single crystal crucibles at a reasonable price, and with minimum probability of destroying the integrity of the internal surface. Therefore, the process was adopted for the 'machining', and the single crystal rod stock was submitted for the preparation of crucibles.*

However, it was reported that the single crystal niobium samples behaved quite differently in their processing than did polycrystalline materials, and several modifications of the technique were explored in order to prepare the niobium and molybdenum single crystal crucibles. As a result of the experimentation with the process, the first niobium crucible delivered had been handled a great deal and showed many surface scratches and dents where the electrode leads were clamped down. There was a question regarding the effect that this mechanical damage to the crystal would have on its retaining its single crystal character when it was heated. In order to remove as much of the damaged material as possible, the crystal was chemically etched rather heavily to remove the deep scratches and dents. It was then electropolished in preparation for a surface area measurement using the Double Layer Capacitance (DLC) technique, described below. However, during the area measurement, the electrode touched the inside

*This work was done by the Sifco Metachemical Division of the Steel Improvement and Forge Company, Cleveland, Ohio.

of the crucible and the resulting arc burned a hole in the crucible wall about 1/4" from the closed end. Upon examination, it was found that the electrochemically machined hole was badly off-center at the bottom, and a rather large region in the vicinity of the penetration was paper thin. In order to recover the crucible as a high purity niobium crucible (but, of course, not single crystal), the closed end was cut off and a taper machined on it to form a plug. Then, a matching taper was cut in the original top-end of the crucible. The plug was inserted and welded. The resulting product is a short, but fully usable, high purity niobium crucible which approaches in quality a true single crystal crucible.

One molybdenum crucible was very successfully prepared by the ECM technique with no complications. However, the single crystal crucibles proved to be so difficult to prepare directly by this process that the second niobium and the second molybdenum crucibles were pre-drilled with an undersize hole using the Elox technique, and were then finished using the ECM technique. Neither of the two tantalum single crystals was machined by the ECM process. These crystals were made into crucibles by the combination of mechanical machining and electropolishing.

The source potassium used in this program was the highest purity product available commercially*. Since this material was to be re-purified for use as is described below, no analyses were performed on it at AI. The analysis provided by the manufacturer is given in Table XII, with those of the purified product.

The material used for the capsule and cap in this program were made of arc melted molybdenum stock. This material was chosen because it was expected to be a relatively pure commercial material. Its nominal purity was quoted to be 99.9+%. The certified impurity levels are: O_2 <3 ppm; H_2, <1 ppm; C, 140 ppm; N_2, 9 ppm; Ni, <10 ppm; Fe, <10 ppm; and Si, <10 ppm. The machining of the capsules and caps was done using chlorethene as a lubricant because it has been found to contaminate the metal surface less than other machining lubricants.

*The potassium was obtained from the Mine Safety Appliance Research Corporation, Callery, Pa.

The method selected for the purification of potassium involves filtering at 90°C, hot gettering at 650°C with zirconium metal, and distillation. The filtering and gettering steps are straightforward, but the distillation poses a potential problem in that the heavier alkali metals are more volatile than potassium and will tend to be concentrated in the distillate. However, the fact that Cs and Rb tend to concentrate in the vapor suggests that one might reduce the amount of these impurities in the final product if a first volume of the distillate were discarded. The remaining potassium then has a lowered impurity concentration. A study of the discard volume required to effect various purification ratios was carried out for a simple pot still and for a still with a fractionating column. Both types of system have been analyzed using the method of Rayleigh, for a two-component system in which the following expression must be evaluated:

$$\int_{B_2}^{B_1} \frac{dB}{B} = \int_{x_{F_2}}^{x_{F_1}} \frac{dx_F}{x_D - x_F} = \ln \frac{B_1}{B_2}$$

In this expression, B is the smount of potassium in the still, x_F is the concentration of the more volatile constituent in the still, and x_D is the concentration of the more volatile constituent in the vapor entering the condenser. Subscript 1 refers to initial conditions and subscript 2 refers to the final conditions. The method of determining x_D differs for the two types of distillation system. For the simple pot still, $x_D = \alpha x_F$ where α is the relative volatility. For the fractionating column system, a McCabe-Thiele diagram can be used to include the effects of ν, the reflux ratio, and N, the number of theoretical plates, on the value of x_D corresponding to a given x_F. These evaluations were made and the quantity D/B_1 computed for various values of α, ν, and N with x_{F1}/x_{F2}, the purification ratio, as a parameter (D is the amount of distillate, $D = B_1 - B_2$).

Table XI shows the vapor pressures and the pertinent relative volatility values for the alkali metals. Figure 44 shows the computed D/B_1 values for the simple pot still. Note that if a purification ratio of 5 is desired for a system whose α is 4, 42% of the original material must be discarded. However, Figure 45, which shows the computed D/B_1 values for a fractionating column with N = 1 and $\nu = 3$, indicates that a purification ratio of 5 can be achieved by discarding only 18% of the original material if $\alpha = 4$. In a two-plate system, only 13% of the material must be discarded.

These results strongly suggest that if Cs and Rb must be removed from the potassium, the use of a modest fractionating column is essential. The column should first be operated under its maximum (Cs) enrichment conditions consistent with a reasonable product rate. Then, after the first fraction is discarded,

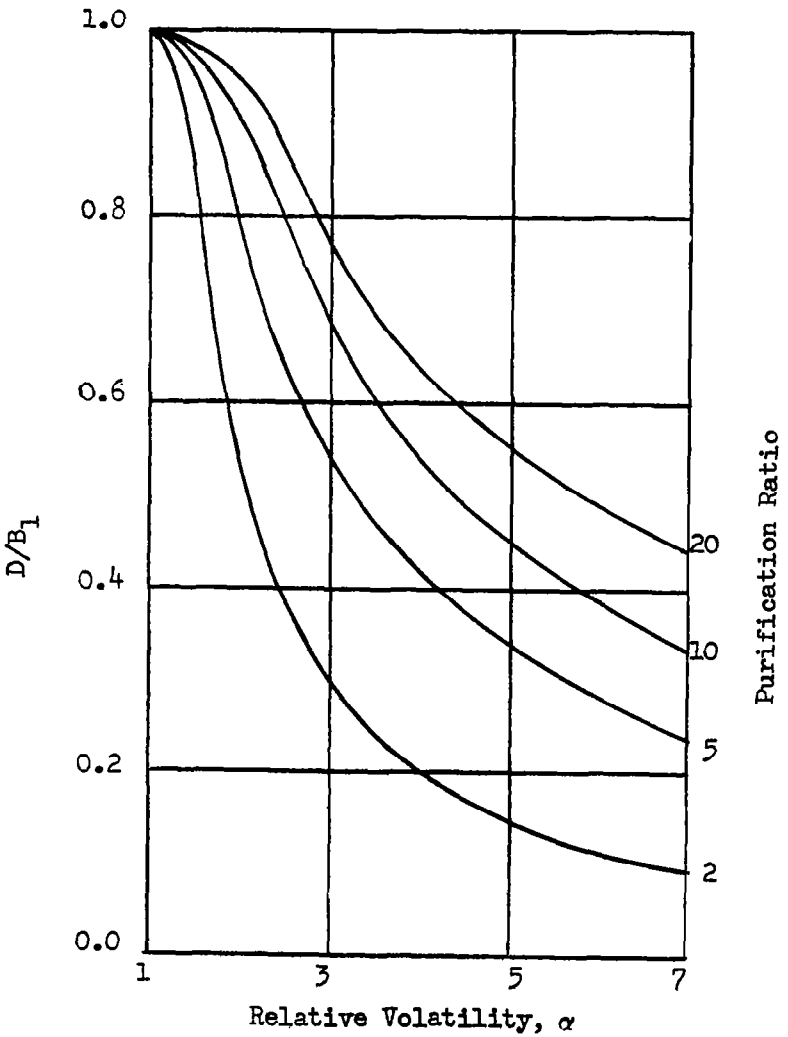

Figure 44. D/B_1 Values for the Purification of Potassium Using a Simple Pot Still.

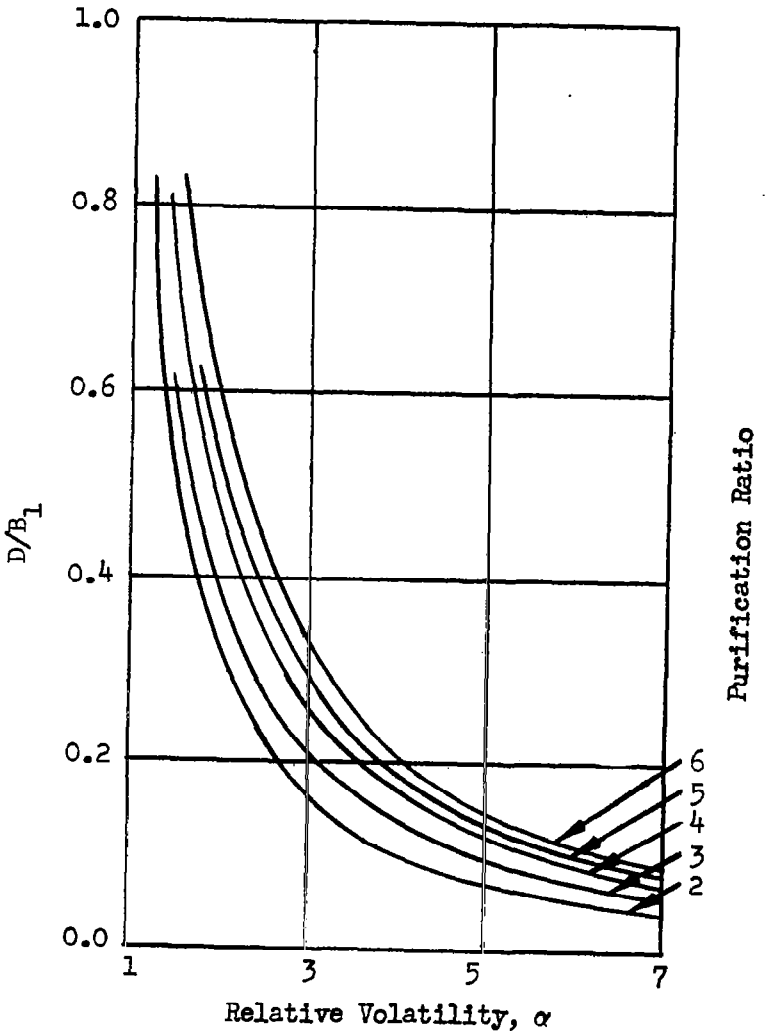

Figure 45. D/B_1 Values for the Purification of Potassium Using a Fractionating Column Having One Theoretical Plate.

Table XI

Vapor Pressure and Relative Volatility Values for Alkali Metals[76]

T °K	p^o_{Cs} atm	p^o_{Rb} atm	p^o_{K} atm	p^o_{Ka} atm
500	2.4×10^{-4}	1.3×10^{-4}	2.9×10^{-5}	7.6×10^{-7}
600	4.6×10^{-3}	2.9×10^{-3}	8.6×10^{-4}	4.8×10^{-5}
700	3.6×10^{-2}	2.5×10^{-2}	9.5×10^{-3}	9.1×10^{-4}
800	1.7×10^{-1}	1.3×10^{-1}	5.6×10^{-2}	8.1×10^{-3}
T °K	α Cs-K	α Rb-K	α Na-K	
500	8.3	4.5	0.026	
600	5.35	3.36	0.056	
700	3.8	2.64	0.096	
800	3.04	2.32	0.145	

the column should be operated with zero reflux (which in effect makes it a zero-plate column, and equivalent to a simple pot still) until about 80% of the remaining potassium is collected as purified product. The remainder of the charge will be enriched in sodium, and should be discarded.

A purification unit was designed and built to carry out the sequence indicated, i.e., filtering, hot gettering, distillation, and purified metal storage and dispensing. The assembly consists of five component parts. The first is a filter unit (working capacity 350 cc) in which the potassium is filtered through a 5 micron stainless steel frit at about 75-85°C. The second unit is a gettering pot containing zirconium foil whose function is to remove traces of oxygen from the potassium. Its operating temperature is 650 $\pm$ 50°C. The third unit is the still pot. This component is sized to provide about 40 sq cm of evaporating surface to ensure an adequate net evaporation rate when operated at a 5-10 Torr pressure level. An oversized area is required to compensate for an expected low evaporation rate coefficient.

The fourth unit is a nominal one-inch diameter fractionating column. Saddles made of tantalum sheet are used as packing, and it is expected that the 9-10 inch depth of packing is equivalent to 2-3 theoretical plates. Reflux control is effected by a partial condenser at the top of the column. The fifth unit is a combination distillate receiver and sample extruder. It collects up to 250 cc of product and delivers it into the test system as a 3/8" diameter extruded slug. Figure 46 shows the assembled unit, and Figure 47 shows a schematic representation of the purification system. Figure 48 shows details of the extruder unit.

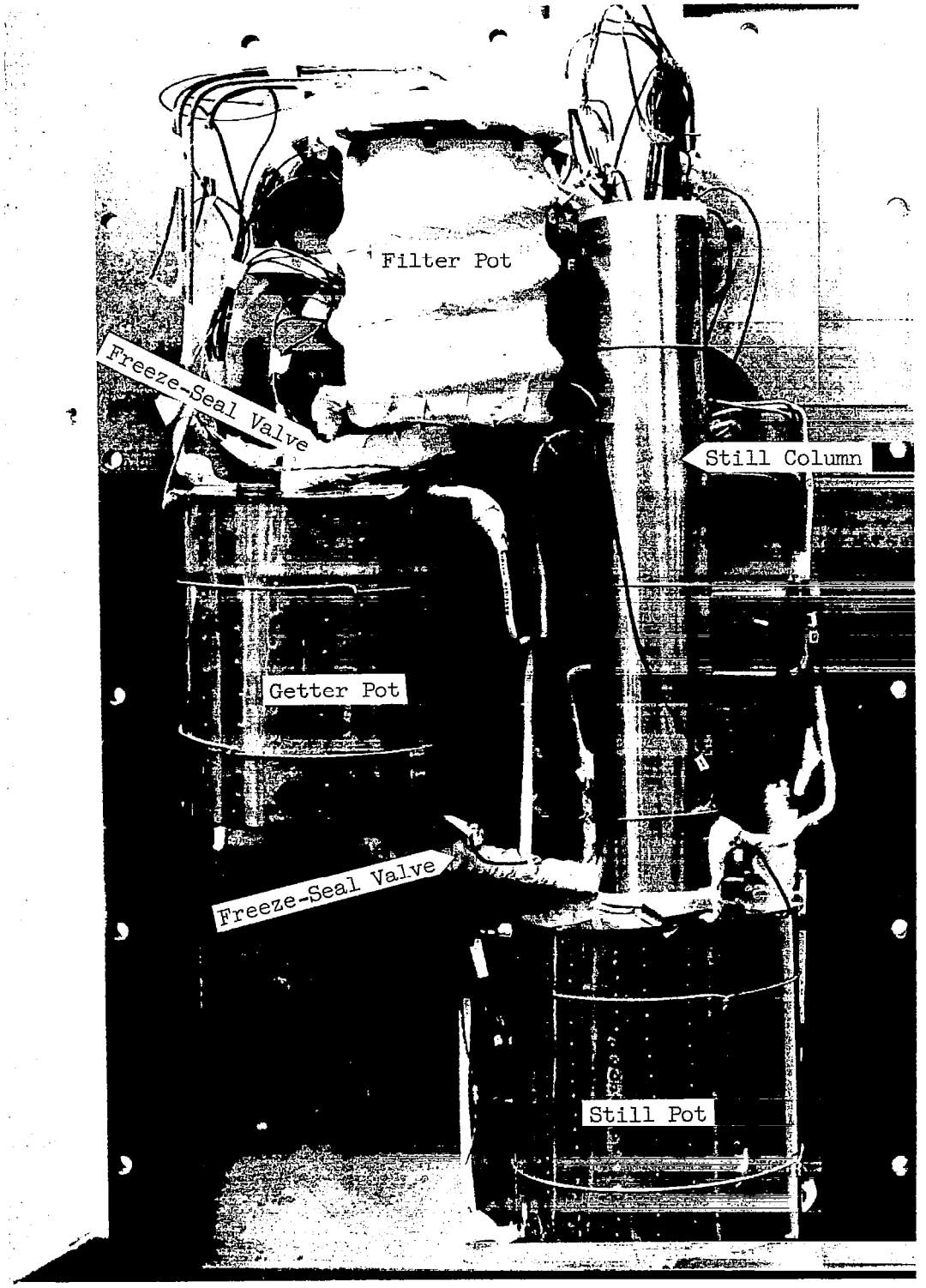

Figure 46. Potassium Purification Unit.

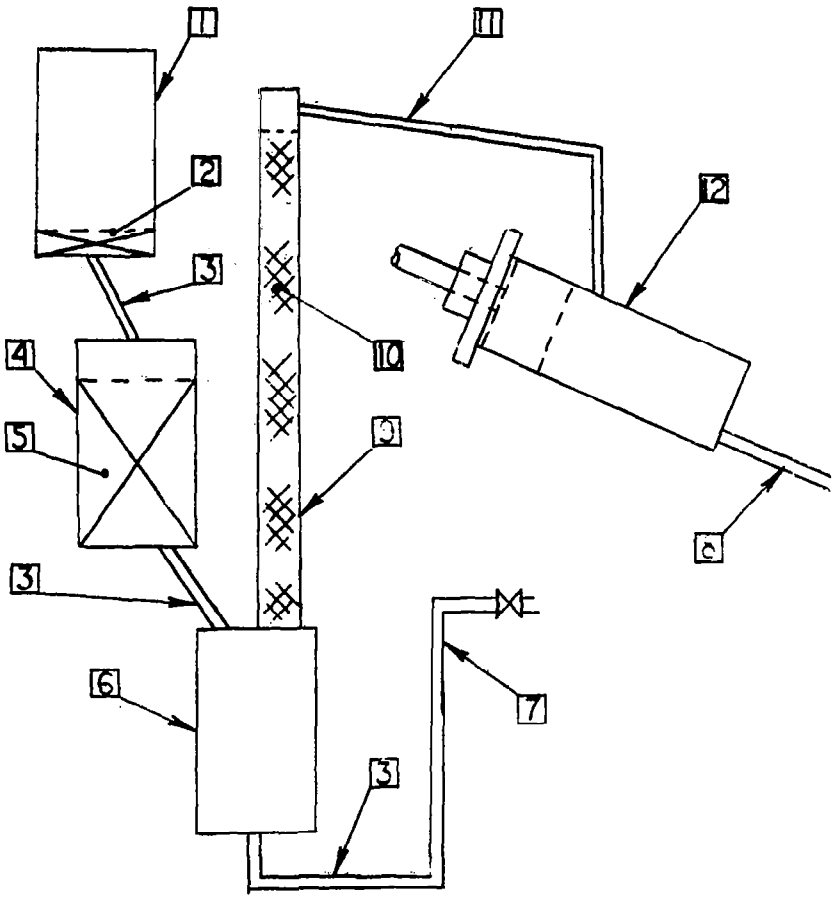

NOTES

1. Filter Pot: 3" Std. wt. #304 Sstl pipe, 5" high with O-ring cover closure.
2. Filter: 5 micron #304 Sstl frit, 1/8" thick.
3. Transfer line and Freeze seal: 1/4" Sstl tubing wrapped with 8 turns of 1/8" Cu tubing for cooling water, and 20 turns of 22 ga chromel wire as a resistance heater.
4. Getter Pot: 3" Std. wt. #304 Sstl pipe, 5½" high, all-welded construction.
5. Getter: 6' of 5 mil flat Zr strip 4" wide, plus 6' of 5 mil corrugated Zr strip 4" wide rolled in alternate layers to form a coil.
6. Still Pot: 3" Std. wt. #304 Sstl pipe, 5½" high, all-welded construction.
7. Drain Line: 1/4" #304 Sstl tubing with Sstl valve at exit.
8. Product Line: 3/8" Std. wt. #304 Sstl pipe, discharges into Chamber #1.
9. Still Column: 1" Std. wt. #304 Sstl pipe, 14½" long, with a 2-mil Ta foil liner.
10. Column Packing: Ta saddles made from 20 mil sheet stock cut into 1/4" x 1/2" rectangles.
11. Condenser: 3/8" #304 Sstl tubing with a 1-mil Ta foil liner.
12. Extruder: See Figure 48 for details.

Figure 47. Potassium Purification Unit, Schematic.

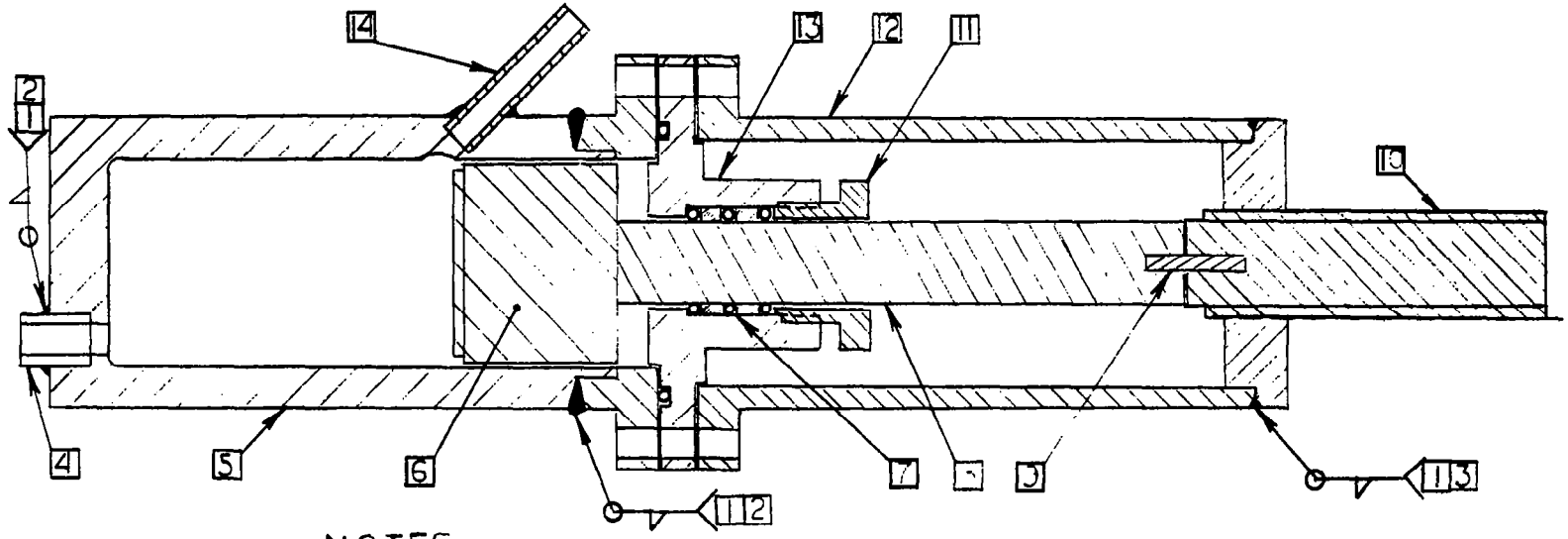

NOTES

1. Weld as per NAA-AI Spec #LA-0107-004-class #2.
2. Vacuum weld.
3. Weld before cutting threads
4. Discharge Line: to Chamber #1.
5. Extruder Barrel: type 304 Sstl., 3½" O.D., 2.500 + 0.002, -0.000 I.D., 8 microinch finish on I.D., 7½" long.
6. Piston: Ketos tool steel; hardened and ground to size, 2.496 + 0.002, -0.000 O.D., 8 microinch finish on O.D., 2" long (continuous with item 8).
7. Seal: Triple O-ring sliding seal with pump-outs.
8. Piston Shaft: Ketos tool steel, hardened and ground to size, 0.980 + 0.002, -0.000 O.D., 4 microinch finish, 7" long (continuous with item 6).
9. Alignment Pin.
10. Drive Screw: Mild steel, 1" Acme thread, 5 turns/inch, 6½" long.
11. Seal Follower: Brass.
12. Extruder Frame: Mild steel
13. Extruder Cover: type 304 Sstl
14. Potassium Inlet Tube: 1/4" Sstl tubing from condenser.

Figure 48. Potassium Extruder Assembly.

Following the assembly of the unit, several batches of potassium were used in a rinsing operation so that all of the internal surfaces of the components were brought into contact with either liquid potassium or potassium vapor. The freeze-seals which are used as on-off valves between the components perform very well, and the movement of potassium through the 1/4" O.D. lines is very easily regulated. The transfer of the metal from the supply tank to the filter pot, and on into the getter pot is readily accomplished using rather small helium pressure differentials (about 1 psi is adequate). The vapor pressure of potassium is adequate to transfer the charge from the getter pot to the still. An operating problem was uncovered in that it was difficult to determine when the proper amount of potassium had been transferred into the filter pot from the supply tank. In the original design, three thermocouples of varying length extended into the chamber. The level of the potassium was to have been detected by sensing the temperature changes occurring as the thermocouples became immersed in the rising potassium. In practice, it was easy to detect the presence of hot potassium at the lowest level, but the responses of the intermediate and upper level thermocouples were not adequate to indicate unambiguously the presence of the potassium at these levels. Since these simple thermocouples have proven to be poor liquid level indicators, they were replaced by two thermocouple wells each of which contains a small heater and a thermocouple. The thermocouple is spark-welded to the inner end of the well. When the heater is operating, and the well is not covered with potassium, the poor heat transfer characteristics of the well cause its temperature to rise 20-30°C above the temperature of the surroundings. Then, as the potassium is transferred into the filter chamber and rises to contact the end of the well, the excess heat is quickly transferred away, and the thermocouple emf drops abruptly. The modified level sensing unit now operates very well and gives the required positive response.

In the early testing of the distillation unit, it was convenient to view the inside of the reflux control condenser by looking through the drop counter window into the condenser tube using an opthalmoscope. In this fashion, condensing potassium could be observed in the reflux control condenser and it was determined that the rates were in general agreement with our expectations from the temperature-levels (vapor pressure-levels) in the distillation column. However, when the temperatures and vapor pressures were high enough to deliver distillate at the desired rate, there was enough streaming of vapor along the condenser tube to slowly cloud and cover the sight glass. Because of the concern that the glass might interact and become an oxygen source in our collected distillate, a baffle was installed to prevent line-of-sight streaming. Although the baffle does prevent the direct visual observation of droplet formation in the condenser, it was found that the drops which form are large enough to fill the diameter of the condenser so that there is a decrease in the observed pressure level reading when the drop fills the condenser tube. As soon as it flows to the end and drops off, the pressure gauge needle jumps. A usable indication of the distillation rate is therefore obtained by merely counting the drops formed per minute.

The distillation is normally carried out with the still pot temperature at $450 \pm 10°C$, and a nominally linear gradient along the packed column to $375° \pm 10°C$ at the reflux control condenser. Under these conditions, the distillation rate is about one gram per minute in this system which has an

evaporating area in the still pot of 40 sq cm. As the level of the potassium drops in the still pot, a temperature difference develops between the upper and the lower level thermocouples on the still pot itself. When only 50 gm of potassium remains in the pot, the difference is about 20°C. This, too, has been a useful operating criterion and is used in conjunction with the estimated product discharge rate to determine the end-point of the distillation.

Four batches of purified potassium have been prepared. There has been a continual decrease from batch-to-batch in the oxygen content of the product, and the most recent batch in particular is considered to be a very high quality material. Table XII shows the analyses of the four product batches of purified potassium, together with the analysis provided by the supplier of the starting material.

The data of Table XII indicate that the purification process is very effective and that the impurity levels of Al, Ca, Cr, Cu, Fe, Mg, Mn, Na, Ni, Si, and O have been markedly reduced. The maximum total value of the impurity levels of the 26 elements for which analyses are available for the AI product is 105 ppm as compared with a total of 250 ppm for the feed stock. It is therefore concluded that this purification process has produced a potassium product of exceptionally high purity.

The potassium is collected in the extruder body, is frozen, and is then dispensed as required into Chamber #1. The extrusion of the potassium is readily accomplished using 75 foot-pounds of torque on the driving screw when the metal is at 25°C, or using 40 foot-pounds of torque with the potassium at 55°C. The extruded metal is not a cyclinder as was desired, but tends to curl quite markedly. Further, the surface of the extruded potassium is very sticky, and it adheres quite tightly to any solid surface so that transferring a solid sample into a vessel is almost impossible. Because of this, the original method of using a blade to cut the extruded potassium was abandoned because the metal could not be separated from the blade. The technique which has proved very successful in separating the samples is a hot wire "cheese-cutter". The unit is shown in use in Figures 49 and 50. In Figure 49 the cutter is shown separating a potassium sample from the end of the extruder. In this phase of the operation the wire is cold. In Figure 50, the potassium sample is in place over the mouth of a sample transfer vessel. When the sample is properly placed, the tungsten wire is heated and the potassium drops off. Figures 49 and 50 also show the method of loading a sample crucible. The funnel rests on a heating coil, so that potassium contacting the funnel melts quickly and flows into the crucible which is placed in the heating block shown under the funnel. Since the crucible is also pre-heated, the potassium flows to the bottom of the crucible and is then frozen in that position.

Table XII

Analyses of Potassium Starting Material and Purified Product

Impurity Element	Starting Material** wppm	Batch #1* 8-24-64 wppm	Batch #2* wppm	Batch #3* wppm	Batch #4* wppm
Oxygen	48	40-70	16.2	14	3.5
Nitrogen					4
Carbon			<5 D		10 ± 3
Ag	<1 ND	<1 ND	<1 D	<1 ND	<1 ND
Al	6	<1 ND	<1 D	1 D	<1 ND
B	<10 ND	<10 ND	***	<10 ND	<10 ND
Ba	<1 ND	<10 ND	<10 ND	<10 ND	<10 ND
Be	<1 ND	<1 ND	<1 ND	<1 ND	<1 ND
Bi		<5 ND	<5 ND	<5 ND	<5 ND
Ca	10	<5 D	<5 D	<5 D	<5 ND
Cd		<1 ND	<1 ND	<1 ND	<1 ND
Co	<5 ND	<5 ND	<5 ND	<5 ND	<5 ND
Cr	<5 ND	<1 D	<1 ND	<1 ND	<1 ND
Cs	<20 ND				<20 ND
Cu	9	<1 D	<1 ND	<1 ND	5
Fe	35	<1 ND	<1 ND	<1 ND	***
Li	0.1	<1 ND	<1 ND	<1 ND	<1 ND
Mg	4	<1 D	<1 D	3 D	<1 D
Mn	5	<1 ND	<1 ND	<1 ND	<1 ND
Mo	<3	<1 ND	<1 ND	<1 ND	<1 ND
Na	30	2 D	10 D	5 D	1 D
Ni	12	<5 ND	<5 ND	<5 ND	<5 ND
Pb	<5 ND	<1 ND	<1 ND	<1 ND	<1 ND
Rb	3				
Si	<25 ND	<5 ND	***	***	5 D
Sn	<5 ND	<5 ND	<5 ND	<5 ND	<5 ND
Sr	<1 ND				
Ti	<5 ND	<10 ND	<10 ND	<10 ND	<10 ND
V	<1 ND	<1 ND	<1 ND	<1 ND	<1 ND
Ta				<2 ND	
Zr	<10	<10 ND	<10 ND	<10 ND	<10 ND

*Spectroscopic analyses, except for O (mercury amalgamation), C (wet oxidation), tantalum (colorimetry), and nitrogen (Kjeldahl).

**Analyses supplied by the supplier, Mine Safety Appliance Research Corp.

***Contaminated in handling.

ND - Not detected.

D - Detected at the indicated level.

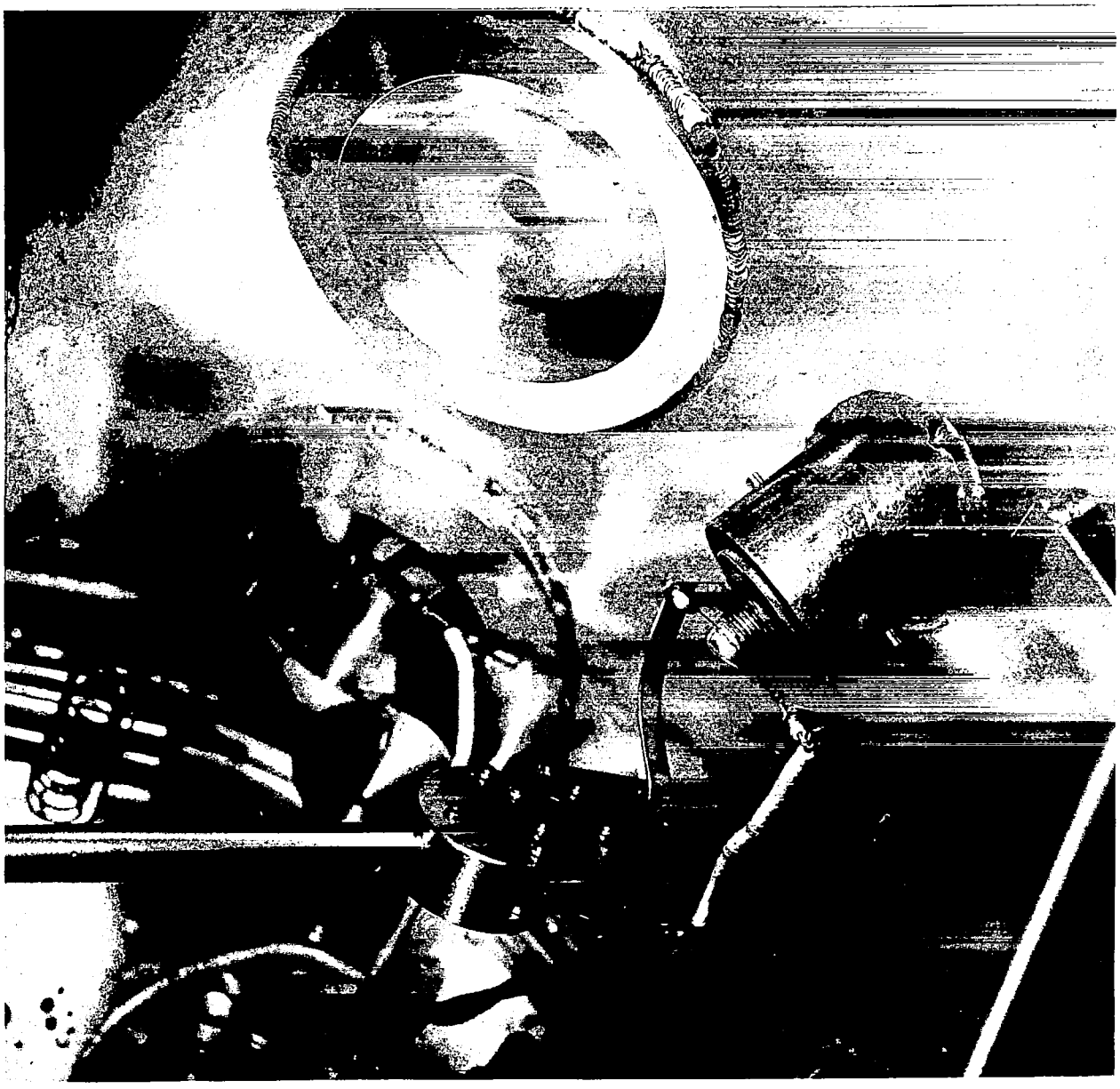

Figure 49. Sample Cutting with Hot Wire "Cheese Cutter."

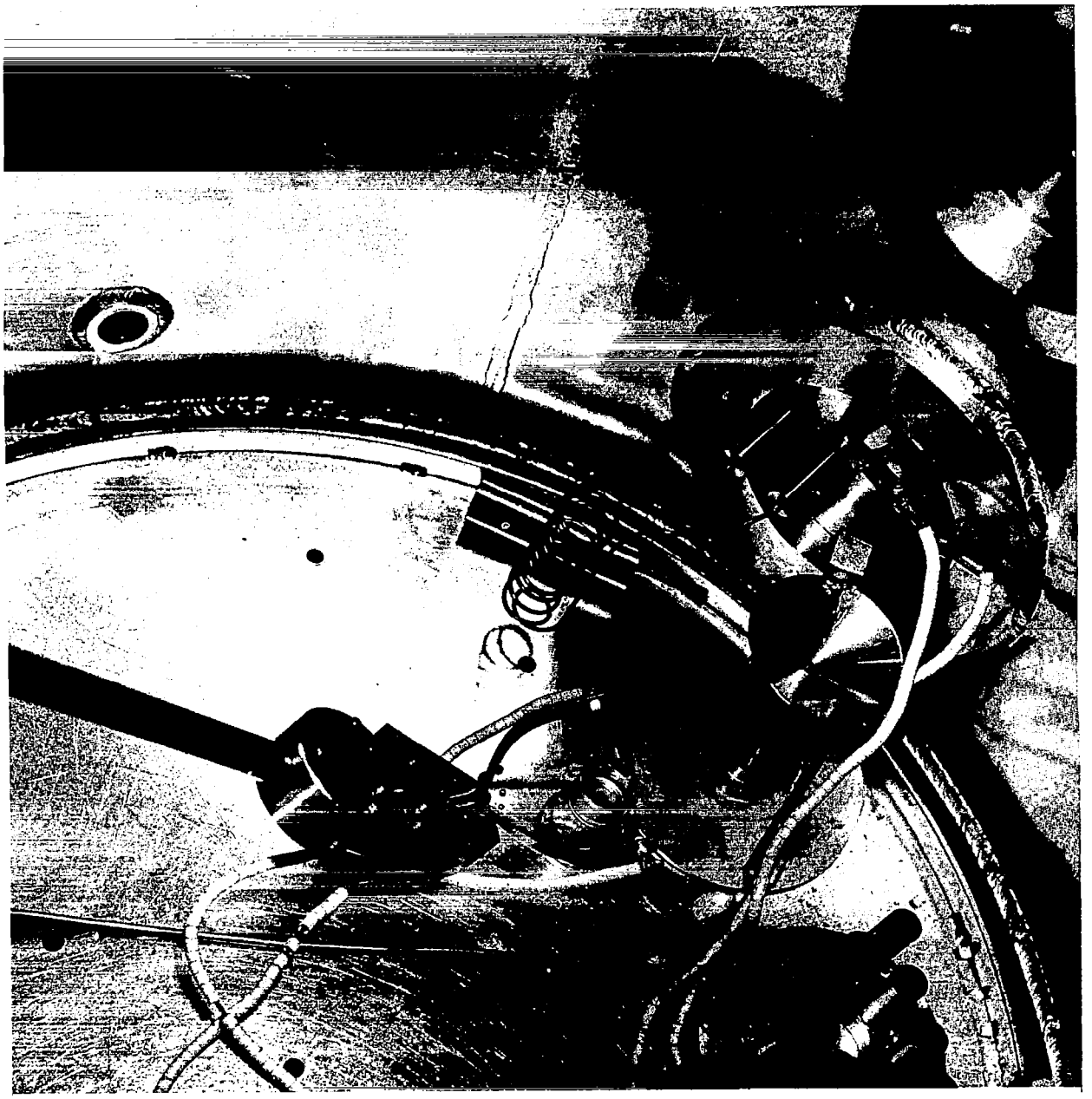

Figure 50. Potassium Sample Ready to Drop Into Transfer Vessel.

CHEMICAL ANALYTICAL TECHNIQUES

A survey of the state-of-the-art analytical techniques for elements of interest in this program was made and techniques were selected for use. The methods were those that afforded the best balance among desirable features such as high sensitivity, good accuracy, precision, speed, reasonable cost, and simplicity in materials and equipment. In order to remain within the limits of the state-of-the-art, methods best known and requiring the least amount of adaptation were given preference.

Following the selection of the preferred analytical procedures, a series of verification tests was performed to confirm the specific usefulness of the procedures. Appendix II is a fully detailed compilation of all of the experimental procedures actually used in the program. Table XIII indicates the state-of-the-art procedures available for determining interstitial impurities. Table XIV indicates the procedures available for determining metallic solutes in potassium. Table XV gives the results of the verification analyses for the spectroscopic analytical techniques used for determining metallic impurities in the test materials. Table XVI indicates the procedures and gives the verification results for the colorimetric methods considered for determining impurities in solute metals. Some of the methods selected in the preliminary survey were found to be unsatisfactory; others were used as necessary. All methods used were restricted to being state-of-the-art.

In the technique verification tests, a procedure was considered verified if 1-10 micrograms of an impurity could be determined in the presence of one gram of the matrix material being analyzed. In many cases, the impurity content of the best available material is too high to permit qualification of a procedure in the concentration range of 1-10 ppm. This has been found to be the case in the determinations of metallic impurities in the zone refined single crystal solute metals. In these cases, the suitability of the method was judged on the basis of its performance at higher impurity levels and the expected possibility of adequate extrapolability to lower impurity concentrations. A more serious problem was encountered in some of the analyses for impurity elements in the solute metals in that interferences between impurity elements were found. For example, niobium and silicon interfere with one another when both are present as impurities in, say, tantalum. The analysis for niobium is also complicated by the presence of tantalum, and by molybdenum.

An attempt was made to set up an ion exchange column to effect the separation of interfering elements, but it was generally unsuccessful. One of the two principal problems encountered results from the "tailing" of the major component during the elution of the minor impurities from the ion exchange columns. The other problem involves the recovery of microgram quantities of impurities from large volumes of elutriant solutions. Although both of these problems can probably be solved, the effort required was not considered to be consistent with the scope of the analytical support program.

Table XIII

Analytical Methods for Determining "Interstitial" Impurities

Element to be Determined	Material to be Analyzed	Method and Description	Sensitivity[a] and Remarks	References
Oxygen	Solute	Micro inert gas fusion or vacuum fusion. Oxygen is converted to CO_2 which is determined manometrically or by gas chromatography.	No firm limits of sensitivity can be established on the basis of published literature. Possibly a sensitivity in the range of 5-10 micrograms can be achieved. However, blank corrections lie in this range, making accuracy and precision difficult to maintain. A sensitivity of 0.3 microgram has been reported(71). This method is used routinely at AI, with a useful lower limit of 10 ppm O. Although a precision of $\pm$ 1 ppm is observed, the absolute accuracy has not been proved because adequate standards are not available.	5, 23, 43, 71, 84
	Solvent	Mercury amalgamation of potassium. Oxide residue is recovered and titrated with standard acid; or potassium in the oxide residue can be determined by flame photometry.	Lower limit 3 ppm $\pm$ 50%. Precision is $\pm$ 2.5 micrograms. Used routinely for for oxygen in Na and K.	21, 39, 62, 63
		Fast Neutron Activation Analysis	For a 10^9 flux and with opposed 3-inch detectors the level of detection is estimated to be 10 ppm with a 5 gram sample. At a higher flux, or using larger detectors, the level can be reduced, but no estimate of the lower limit has been made.	92

Table XIII (Continued)

Element to be Determined	Material to be Analyzed	Method and Description	Sensitivity[a] and Remarks	References
Nitrogen	Solute	Micro-Kjeldahl. Nitrogen is converted to ammonia which is determined spectrophotometrically with Nessler's Reagent.	1-2 micrograms. Used routinely.	12
	Solvent	Micro-Kjeldahl.	1.0 ppm. Used routinely, range 1-5 ± 0.2 ppm.	54,85
Hydrogen	Solute	High temperature vacuum extraction of hydrogen which is then determined manometrically or by gas chromatrography.	1.0 microgram. Used routinely. 1 ppm H_2 can be determined.	14, 33, 48 88
	Solvent	High temperature extraction in iron capsule. Hydrogen diffuses from capsule and is determined manometrically or by gas chromatography.	1.0 ppm. Used routinely.	66
Carbon	Solute	Micro combustion to CO_2 which is determined manometrically, by gas chromatography, or by conductometric readout.	1-10 micrograms. Equipment and blanks limit precision and accuracy. Used routinely for samples containing more than 50 ppm C.	20, 28, 64
	Solvent	Wet oxidation to CO_2 which is then determined by gas chromatography.	2 ppm; at this level good accuracy and precision are not expected. No firm data available. Accuracy and sensitivity limited by the reagent blank.	36, 65, 69

Table XIII (Continued)

Element to be Determined	Material to be Analyzed	Method and Description	Sensitivity[a] and Remarks	References
Sulfur	Solute	Wet oxidation to sulfate followed by reduction to sulfide which is determined spectrophotometrically with p-aminodimethylaniline.	1.0 microgram. Method in occasional use.	73
	Solvent	Same as above.	1 ppm.	73
Phosphorus	Solute	Convert to phosphate and determine spectrophotometrically as molybdenum blue.	2 micro grams. Used routinely.	4, 74
	Solvent	Same as above.	Verified at 1-10 ppm ± 5% in potassium.	4, 74

NOTE: (a) Sensitivity is used here to mean the lowest concentration or amount of a substance which can be determined routinely with reasonable accuracy and precision. Except as noted in the Table, data on accuracy and precision which are applicable to the concentration range or to the system of interest are not available in the literature.

Table XIV

Analytical Methods for Determining Solutes in Potassium

Element to be Determined	Method and Description	Sensitivity (in micro grams)	References
Iron	Spectrophotometric, with o-phenanthroline.	0.01-5.0 (± 2%)	27, 46
Niobium	Spectrophotometric, as the reduction product of the complex molybdo-niobate.	0.1-10 (above 1 ppm ± 2%).	34
Tantalum	Spectrophotometric, with malachite green.	1-2 (to better than ± 5%; estimate).	42
Molybdenum	Spectrophotometric, as the thiocyanate, or dithiol complex.	1.0 (± 2%).	32, 70, 72

Table XV

Spectroscopic Methods for Metallic Impurity Analysis

Material to be Analyzed	Description of Method	Typical Impurities and Reported Limits of Detection	Ref.	Remarks*
Potassium	Flame Photometry.	Other alkali metals can be determined with high accuracy and precision at concentrations near 1 ppm.	49	Atomic Absorption spectrophotometry used instead of flame analysis for determination of Na. Method verified in range of 1-50 ppm ± 0.2 in KCl matrix.
	Emission spectroscopy - Samples converted to chloride, fused, finely ground, mixed with graphite, d.c. arc, graphite cup.	1 ppm - Mo, Mn, V. 1-2 ppm - W, Cr, Ni, Fe. 5 ppm - Zn. 10 ppm - Ta, Nb.	41 49	Used routinely. Extreme care is needed in handling ultra-pure potassium samples to prevent contamination.
Iron	Emission spectroscopy - direct analysis of metal sample using spark technique; or metal sample converted to oxide, mixed with graphite and analyzed.	1-10 ppm - B. 10-50 ppm - Al, Co, Cu, Cr. Mn, Mo, Ni, Pb, Si, Sn, Ti, V.	3, 35, 57, 86	Samples from polycrystalline iron crucible material analyzed (as metal). Only impurities found were Mg, Si and Mn, all at concentrations of less than 5 ppm.
Niobium and Tantalum	Emission spectroscopy - sample converted to oxide, Li_2CO_3 used as a buffer, and Ta as internal standard, d.c. arc; or carrier distillation method, oxide plus Ga_2O_3.	1 ppm - B. 10 ppm - Al, Cd, Cr, Co, Fe, Mn, Mo, Ni, Si, Sn Ti, Zr. 250 ppm - Ta (in Nb).	26	Analysis of two samples (oxide form) from tantalum single crystals showed only Fe (<50 ppm), Nb (<100 ppm), and Si (150 ± 75 ppm) as impurities. Niobium samples not analyzed.

Table XV (Continued)

	Description of Method	Typical Impurities and Reported Limits of Detection	Ref.	Remarks*
Molybdenum	Emission spectroscopy - samples buffered with graphite mixtures containing internal standard of Cu or Ni. Both high voltage a.c. arc and d.c. arc used.	1 ppm - Ca, Cu, Mg, Mn. 4 ppm - Ba, Na. 5 ppm - Al, Fe, Si. 6 ppm - Cr, Ni. 8 ppm - Sn. 10 ppm - K, Sr. 100 ppm - W.	22	Spectrographic analysis (using metal) showed that samples from two single crystals contained only Fe (<50 ppm) and Si (10 ppm) as impurities.

*Most of the techniques described are used at AI. Verification was limited to materials which were on hand. The most serious problem encountered is that of pure standards: Materials used on this project are of higher purity than spectrographic standards, thereby limiting applicability. "Less than" values must be reported in most cases.

Table XVI

Analytical Methods for Determining Impurities in Solute Materials

Matrix Element	Element Determined	Method	Remarks
Iron	Copper	Biquinoline	Method verified in the range of 1-10 ppm.
	Molybdenum	Thiocyanate	Method has been verified in the range 1-10 ppm ± 5%.
	Silicon*		Several methods tested. None satisfactory at concentrations near 10 ppm.
	Manganese	Permanganate	Methods verified in range of 1-10 ppm.
Niobium	Tantalum	Malachite Green	Method is not satisfactory.
	Iron	Ortho-phenanthroline	Method verified in the range 1-10 ppm ± 5%.
	Silicon*	Molybdenum blue	Method is not satisfactory. Work discontinued.
Tantalum	Iron	Batho-phenanthroline	Method verified in the range of 1-10 ppm ± 5%.
	Molybdenum	Dithiol	Method verified in the range 3-25 ppm to better than ± 10%.
	Niobium	Thiocyanate	Method verified in the range of 2-12 ppm ± 5%.
	Silicon*		No satisfactory method. Several tested.
Molybdenum	Iron	Batho-phenanthroline	Method verified in the range of 1-10 ppm ± 5%.
	Niobium	4-(2-pyridylazo-resorcinol), PAR	Method verified in range of 5-30 ppm ± 5%.
	Silicon*		Several methods tested. None satisfactory in range of interest.

*There is a need for research which will provide satisfactory methods for the determination of silicon at levels near 10 ppm.

Several approaches to the problem of determining silicon by wet chemistry techniques in niobium, tantalum, and molybdenum have been investigated. None of the state-of-the-art methods tested provided adequate sensitivity or accuracy for the determination of silicon in the <20 ppm range in these metals. Therefore silicon was determined spectroscopically when required.

An interesting observation was made in connection with the analysis of potassium for oxygen by the mercury amalgamation technique using transfer vessels of the original design, requiring revision of the sampling procedure. Figure 51 shows one of these original transfer vessels. During the analytical procedure, the mercury was introduced into the vessel through a lightly-greased stopcock. In some of the analyses, the mercury would carry a few milligrams of the stopcock grease into the vessel. This grease tended to collect on the inner wall of the vessel and would frequently trap a small amount of raw potassium there. The presence of grease was accompanied by the development of a dark coloration on the mercury amalgam surface. Apparently, the trapped potassium was not washed away in the normal sequence of mercury washing, so that it remained on the wall until the final aqueous washing step, at which time it would dissolve. Since there is no way of avoiding the grease in the vacuum stopcocks, the planned handling technique had to be abandoned.

The present sampling technique consists of dropping the potassium sample from the cutter wire directly into a small weighing bottle. Care is exercised to keep the potassium from touching the lip of the bottle. The bottle is then closed, using vacuum grease to seal its ground glass joint. The closed bottle is then removed from the vacuum system and placed in a scavenged-atmosphere argon dry box for analysis. The cap is removed, the piece of potassium is picked up on a metal stirring rod and is placed for analysis in a separatory funnel having a greaseless teflon stopcock.

This technique has been quite successful, and was used in making the oxygen analyses shown in Table XII. Proof that the procedure is a good one is unambiguously shown by the quadruplicate measure of oxygen in the fourth batch of potassium. The four measurements were reported as 3.5, 3.8, 3.4, and 3.3 ppm O for the average of 3.5 ppm O as reported in the Table.

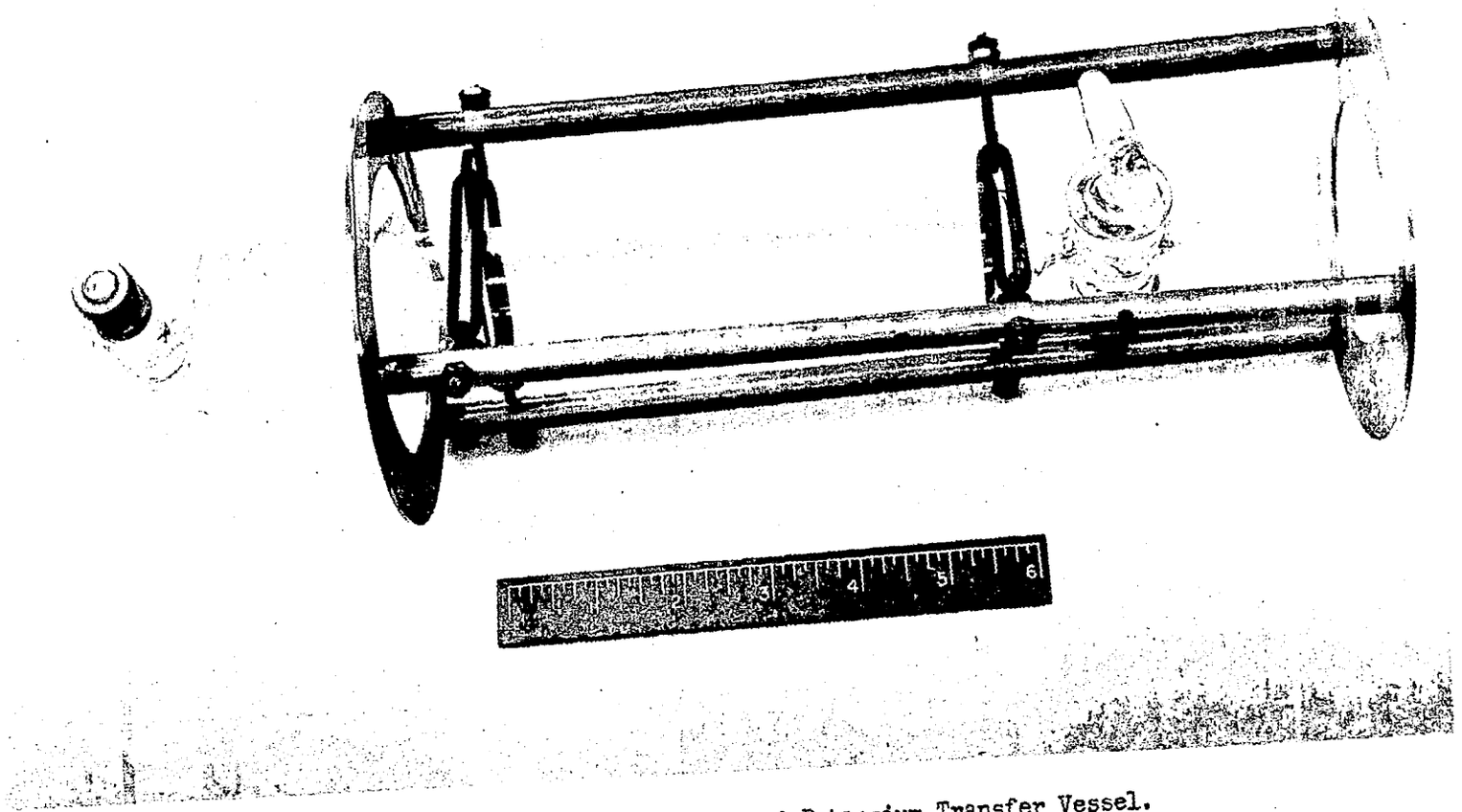

Figure 51. Original Design of Potassium Transfer Vessel.

TECHNIQUE FOR SURFACE AREA MEASUREMENT

The interpretation of solution rate data requires knowledge of the true dissolving surface area which is exposed to the solvent. Since it is well known that surfaces formed by ordinary means are rough on an atomic scale, and are likely to be non-reproducible, the decision was made to attempt to form a smooth surface for use in the kinetic studies. Therefore, the surfaces of the solutes exposed to the solvent were all finished by electropolishing because this process is known to produce a very uniform surface. The measurement of the surface area using the double layer capacitance (DLC) technique as a measuring tool was explored. An aqueous electrolyte of 0.1N Na_2SO_4 in contact with a mercury surface was used as a standard system in the evaluation study, and the associated DLC was measured using the technique of McMullen and Hackerman(56). Values of 18 and 19 μf/sq cm were obtained. These values compare well with the reported literature values, which range from 16 to 20 μf/sq cm for mercury.

Measurements of the DLC of electropolished platinum were also carried out using rectangular, flag-type electrodes. The electrodes were cleaned by heating to redness in an oxidizing flame. They were then placed in a measurement cell and biased cathodically at 2 volts for 10 to 15 seconds to liberate hydrogen. This hydrogen evolution was used to clean the electrode surface of any oxide. The differential capacity of the electrode was then determined as a function of voltage. During the early measurements, a minimum was observed around the electrocapillary maximum (which corresponds to the zero point of charge, ZPC) of 0.5 v with respect to the standard calomel electrode. This behavior was unexpected. It was found that this minimum disappeared if the electrode was allowed to stand for 10 minutes after the hydrogen evolution was completed. This indicated that the hydrogen on the surface had not completely desorbed and that this 10 minute interval was needed for the desorption process to be completed. The results of the final steady state measurements are given in Table XVII. The agreement with literature data prompted the start of measurements on refractory metals.

Table XVII

DLC/sq cm for Platinum

(ZPC* = +0.5v)

Apparent Surface Area	Capacitance μf/sq cm	Remarks
2.5 sq cm	22	Hackerman's data(56)
5.9 sq cm	23	AI data
2.4 sq cm	22	AI data
3.3 sq cm	24	AI data

*All DLC values reported were measured at a voltage which is 100 to 200 mv cathodic of ZPC.

Tungsten was the first refractory metal studied. Sample coupons were electropolished in a saturated solution of sodium nitrite at 10 volts a.c. for 20 seconds. They were then washed with distilled water and placed in the capacitance cell. The data are summarized in Table XVIII.

Table XVIII

DLC/sq cm for Tungsten (Electropolished)
(ZPC = -0.6v)

Apparent Area	Capacitance μf/sq cm	
3.4 sq cm	39	
4.1 sq cm	42	Avg. 42.0
2.1 sq cm	43	
1.3 sq cm	44	

In order to become better acquainted with the process, a series of measurements was made on mechanically polished samples. Table XIX shows the results obtained on highly polished Ta, Mo, Nb, and W.

Table XIX

DLC Values for Mechanically polished Refractory Metal Samples

Material	Crystalline Character	Apparent Area, cm^2	Capacitance* $\mu f/cm^2$
Tantalum	Poly Crystal	0.32	7.2
Molybdenum	Single Crystal	0.22	95
Niobium	Poly Crystal	0.32	11.0
Tungsten	Poly Crystal	0.32	45.5

*These data were calculated from the flat portions of the capacity vs emf curves on the cathodic side of the zero point of charge (ZPC). Measurements on the anodic side are complicated by oxide formation.

The DLC values for Ta are generally in agreement with literature values, which range from 4.5 to 9 μf/sq cm.(56,89).

Tests were made on both mechanically polished and electropolished iron surfaces of the same high purity metal. The unit capacitance values of the mechanically polished iron ranged from 5 to 7 $\mu f/cm^2$, while those for the electropolished surfaces were uniformly 10 $\mu f/cm^2$. The variance in the mechanically polished

surfaces is probably caused by the local differences in the character of the rather soft pure iron, and the resulting difference in the nature of the polished surface.

Further study of the DLC method led to the observation that refractory metal measurements are sometimes complicated by the persistence of the very thin oxide film which invariably forms on the surface of the electrode specimen. Therefore, an electropolishing technique that will produce surfaces which give consistent capacitance measurements is needed for each metal. A suitable electropolishing scheme, if properly carried out to achieve a minimum surface roughness, is believed capable of producing surfaces of a roughness factor of about 1.1(58). The procedures developed for use on the sample materials are described in detail in Appendix III. These were used to perform the various measurements on the solute crucibles shown in Table XX. An examination of the ratio of the DLC area and the geometric area indicates that the electropolishing treatment given the crucibles produces a very smooth surface which is nominally equal to the geometric area, within the uncertainty of the DLC measurement itself ($\pm 10\%$).

Table XX

DLC Values for Solute Samples (Electropolished)

Material	Geometric Area, A_G cm^2	DLC Area, A_D cm^2	Ratio A_D/A_G	
Fe-1	20.6	19.6	0.952	Avg. 1.017
Fe-2	19.2	20.8	1.082	
Mo-1	18.82	20.4	1.082	Avg. 1.080
Mo-2	18.38	19.8	1.078	
Nb-1	16.46	15.45	0.938	
Ta-1	16.56	15.24	0.921	Avg. 0.983
Ta-2	17.47	18.22	1.044	

SOLUBILITY TEST PROCEDURE

The solubility test capsule and associated parts and their relative positions are shown in exploded view in Figure 52. The parts are prepared for use in the tests by first washing them in solvent to remove oil and then outgassing them at high temperature in the apparatus shown in Figure 53. The outgassing temperature conditions for molybdenum parts involve holding them at 1800-1850°C until the system pressure drops to 1×10^{-6} torr. For tantalum, the hold temperature is 2000-2100°C. A flow sheet for the test procedure is shown in Figure 21.

The first trial solubility test run was made using a high purity polycrystalline iron crucible. The test (#311) was scheduled as an 8-hour run at 800°C. Although the oxygen content of the potassium then available was higher than was desired for use on the program, a couple of initial tests were scheduled to obtain operating experience with the system. This test was terminated after 2 hours and 35 minutes because a vacuum leak developed at the ball joint of one of the manipulators. As soon as possible after the leak developed, the power was turned off, and the test capsule was moved into the chill block in order to salvage the sample. The leak was quite large and developed suddenly so that the furnace heating element was very badly damaged, and the furnace radiation shields were also markedly affected. The surface of the test capsule was oxidized, but examination of the opened test capsule showed no evidence that the internal parts had been affected. Because there seemed to be no adverse effects on the sample, the potassium was submitted for analysis of its iron content.

The repair of the furnace involved replacing the tantalum heating elements, cleaning the radiation shields and the cup in which the test capsule seats, replacing the TZM shaft which supports the cup and capsule in the furnace, and repairing some of the thermocouple feed-through seals.

The second test was run for 2.6 hours to be comparable with the first. However, the problem of potassium transfer out of the crucible-collector sub-assembly was first noted in this test. This potassium transfer has proven to be the most severe experimental problem encountered. Normally, one would expect a small amount of potassium to be found between the crucible and the capsule, because potassium vapor will fill all of the open space within the capsule during testing. Upon cooling at the end of a run, this vapor will condense to leave a small amount of potassium ($\sim$0.1 gm) outside the crucible. Much more has frequently been found. Because of the uncertainties associated with the interpretation of the solute analysis and the evaluation of the solubilities when the potassium transfers, a number of techniques for effecting a mechanical seal between the crucible and the collector were tried. However, the desire to maintain and preserve the integrity of the single crystal crucibles originally restricted the choices of possible techniques to those which would not damage the crucible material.

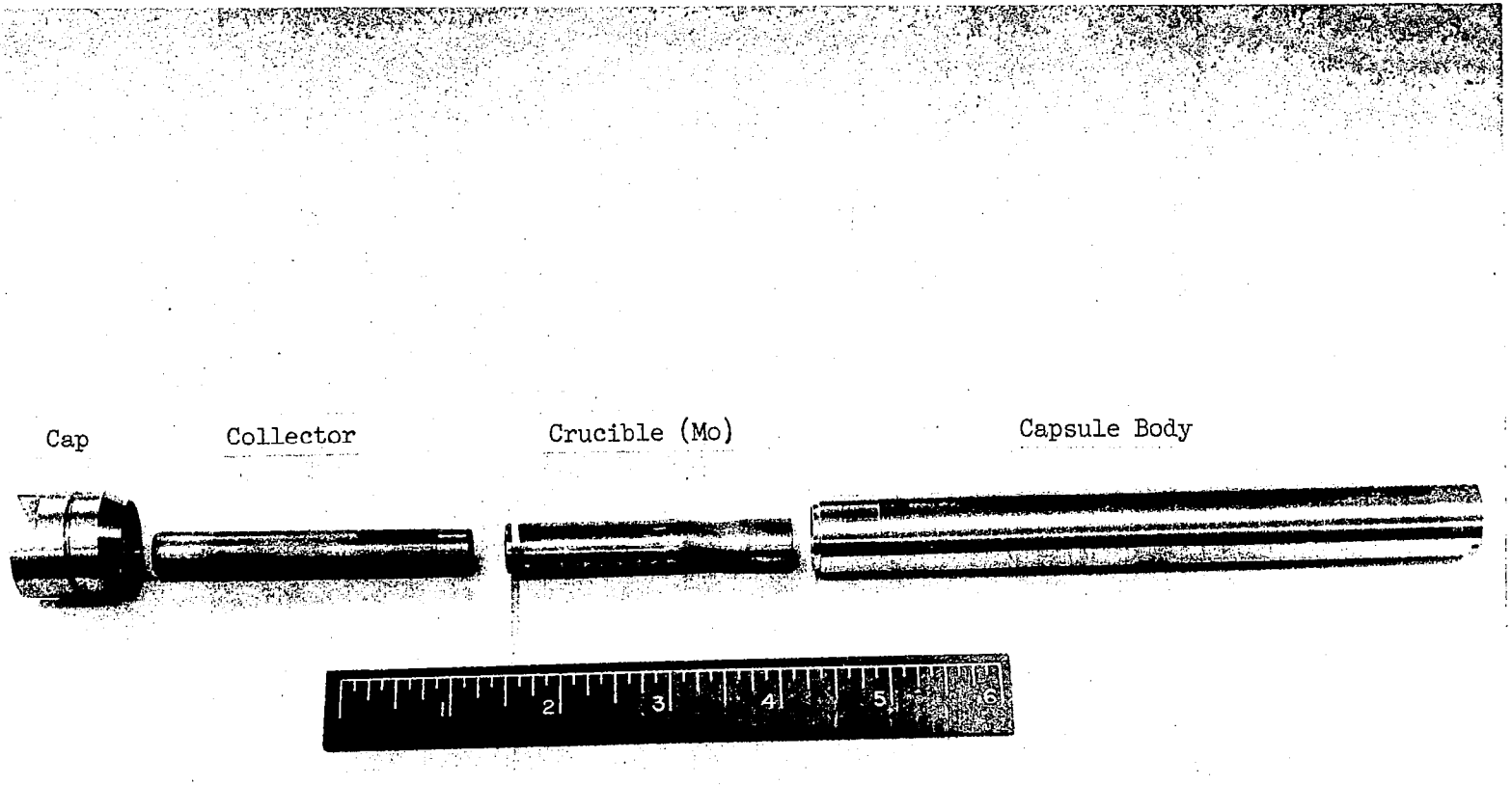

Figure 52. Exploded View of Solubility Test Components.

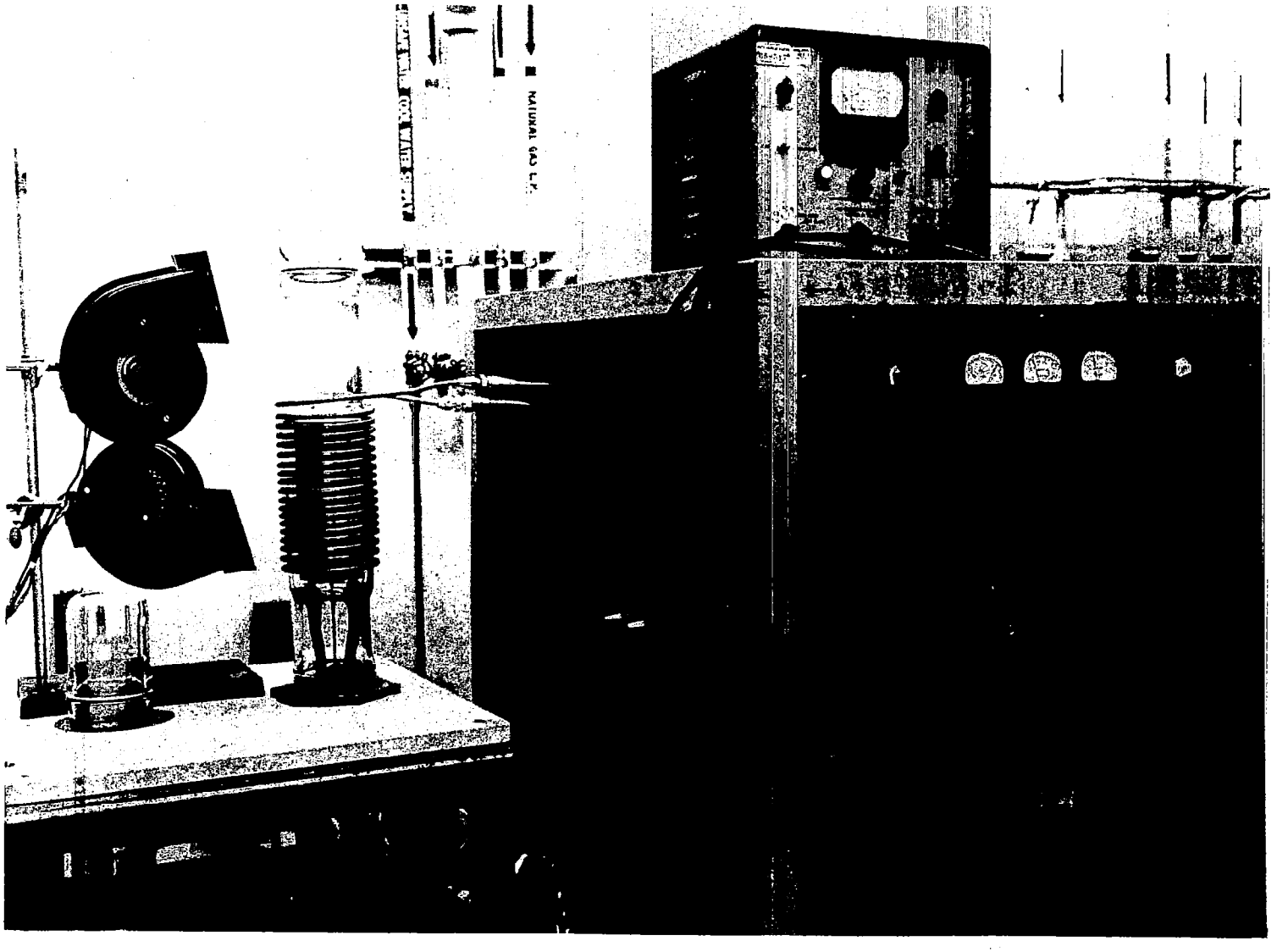

Figure 53. High Temperature Outgassing System.

An analysis of the test sequence leads to three possible mechanisms by which massive amounts of potassium might transfer out of the crucible-collector sub-assembly. First, there may be spillage of the potassium as the capsule is inverted and the metal flows into the collector. The joint between the two parts is not sealed and it is possible that some material could run out. However, tests using acetone and water as fluids indicated that only a few drops would spill under the worst conditions if the collector is properly seated in the originally designed crucible lip. One would not expect losses of a half gram or more from this source if the collector mouth is maintained in position in the crucible lip.

The second mechanism considered was the evaporation-condensation transfer of the potassium during the test period under the influence of a temperature gradient along the length of the crucible. In the early tests, the temperature difference between the upper end of the capsule and the center was 15-20°C, and that between the bottom and the center was 20°-25°C. By careful trimming of the heating element to provide an incremental heating at the top and bottom, the temperature differences have been reduced to about 5°C. The tendency here is for the metal to collect at the coldest part of the capsule. It is therefore advantageous if the crucible end of the capsule runs a few degrees cooler than the middle and the top of the capsule during the test period. The reduction in the temperature differences along the capsule effected by trimming the heating element is therefore expected to have reduced markedly the potassium transfer by this mechanism, particularly since the top of the capsule typically runs slightly hotter than the bottom.

The third mechanism considered also involves vapor transfer, but was postulated to take place during the quenching step. During this period, the capsule wall is deliberately cooled. Since the heat transfer to and from the capsule-collector sub-assembly to the wall is relatively poor, the wall temperature could drop, say, 30-40°C before the collector and its collected potassium begins to cool. Under these circumstances, the potassium could readily vaporize, pass through a loose capsule-collector joint and condense on the cooled wall of the capsule. At present, this is thought to be the major mechanism contributing to the observed potassium transfer.

The first step taken to control these transfer problems was the reduction of the temperature gradient as noted above. In addition, an improvement of the quenching action and the reduction of the time required to cool the capsule was initiated as another possible means of controlling the potassium transfer. Figure 42 shows a typical quenching curve of a capsule which is cooled from 1000°C and the corresponding temperature history of the chill blocks. The dashed curve represents a typical temperature history of the capsule wall. The collector, which presumably now contains the test potassium, is expected to follow a curve similar to the dashed curve shown in Figure 42 but which is displaced about 10-15 seconds to the right. Thus, in the first few seconds, a 30°-40°C temperature difference between the capsule wall and the collector is developed. This difference decreases as the temperature level drops and is expected to be quite small by the time the capsule temperature has dropped to that of the chill block. With the chill blocks, the time required for the

capsule to cool to the melting point of potassium was four to six hours. Ideally, this time should be quite short, and the water-cooled quenching device shown in Figure 41 was designed to replace the chill blocks. With this device, the potassium in a capsule cools from 1200°C to the melting point of potassium in less than 20 minutes.

The techniques used to control the potassium transfer by modifying the crucible-to-collector seal have been: 1) the use of a solid spacer inside the capsule such that the top of the collector was supported at a level slightly above the lip of the crucible at the time the welding cap was attached, 2) the use of a matching low-angle bevel on the collector and on the crucible to form a tapered joint, and 3) sealing the capsule with a compressed coil spring beneath the crucible-collector sub-assembly so that the sealing force would continue to be applied to the tapered joint during the test period, d) the use of K between the crucible-collector sub-assembly and the inner capsule wall, and 5) brazing the joint between the crucible and the collector.

Three runs were made using carefully sized spacers inside the capsule to hold the crucible-collector under slight compression during the runs. Further, in one of the runs, a flat strip of molybdenum was also placed inside the capsule to aid in maintaining the crucible and collector in axial alignment. Nevertheless, significant losses of potassium were experienced in all of the runs. Apparently, the potassium transfers unless the joint becomes sintered and forms a metallurgical bond. However, the number of sintered joints that were formed is small. One reason for this may be that the test temperatures and the developed forces on the joint are too low to encourage sintering. Another reason may be that the spacer does not maintain a steady force on the collector-crucible sub-assembly during the entire run. At the beginning, all of the internal parts expand during heating. Since the usual collector is tantalum, and because tantalum has a greater expansion coefficient than molybdenum, an expansion-induced axial force develops during the initial approach to the test temperature. During the higher temperature runs in particular, the axial stress in the tantalum may exceed its short time compressive yield strength and it may plastically deform. Then, as the test proceeds at constant temperature (whether there has been previous yielding or not), the tantalum collector will tend to undergo plastic deformation as controlled by its creep properties, and, as a result, the stress level in the collector will decrease with time. Then, as the test is ended and the capsule cools, there is at first a compression action on the tapered joint, followed by a relaxation of stress to zero, as the contraction of the now-deformed tantalum collector exceeds that of the molybdenum capsule.

The result of this sequence is that the sealing force on the crucible-collector joint could vary by a large factor during the test period, but it seems inevitable that the force must drop to zero during the quench period. Thus, unless sintering occurs near the start of the test, the loss of potassium during the quench operation is a distinct possibility.

Another attempt to contain the potassium within the collector-crucible sub-assembly was made by trying to cause a pressure-weld to form between the collector and the crucible lip. In this case, the collector lip was cut with a

45° bevel, and the lips on the (iron) crucibles were machined to be square and true. Then the capsule was loaded with about a half gram of potassium outside the crucible. A spacer was used to ensure that pressure was applied to the joint. The external potassium provided a slightly improved heat transfer bond between the capsule and collector, but primarily it provided material to maintain the vapor pressure of potassium external to the crucible. In these tests, the intent was to develop a pressure-induced diffusion bond seal during the initial part of the test period. To this end, the spacers used in the assembly of the capsules were made long enough so that the end of the collector extended about 1/32 inch above the top of the capsule. Then the cap was pressed firmly against the collector and welded to maintain the pressure on the collector-crucible sub-assembly. The combination of pressure and the sharp edge on the collector was intended to lead to the development of a diffusion bond and a seal. However, the yield of good seals was not high, and another method of attempting to form a seal was tried. This involved machining a matching taper on both the crucible and the collector. In addition to the tapered joint, a spring was used beneath the crucible. It was intended that before and during welding the spring would be compressed enough to develop about a 3 lb axial force on the joint and would continue to apply that force during the heating period, at least until its modulus began to decrease. In this assembly, the spring is the most heavily stressed element in the capsule, and it would normally be subject to creep. Accordingly, the applied force from the spring should decrease during the test and, if the creep deformation is excessively large, the spring action may fail entirely. In such a case, the spring is no more effective than the solid spacer. On the other hand, if a creep-resistant spring is used, it should maintain a force on the crucible-collector joint through the entire test period, and, even if sintering of the joint does not occur, the spring may hold the tapered joint together.

Refractory alloy springs were used in this application. The springs were made of nine turns of 25-30 mil wire, and were 7/8 inch long and 3/8 inch in diameter. The springs were placed beneath the crucibles and collectors in the assembly of the capsules, as shown in the exploded view of a capsule and contents in Figure 53. Before the capsule cap was put in place, the top of the collector extended about 3/8 inch above the top of the capsule. Three spring materials were used and all were found to be unsatisfactory. These are: tungsten, the niobium-base alloy C-129Y, (Nb-10W-10Hf-0.2Y) and the tantalum base alloy T-111 (Ta-8W-2Hf). The tungsten springs were used at 600°, 800°, 1000°, and 1100°C for test periods up to eight hours. In all cases, the springs were found to be collapsed when the capsules were opened. The C-129Y springs were used at 800°, 1000°, and 1200°C for periods up to eight hours. In all cases the C-129Y springs had relaxed so that they just filled the space, but they did not appear to be applying any force. The C-129Y springs were brittle after use, and one of them fractured into several parts when it was subsequently compressed. The T-111 springs were also used at 800°, 1000°, and 1200°C for 8 hours. In all cases the T-111 springs had relaxed so that they filled the available space inside the capsules, but little or no force was being applied. These T-111 springs, though shortened, did continue to possess spring-like qualities and could be flexed without damage.

Although all of the various springs relaxed during the tests, the amount of potassium transferred varied. In some cases, a large fraction of the potassium was retained in the crucible-collector assembly, but in other cases most of the potassium escaped to the exterior of the crucible. From the results of these various tests, it became obvious that some means other than spacers and/or springs must be used to form a seal. The only method which seemed feasible was the use of a braze or a weld. The choice between these two sealing techniques was made on the basis that the braze joint requires the use of a lower temperature, which minimizes the heating of the potassium in the crucible. It is feared that the use of welding temperatures for molybdenum and niobium (which temperatures are above 2500°C) would be quite likely to cause the volatilization and loss of the potassium in the crucible. An additional consideration was the fact that a welding operation would almost certainly destroy the single crystallinity of the crucible in the region of the weld, and would thereby severely limit the number of times a given crucible could be re-used. The braze seal, however, allows the use of a much lower seal temperature (about 1600°C for a nickel braze, and 1900°C for a zirconium braze) and lowers the probability of the loss of potassium by volatilization. For this reason, the lower sealing temperatures are strongly preferred. Further, the use of a braze is less damaging to the crucible and would allow its re-use for a greater number of tests than would be possible with a welded joint. We deliberately avoided this sort of closure in the early tests because of the concern about contaminating the single crystal crucibles with the braze metal, but it finally appeared to be the only way of effecting the required seal (other than welding).

The first braze metal chosen for testing was nickel. The procedure involved electroplating nickel on the upper portion of the taper which is machined on the sample collector. The last 1/6" of the taper is masked to prevent deposition there and thereby to reduce the chance that nickel would be dissolved in the potassium. A typical plated collector is shown in Figure 55. The amount of nickel used is 25 to 30 mg, which produces a plate about 0.001" thick on the tantalum. The plated collector is mated to the taper on the sample crucible, and the braze is effected by heating the joint area above the melting point of nickel, while a weight on the collector maintains a tight joint as the nickel softens. The concern that the nickel braze would interact with the potassium and complicate the interpretation of the experimental results was allayed by the finding that no nickel was detected in the solvent potassium at the end of the tests.

Identical brazed joints have been made to join tantalum crucibles to molybdenum sample collectors, with the nickel plate being applied to the molybdenum. An alternate braze metal which might be considered for higher temperature experiments is zirconium. A nickel braze was attempted for the joining of the iron crucibles to the tantalum collectors, but the melting points of iron and nickel were found to be too close together and the temperature control required to prevent melting the iron could not be achieved. The use of copper, applied as a loop of wire which is melted to form a fillet at the outer interface of the tapered joint, appeared satisfactory. However, the melting point of copper limits the operating temperature of experiments in which this braze is used to about 1000°C.

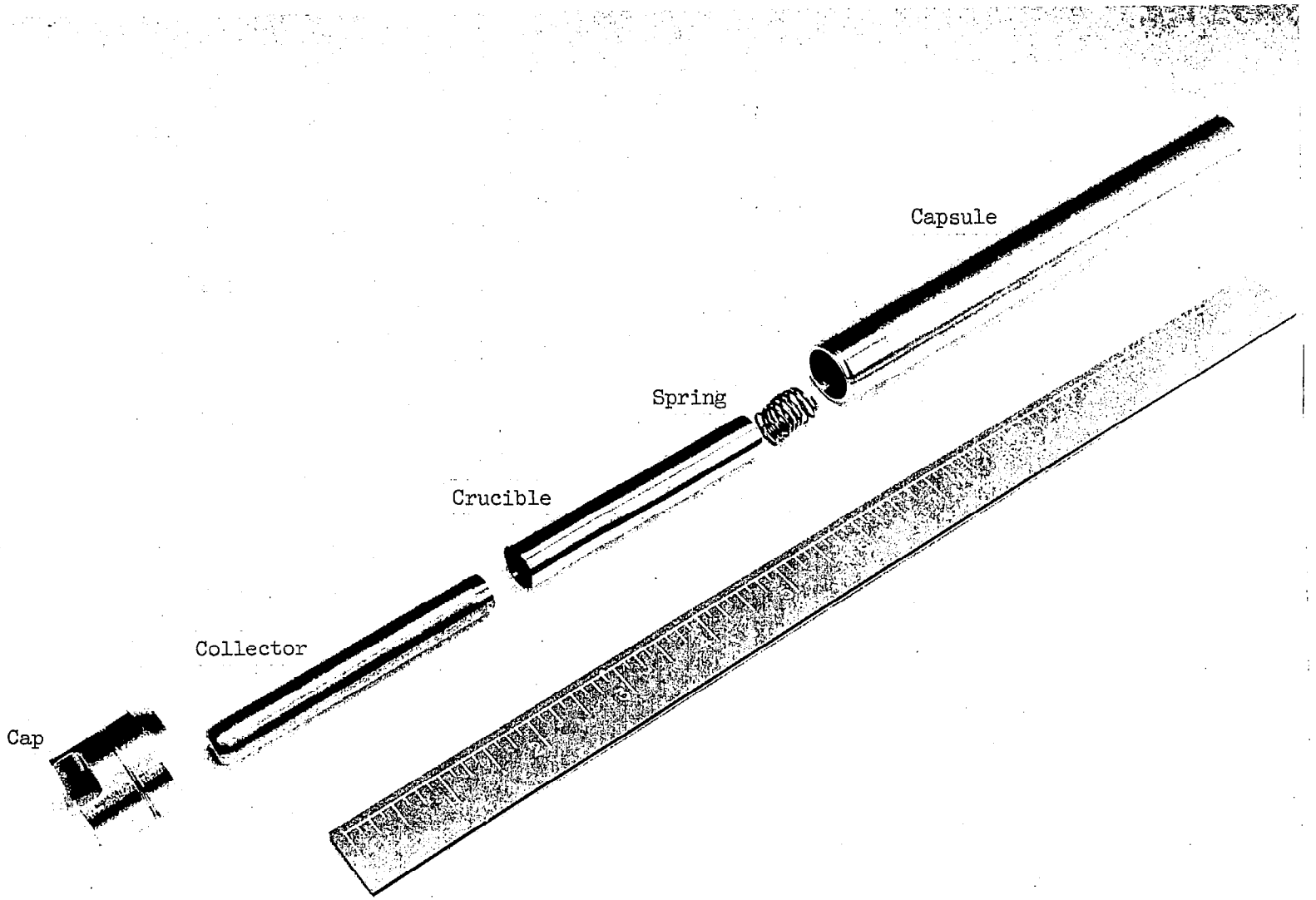

Figure 54. Exploded View of Capsule Components with Spring.

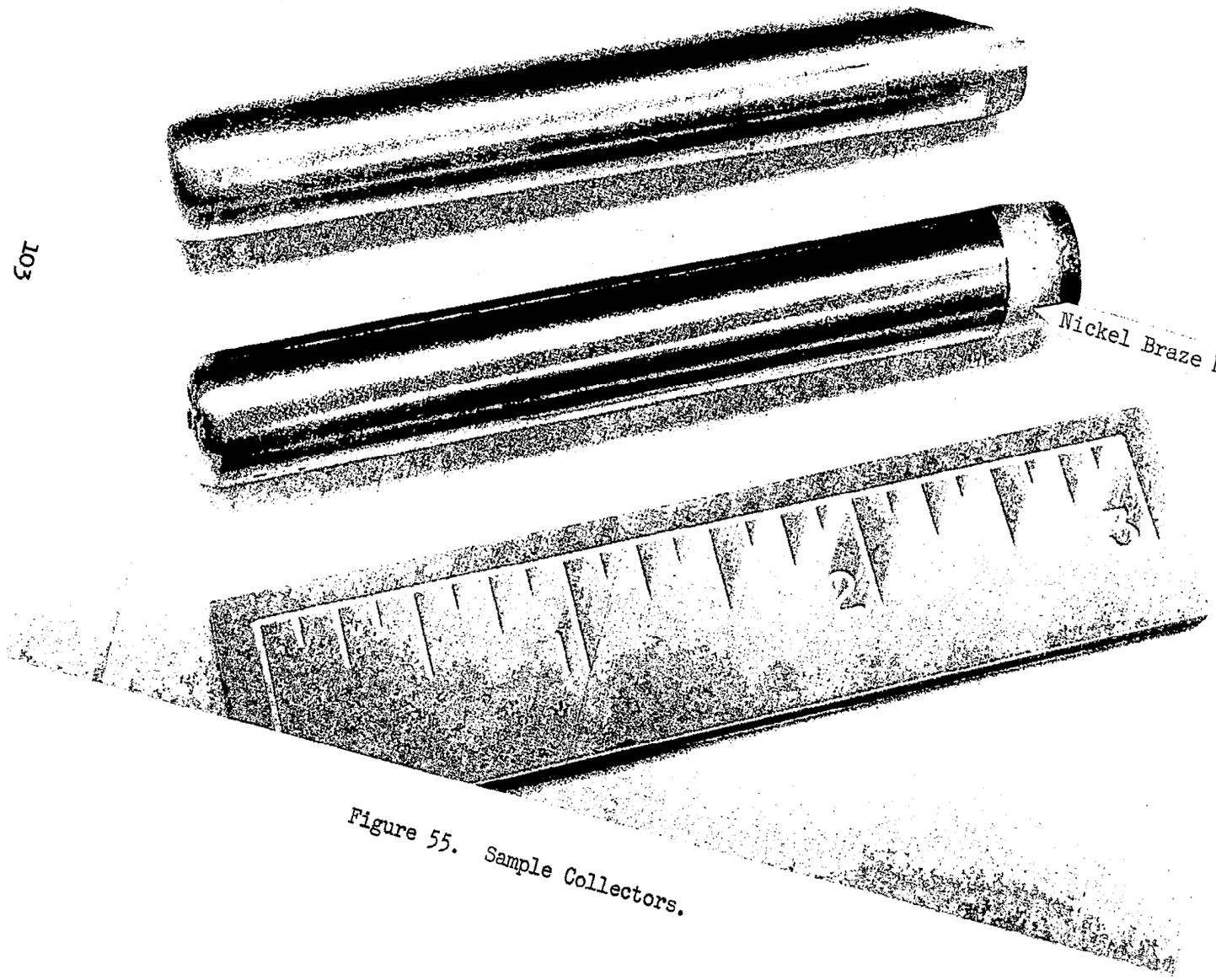

Figure 55. Sample Collectors.

The use of the braze joint successfully solved the problem of transfer of potassium from the interior of the crucible-collector assembly to the space outside it. The practice of placing a small amount of potassium external to the crucible was continued, however, to minimize the pressure difference across the crucible-collector subassembly, since these components are not designed to be pressure vessels. The major advantage derived from the routine use of brazed joint seals is the removal of any uncertainty about the amount of potassium associated with any solubility experiment. The total amount of potassium found in the collector at the end of a test is that which was originally loaded into the crucible. Earlier attempts at estimating the amount of potassium loaded by using a "dip stick" after the potassium had solidified in the crucible were marginally successful. The inauguration of brazing as a sealing technique rendered the "dip stick" measurement both inadequate, since the crucible length changes with each machining operation, and unnecessary, since the amount of potassium can be determined unequivocally at the end of the experiment. A disadvantage is that the third component may complicate the solubility measurements.

The experimental procedure used for the experiments carried out after the problems of the crucible-collector joint and the quenching rate were solved is described in the following paragraphs.

The four parts for an experiment (i.e., crucible, collector, capsule, and cap) are collected in Chamber #1 of the environmental test system after high temperature outgassing. All parts then receive an outgassing at 350°C in the heater in Chamber #1 to remove adsorbed gas. At the end of the outgassing, the vacuum in Chamber #1 is about 3-5 x 10^{-7} torr with the furnace hot, dropping to less than 1 x 10^{-7} torr when the furnace cools.

The solute crucible is set in place under the heated funnel, and the capsule body placed in the coil heater designed for it. The protective cap is removed from the extruder delivery tube and about 0.5 gram of potassium is extruded, cut off with the "cheese cutter", and discarded. Then about 0.2 gram of potassium is extruded, cut off, deposited in the capsule body, and allowed to melt and flow into the bottom of the capsule. The capsule is then removed from the heater and the potassium allowed to cool. The amount of potassium solvent to be used in the experiment (0.75 to 2 grams, depending on the crucible being used) is then extruded, cut off, and dropped onto the heated funnel, through which it flows into the crucible. The crucible is then removed from the funnel stand and the potassium is allowed to solidify. When all the potassium is solid, the sample collector is placed carefully into the crucible and then given several firm taps with the manipulator in the top of the chamber, being careful to align the crucible and manipulator so as not to exert any lateral pressure on the ball joint seal. During these operations, careful, patient work with the manipulators can keep the pressure from exceeding 6 x 10^{-7} torr in the chamber. The crucible-collector assembly, and the separate capsule body and cap, are then passed through the gate valve into Chamber #2, which is also under high vacuum.

The crucible-collector assembly is inserted in the welding chuck and the braze operation completed as the assembly rotates. The brazed assembly is removed from the chuck and the capsule body set into the chuck. The crucible-collector assembly is then put into the capsule body, the cap placed in position on the capsule, and the weld to close the capsule completed.

After cooling, the welded capsule is transferred to Chamber #3 and placed in position in the test furnace. The six thermocouples are adjusted to bear on the capsule, and contact with the capsule is verified by measuring the electrical continuity from the external thermocouple leads to ground. Then, after the chamber has been evacuated to 2×10^{-6} torr, the furnace is heated and controlled at temperature for the required time.

At the conclusion of the experiment, the thermocouples are pulled away from capsule and the movable half of the test furnace swung open at temperature. Then the capsule is permitted to swing out of the furnace and down into the water-cooled quenching device. Power to the furnace is then turned off.

When the system is cold, the capsule is removed from the furnace and the cap is cut off at the machined groove by means of a tubing cutter. The crucible-collector assembly is removed from the capsule, and washed free of the small amount of potassium adhering to its exterior. Then, the collector is separated from the crucible by cutting with a small tubing cutter. The separated collector is placed in a closed container to prevent excessive oxidation which would make removal of the sample from the collector more difficult, and submitted for chemical analysis. The crucible is machined to remove the end of the collector which remains with the brazed joint, and prepared for a subsequent experiment.

RESULTS AND DISCUSSION

In the preceding sections, the various aspects of the development of the experimental procedure have been discussed in detail. This work focussed on the problem of obtaining a seal between the collector and the crucible without compromising the single crystallinity of the test crucibles. The solution involved the use of a braze made in a way which inhibits the braze metal (which is used in very small amount) from contacting the potassium. Because the braze is made at a relatively low temperature (compared with a weld), the crucible integrity is not affected by the temperature. However, the upper end of the crucible is expected to change in composition as the braze metal slowly diffuses into it. In spite of this objection to the sealing technique, it does give an answer to the question of the amount of potassium which acts as solvent in a test. Therefore, only tests in which the potassium can be shown to have been retained within the crucible-collector sub-assembly are considered to have produced usable results. All of such data are shown in Tables XXI through XXIV, and in Figures 56 through 59.

Table XXI and Figure 56 summarize the data for the solution of iron in potassium. In all, more than twenty tests were made with the iron crucibles, since they were used for many of the development tests of the crucible-collector seals. Although most of the early techniques for retaining potassium within the crucible-collector sub-assembly were unsuccessful, two experiments, #311 and #333, retained the required amount of potassium to warrant their inclusion in the final grouping of test data. The spread in the values of the data for tests which did meet the nominal 100% retention criterion is nominally an order of magnitude, as shown in Figure 56. This degree of variation of the data was not expected in these tests in which very pure solute materials and purified potassium were used as sample materials. The data do suggest a trend with temperature, and have been analyzed by the use of the least squares technique to yield the best curve,

$$\log (\text{wppm Fe}) = 3.4 - 1700/T.$$

This curve shows a ΔH_S of 7700 cal/mol, which value is close to, but higher than, the 'simple solution' range of values described in the "Introduction" section above. However, it is significantly lower than the ΔH_S given by Swisher(77) who reports a value of 28,200 cal/mol. In addition, the present curve shows a value of about 115 wppm at 1000°C while Swisher reports a measured value of 1000 wppm at the same temperature. Ginell and Teitel(29) report a single value at 1000°C of 500 wppm. At 800°C, the present curve shows a value of iron concentration of 65 wppm. Swisher's value from his reported curve(77),

$$\log \text{ppm alpha iron} = 8.193 - 6166/T,$$

is 285 ppm.

TABLE XXI

Summary of Test Data for Iron

Test No.*	Temp. °C	Time hr.	Oxygen Content of Potassium ppm	K gm	Fe µgm	Fe Conc. wppm
311	800	2.6	40	1.46	37.5	25
333	1000	4.0	16	2.11	89.	43
182	800	8.0	14	1.70	250.	147
183	800	4.0	14	1.36	99.	74
196	1000	8.0	14	1.01	179.	177
197	1000	4.0	14	1.13	223.	197

*The tests listed are shown on Figure 56 with the test numbers.

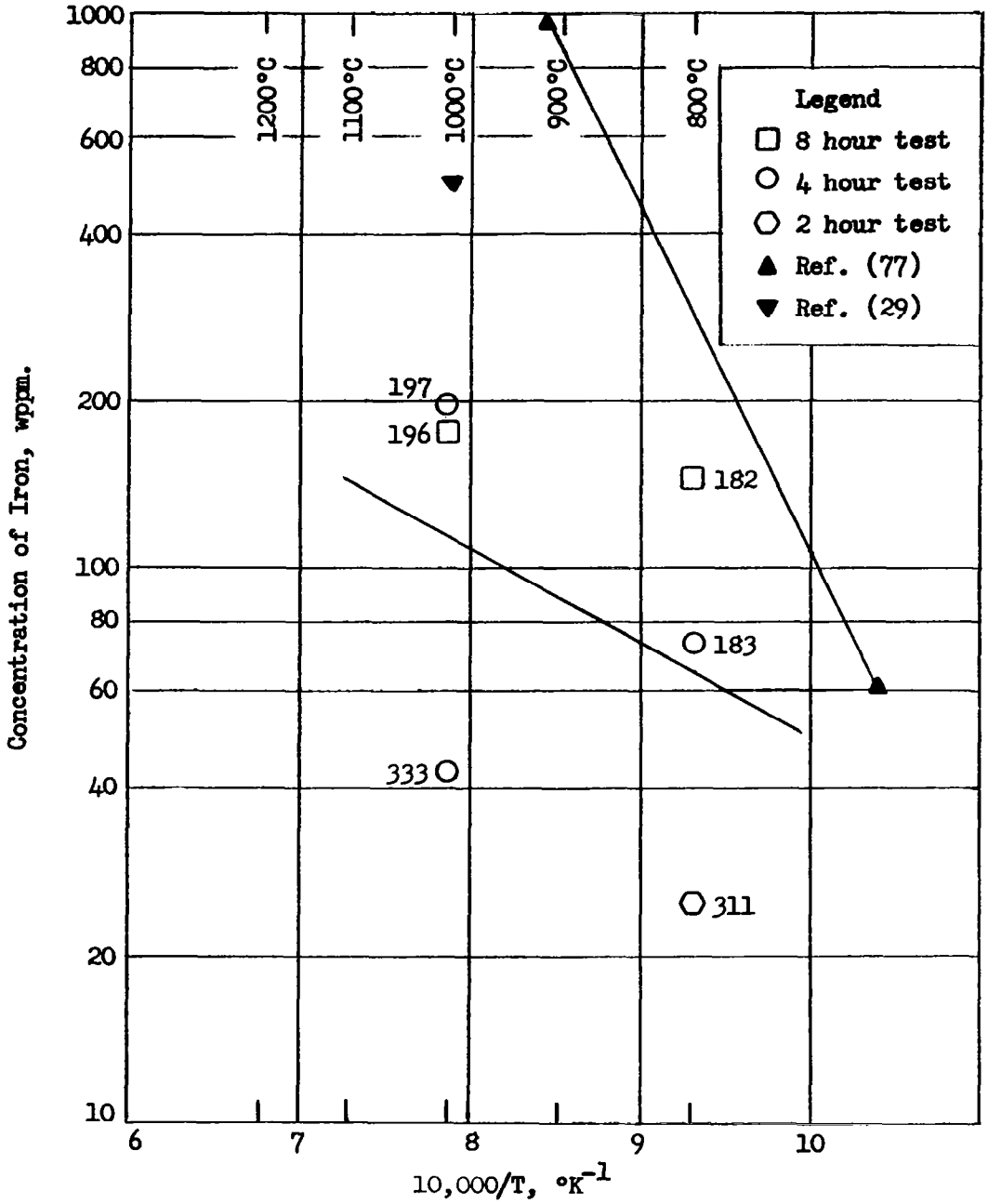

Figure 56. Concentration of Iron Dissolved in Potassium. (Data from Table XXI.)

The difference in the concentration levels between the present data and Swisher's data may be explained by the difference in the purity levels of the test materials. The triple-pass zone-refined iron used in the present tests is much purer than the Armco iron used by Swisher (whose iron had an oxygen content of 510 ppm). In addition, the oxygen level of the potassium used in all but one of the present tests is 14-16 ppm, while Swisher's was nominally 20 ppm. The oxygen content of Ginell and Teitel's potassium was 10 ppm, and their iron sample was made from "Puron"* high purity iron, which is reported by the manufacturer to have a typical oxygen content of 400 ppm. It therefore appears that there may be a trend in the level of the solubilities with the oxygen levels of the solute materials. If this is the only cause, then it might also explain the difference in slopes of the two curves. Oxygen has been reported to react with iron to form complex species in sodium(37), and one would expect similar behavior in potassium. Thus, Swisher's higher oxygen content may allow a reaction to occur, which reaction might account for his ΔH_S value of 28,200 cal/mol. Further, it seems possible that some reaction might also be affecting the data of the present experiments because the ΔH_S here is 7700 cal/mol, which is perhaps twice the expected value for the simple solution of iron in sodium. However, this is a very tenuous possibility, because the present data have quite a large spread.

Table XXII and Figure 57 summarize the data for the solution of molybdenum in potassium. About twenty tests were performed with the molybdenum crucibles. About half of these were tests made with the various non-brazed seals. In none of these did more than 75% of the potassium remain in the crucible. Of the remainder, there were several in which the nickel braze was faulty, probably due to the failure to melt the nickel. In preparing the first group of nickel joints, the nickel plate was limited to a 1/8-inch strip about 1/16 inch away from the tip of the taper on the collector. When such a plated collector is seated in the crucible, none of the nickel can be seen. It was therefore no possible to be certain when the brazing temperature had been reached, and in the care to avoid overheating, which would cause the potassium sample to vaporize during the braze, the braze metal was probably not melted. In later tests, the nickel plate was carried up the full length of the taper on the collector so that it can be seen by the welder, and the heat applied until the visible nickel was observed to melt. The braze joints prepared in this way are substantially better than those made earlier.

The data obtained in the final molybdenum tests is generally consistent, except for test 177. Since there is no indication that the test was invalid, the data point has been retained and used in the evaluation of the least squares curve representing the data,

$$\log (\text{wppm Mo}) = 4.8 - 5600/T.$$

The ΔH_S of this curve is 25,500 cal/mol, which suggests that there may be a reaction involved in the present solution process for molybdenum. The oxygen content of the potassium used in all tests was 14 wppm, and the molybdenum

*A product of the Westinghouse Electric Co.

Table XXII						
Summary of Test Data for Molybdenum						
Test No.*	Temp. °C	Time hr.	Oxygen Content of Potassium ppm	K gm	Mo µgm	Fe Conc. wppm
166	1200	4.0	14	1.15	16	13.9
167	1200	8.0	14	1.22	16	13.1
173	1000	8.0	14	1.38	6	4.3
176	1000	4.0	14	1.54	5	26.
177	1100	8.0	14	1.50	2	1.3
203	1100	4.0	14	1.84	24	13.

*The tests listed are shown on Figure 57 with the test numbers.

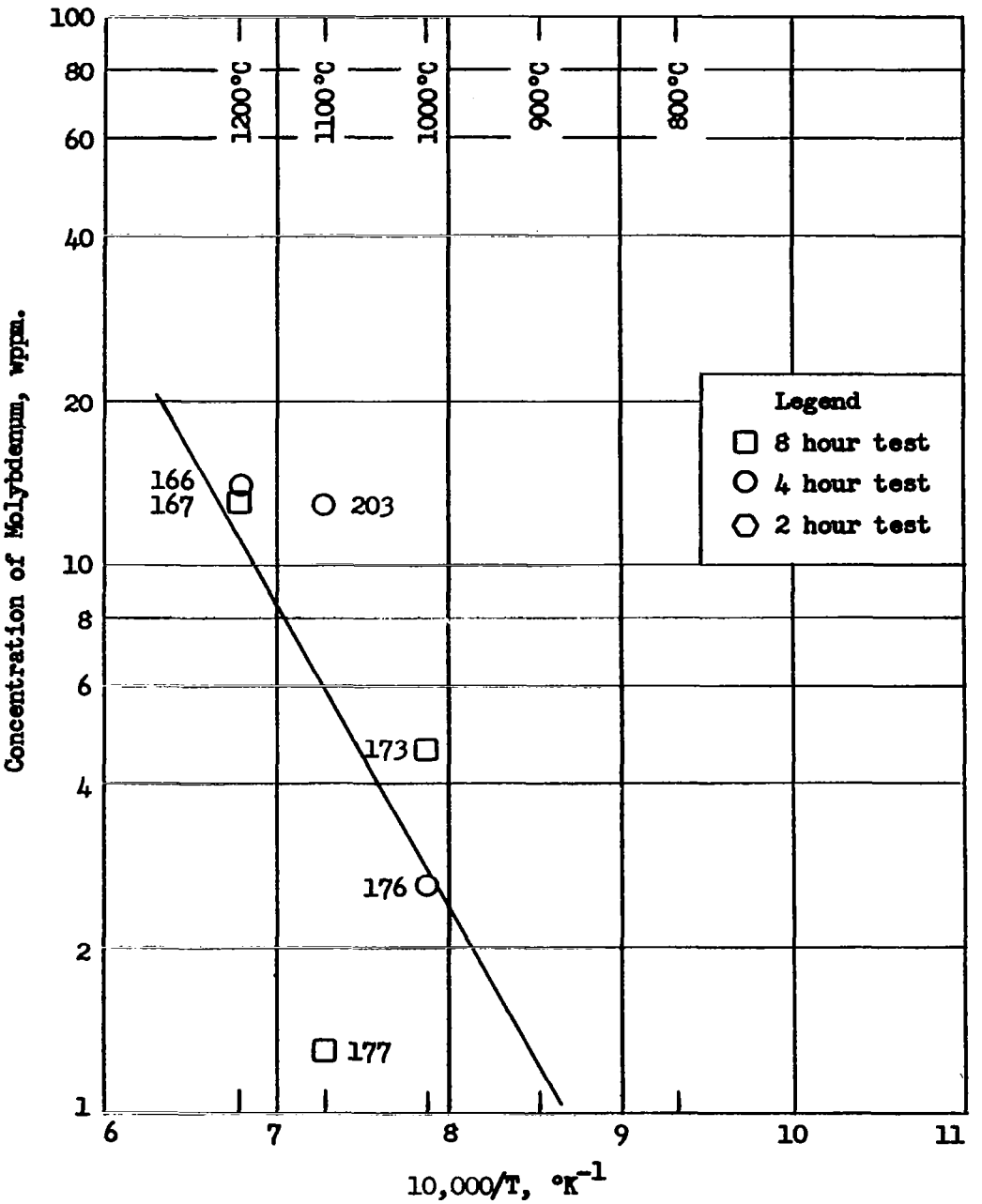

Figure 57. Concentration of Molybdenum Dissolved in Potassium. (Data from Table XXII.)

crucible is made from a triple-pass zone-refined single crystal so its oxygen content is quite low. Another source of oxygen is the tantalum collector, but the collectors were all outgassed quite thoroughly by heating in high vacuum to 2100°C for several hours. Further, in order for any oxygen from the collector to be available for reaction with the molybdenum, it must have been transported to the liquid potassium pool in the crucible. So long as the collector is held at a slightly higher temperature than the crucible during the test period, there is a limited amount of potassium moving about the system. It therefore appears that there is some oxygen available to the molybdenum, and a reaction to form a Mo-O complex is possible. It is not possible, however, to determine whether this is indeed the cause of the high ΔH_s value shown by the data.

Table XXIII and Figure 58 summarize the data for the solution of niobium in potassium. In all, seventeen tests were performed with the niobium crucibles. Eleven of these showed full retention of the potassium and are listed. Of the samples whose potassium retention was low, four were the result of faulty brazes and the others were tests performed with non-braze joints. In addition to the tests of pure niobium, two tests of a niobium-1% zirconium alloy were performed and are reported in Table XXIII. The niobium data are plotted in Figure 58 and show a most peculiar pattern. First, the data scatter quite badly; second, there seems to be a reversal in the trend of solute concentration vs temperature; and third, there is no evidence of a kinetic effect for the one-half hour and the one hour tests.

The reason for the spread in the data is not known. The magnitudes of the concentrations are in the 10-200 wppm range, and the analytical chemistry procedures have been demonstrated to be accurate in this range. The formation of a $Nb-O_x$ dissolved species is a possibility, since such entities have been observed in other systems(44). In this connection, one can examine the possible sources of oxygen which might have access to the interior of the crucible-collector sub-assembly. First, there is the potassium itself, which for five of the runs had 14 wppm oxygen, and for six of the runs had 3.5 wppm oxygen. From this source, therefore, one can account for as much as 20 micrograms of oxygen being present in Runs 169, 171, 195, 199, and 200. In Runs 207, 209, 210, 215, 222, and 225, no more than 5 micrograms of oxygen is available from the potassium. The second source of oxygen is the crucible, whose initial oxygen content was reported to be 10 ppm. At this level one can account for about 200 micrograms of oxygen in the crucible metal. In addition, there is an unknown amount of oxygen which is introduced into the metal, even though steps were taken to minimize this source of contamination. However, one full monolayer of oxygen on the inner surface of the crucible would account for only two micrograms of oxygen. The third possible source of oxygen is the collector, although its outgassing treatment in vacuum at >2000°C is believed to reduce its oxygen content to a few ppm. The fourth possible source of oxygen is the capsule and cap material, although any oxygen originating from them would have to diffuse through the crucible or the collector wall, after being transported from the inner capsule wall. The probability of this transfer occurring during the solubility tests seems small in view of the fact that all the capsule parts were outgassed at 1800°C for several hours prior to their use at the lower temperatures. If any gaseous products were going to transfer from the capsule material, it seems quite likely that the transfer would occur much more

TABLE XXIII

Summary of Test Data for Niobium

Test No.*	Temp. °C	Time hr.	Oxygen Content of Potassium ppm	K gm	Nb µgm	Nb Conc. wppm
169	1200	8.0	14	0.9	31	33
171	1000	8.0	14	1.45	22	15
195	1200	4.0	14	1.19	41	34
199	1000	4.0	14	1.36	78	57
200	1200	1.0	14	1.40	86	61
207	1200	1.0	3.5	0.81	21	26
209	1200	0.5	3.5	1.21	87	72
210	1200	0.5	3.5	1.53	26	17
215	1200	4.0	3.5	1.47	43	29
222	1000	4.0	3.5	1.49	255	171
225	1000	8.0	3.5	1.35	118	88
219**	1000	8.0	3.5	2.27	N.D.	<1
224**	1200	4.0	3.5	1.84	11	6

*The tests listed are shown on Figure 58 with the test numbers.
**Nb-1% Zr alloy solute samples, shown in Figure 59.

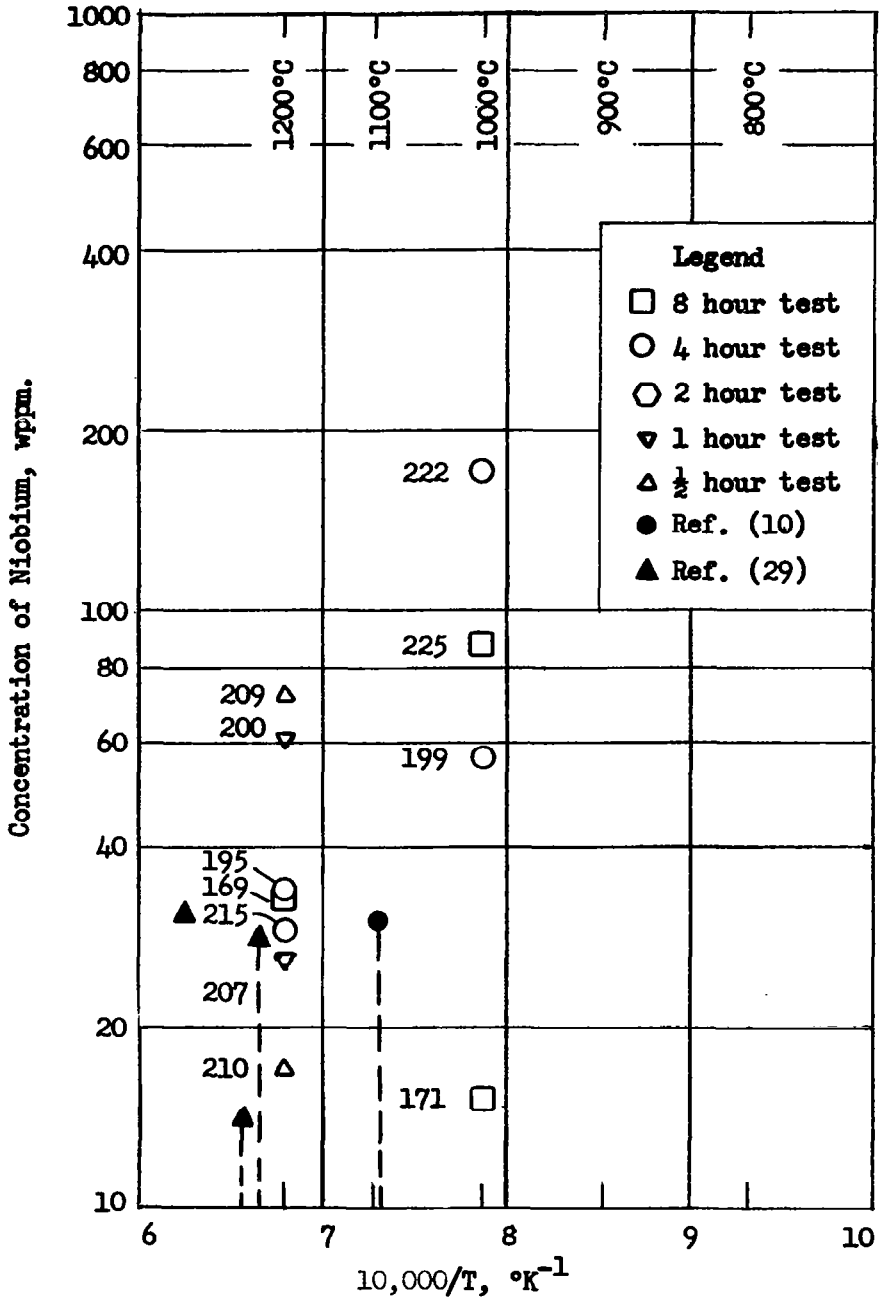

Figure 58. Concentration of Niobium Dissolved in Potassium. (Data from Table XXIII.)

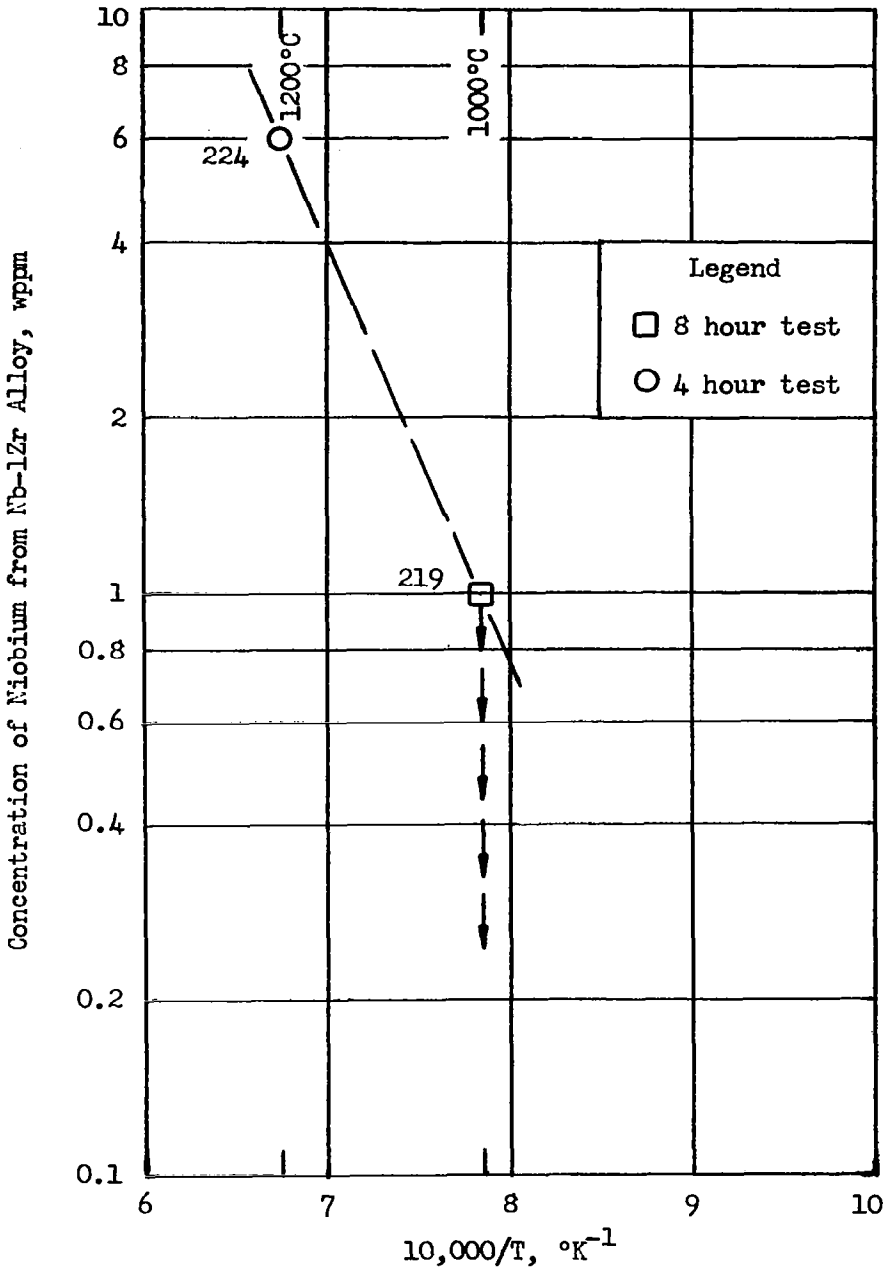

Figure 59. Concentration of Niobium from Nb-1Zr Alloy Dissolved in Potassium. (Data from Table XXIII.)

readily at the high temperature, and that the volatile components would be reduced to a concentration level at which the loss rate at even 1200°C would be extremely small.

Therefore, one can reasonably account for perhaps 250 micrograms of oxygen in each of the niobium crucibles. If all of this oxygen were to be combined with niobium as a Nb_2O_5 species, about 600 micrograms of niobium could be involved. Actually, the total amount of niobium found in the various niobium tests was in the range 400-500 micrograms per crucible. However, most of the oxygen which might be presumed to be available to complicate the niobium solution process is present in the niobium crucible. Therefore, its availability must be diffusion-controlled, and, because of this, one should find a greater influence of this oxygen in the early tests. As the crucible is used in successive tests and its contained oxygen is removed, its rate of transport to the surface must decrease, and the effect on the niobium solution should decrease. This is not borne out by the data. Examination of Figure 58 shows the results of tests to be mixed, with the later tests at a given temperature actually showing higher niobium concentrations. This observation does not negate the possible effect of oxygen on the solution of niobium in this system, of course, but it does suggest that the factor which is causing the scatter in the present data must involve other factors which are not yet understood.

The two tests of the Nb-1% Zr alloy shown at the bottom of Table XXIII are plotted in Figure 59. In the 1000°C measurement, no niobium was detected, so that its concentration was quoted as <1 wppm on the basis of the analytical limitations. A very tentative curve has been drawn on Figure 59, merely to show the minimum ΔH_S indicated for this solution process. This value is 32,700 cal/mol. However, one should use this ΔH_S with extreme caution because of its very tenuous foundation. The levels of concentration of niobium from the Nb-1Zr alloy are, however, quite interesting because in tests performed in exactly the same manner as those with the pure niobium, the observed amounts of dissolved niobium in the potassium solvent are nominally an order of magnitude less than the corresponding pure niobium data. This behavior has been attributed by others to the gettering effect of the zirconium. If this view is correct, then the solution of niobium must be quite dependent upon the oxygen content of the solute.

The present data are scattered in range of 10 to 100 wppm in the temperature range 1000° to 1200°C. Blecherman(10) gives data at 1095°C, which data show a slight dependence upon the oxygen content of potassium up to 3000 ppm, and then a large dependence between 3000 and 5000 ppm. Ginell and Teitel(29) show data for temperatures of 1130° to 1330°C, and report values from 10 to 31 ppm for niobium dissolving in potassium having 10-23 ppm oxygen. All these data are included in Figure 58. With the exception of the 1000-3000 ppm data of Blecherman for solution in potassium of very high oxygen content, the reported data and the present data are in qualitative agreement. There is an anomaly here, however, in that there does not appear to be a significant effect of oxygen on the data. Blecherman used potassium whose oxygen content was as high as 3000 ppm; Ginell and Teitel had 10 and 23 ppm O in their potassium, and the present work had 3.5 and 14 ppm O in the potassium. In spite of this 1000-fold variation in oxygen content, the reported values of niobium content do

not reflect this variation. However, an order of magnitude effect is observed in the present, low-oxygen-content potassium between the pure niobium and the Nb-1% Zr alloy tests. If the reason that the alloy is less soluble is that the zirconium acts as a getter for oxygen, should not the 1000 and 3000 ppm O data for pure niobium be higher than that for 3.5 - 23 ppm O? It therefore seems that one must conclude that the mechanism of solution of niobium in potassium is not yet understood.

Table XXIV and Figure 60 shows the data which were obtained from the tantalum tests. A total of fourteen tests were run, two of them being rejected due to operating difficulties. The data shown in Table XXIV are generally consistent and define a curve which has been evaluated by a least squares treatment to be,

$$\log (\text{wppm Ta}) = 5.2 - 2900/T.$$

The ΔH_s of this curve is 13,200 cal/mol, which suggests that there may be a reaction involved in the solution process for tantalum. This is not too surprising, in that the molybdenum data also show a moderately large ΔH_s. However, the level of the data is quite high in comparison with that obtained for niobium and molybdenum. One would expect the solubility of the more refractory tantalum to be in the same range as that of niobium, or possibly somewhat lower. The reason for its order-of-magnitude higher level is not at all clear.

The procedure used in these tests was the same as that used in the other tests, with the exception that a molybdenum collector was used instead of the usual tantalum collector. Because of this, the question was raised about the possibility of the molybdenum's effect on the test, and, specifically, whether it might be a source of a contaminant. Test #221 was therefore run using one of the triple-pass zone-refined iron crucibles as a collector. Examination of Figure 60 shows that its test result lies in the center of the pattern of data taken with the molybdenum collectors. Therefore, one must conclude that the presence of the molybdenum collector does not affect the solution process.

However, a difficulty was uncovered in the tantalum tests in that the chemical analysis for tantalum was found to be seriously affected by molybdenum. Since there were always many milligrams of molybdenum introduced in the etch processes, it was necessary to develop the two-stage extraction procedure described in Appendix III to separate the two metals. Because each additional handling step required in the analysis of the solutions introduces a small element of uncertainty in the final result, the uncertainty of each tantalum data point is higher than that for the other metals. However, this uncertainty is, at most, $\pm$10 ppm, so that it cannot reasonably be expected to affect the validity of the results.

The only other data reported for the solution of tantalum in potassium is that by Ginell and Teitel(29), who show values in the 17 to 138 wppm range in the temperature range 1130 to 1330°C. These data fall below the present data by a factor of about 20. These authors used their centrifuge apparatus with a vapor-deposited tungsten collector for these tests, and did not experience any complications in their analysis. This problem of the interference in the

TABLE XXIV

Summary of Test Data for Tantalum

Test No.*	Temp. °C	Time hr.	Oxygen Content in Potassium ppm	K gm	Ta ugm	Ta Conc. wppm
180	1000	8.0	14	0.94	490	552
181	1000	4.0	14	1.32	490	371
187	1100	8.0	14	0.69	475	688
188	1000	2.0	14	0.63	505	802
190	1100	4.0	14	1.09	2500	2290
191	1200	8.0	14	1.29	3717	2880
201	1200	4.0	14	0.50	760	1520
202	1000	4.0	14	0.89	728	817
206	1200	4.0	3.5	1.12	2062	1840
212	800	8.0	3.5	1.09	450	413
216	1000	4.0	3.5	0.71	1935	2730
221**	900	8.0	3.5	1.31	750	572

*The tests listed are shown on Figure 60 with the test numbers.

**Triple-pass zone-refined iron collector. All other tests used a molybdenum collector.

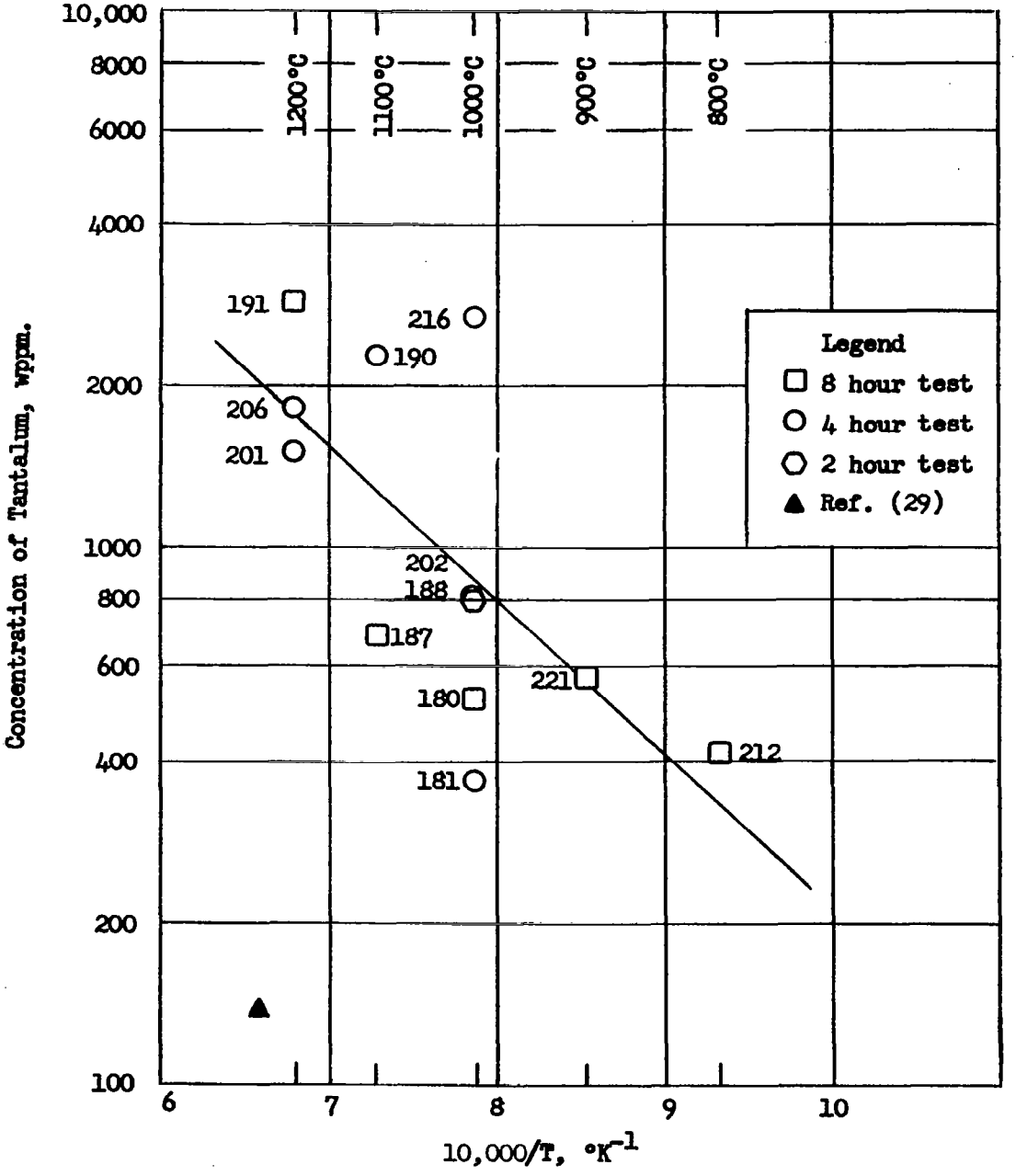

Figure 60. Concentration of Tantalum Dissolved in Potassium. (Data from Table XXIV.)

analysis remains as the major note of uncertainty in the present tests, but it cannot be resolved without additional work.

The question of oxygen and the formation of Ta-O_x species seems to be self-limiting in that the amounts of tantalum involved are very large, and would require as much as several tenths of a milligram of oxygen. Since no difference in the tantalum concentration was observed between the molybdenum and the zone-refined iron collectors, these are not likely to be a major source of oxygen. That leaves only the crucible and the potassium as potential oxygen sources. The potassium has from five to perhaps twenty micrograms of oxygen dissolved in it. The tantalum crucibles were used repeatedly, so that even if there were some oxygen initially in the crucibles it would certainly be noticeably depleted after several tests. Since there was no such indication, the crucibles must be ruled out as a significant source of oxygen. Therefore, it is unlikely that tantalum can be present in the solution as a TaO_x complex. There is, of course, the possibility that the small amount of oxygen which is known to be present might act as a catalyst and attack the tantalum wall to form a TaO_x species which then moves into the bulk potassium and decomposes to free the oxygen. But, there is a flaw in this hypothesis, too, in that if the presumed TaO_x species is not stable in bulk potassium, why should it form at all? Further, if this catalyst action is, in fact, operative in the tantalum-potassium system, why does it not appear in the niobium-potassium system? The answers to these questions are not immediately apparent.

At the outset of the program, it was intended that in addition to measuring the solubilities of the metals, an attempt would also be made to determine their rates of solution. To this end the surfaces contacted by the potassium were carefully treated by electropolishing to arrive at a reproducible surface condition. This surface area was then measured using the DLC technique and it was found that the 'true' area was within 10% of the projected area. Since 10% is the nominal uncertainty of the DLC technique, the electropolished crucible surfaces are considered to be smooth and their areas are equal to their projected areas.

In general, tests were run at 2, 4, and 8 hour durations as shown in Tables XXI-XXIV. Within this time span, the indications of a kinetic effect are sparse. The 800°C data for iron (Figure 56) suggest a trend, but at 1000°C run 197 (4 hrs) shows a higher iron concentration than does run 196 (8 hrs). In Figure 57, the 800°C molybdenum data run 176 (4 hrs) and run 173 (8 hrs) are in the correct relative position if there were a kinetic effect operating, but the 1100°C and the 1200°C data show the 8 hr data lying below the 4 hr data. In Figure 60, the 1000°C tantalum data are mixed. The highest and the lowest points are for 4-hour tests, while both 2-hour and 8-hour tests lie between. At 1100°C the 4-hour data lies above the 8-hour point. At 1200°C, however, the 8-hour point lies above the two 4-hour points.

Using these data as a basis, it was concluded that for these tests, there was no evidence for assuming that the solution process was not complete in two hours. For this reason, four tests were made at 1200°C in the niobium system in order to investigate kinetics in 1/2-hour and the 1-hour periods. Again, the data were inconclusive in that test 210 (1/2-hour) showed the lowest value

observed, but test 209 (1/2-hour) showed the highest value observed. Further, while test 207 (1-hour) showed the second lowest result, test 200 (1-hour) showed the second highest result. 4-hour and 8-hour values lie between the 1-hour (and the 1/2-hour) values. Again, in the 1000°C niobium data, the highest value is from a 4-hour test (run 222) and the lowest value is from an 8-hour test (run 171).

Therefore, the analysis of these data for their kinetic implications is not warranted. Further, the indications are that the factors which are operative in producing large variations in the solubility test results must be identified and controlled before meaningful data can be obtained.

In summary, the present studies, which were carried out under high vacuum conditions to minimize the contamination of the samples during testing and with very high purity solute and solvent materials have yielded data having a large amount of scatter for all four solutes tested. The present results obtained for the solution of iron in potassium are lower in magnitude than those reported by Swisher(77), whose materials were somewhat less pure, and they show a ΔH_S value which approaches that corresponding to a simple solution process. The molybdenum data, on the other hand, show rather low concentration levels, but do have a ΔH_S which is significantly larger than that which would correspond to a simple solution process. The niobium data are widely scattered, but are generally in agreement with the data presented by others. The reason for the variation in the niobium solution data is not known. The tantalum data show a well defined curve, and, although the concentration levels are high, the data appear to be consistent.

It is apparent that there are facets of liquid alkali metal solvent behavior which are little understood. The present study was initiated with the thought that by using very highly purified sample materials, and by preventing their contamination during handling and testing, one could obtain highly reproducible solution process data. Although the data obtained in the present study in which these precautions were taken does not meet the expectations of reproducibility, one cannot yet conclude that the original premise is wrong. However, to prove it to be correct may require such extreme measures with regard to sample purity and handling procedures that the cost of such research would be quite high.

PROJECT REPORTS ISSUED ON THIS CONTRACT

R. L. McKisson, R. L. Eichelberger, and J. M. Scarborough, "Solubility and Diffusion Studies of Ultra Pure Transition Elements in Ultra Pure Alkali Metals," First Quarterly Report, AI-9151, November 6, 1963.

R. L. McKisson, R. L. Eichelberger, and G. R. Argue, "Solubility and Diffusion Studies in Alkali Metals," Second Quarterly Report, AI-64-5, February 7, 1964

R. L. McKisson, R. L. Eichelberger, G. R. Argue, and J. M. Scarborough, "Solubility and Diffusion Studies in Alkali Metals," Third Quarterly Report, NASA-CR-54093 (AI-64-75), May 11, 1964.

R. L. McKisson, R. L. Eichelberger, G. R. Argue, and J. M. Scarborough, "Solubility and Diffusion Studies in Alkali Metals," Fourth Quarterly Report, NASA-CR-54094 (AI-65-156), August 10, 1964.

R. L. McKisson and R. L. Eichelberger, "Solubility and Diffusion Studies in Alkali Metals," Fifth Quarterly Report, NASA-CR-54095 (AI-64-235), November 16, 1964.

R. L. McKisson and R. L. Eichelberger, "Solubility and Diffusion Studies in Alkali Metals," Sixth Quarterly Report, NASA-CR-54096 (AI-65-15), March 5, 1965.

R. L. McKisson and R. L. Eichelberger, "Solubility Studies in Alkali Metals," Seventh Quarterly Report, NASA-CR-54097 (AI-65-93), June 2, 1965.

AI INTERNAL REPORTS ISSUED ON THIS CONTRACT

G. R. Argue, W. A. McCollum, and H. L. Recht, "Double Layer Capacitance Measurements on Ta, Mo, and Nb," AI-TDR-9773, May (1964).

R. L. McKisson, "Analysis of the Freezing Point Depression Technique of Determining Impurity Content of Alkali Metal," AI-TDR-9404, March (1964).

G. R. Argue, H. L. Recht, and W. A. McCollum, "Double Layer Capacitance Measurements on Iron Crucibles to Determine Surface Area," AI-TDR-64-229, December (1964).

APPENDIX I

Specification for Environmental Test System for NASA Contract NAS3-4163, (Revised)

1. Scope

This specification defines a complete set of high vacuum chambers for use in performing solubility studies of ultra pure transition elements in ultra pure alkali metals. All work from design through installation and testing shall be provided by the supplier.

2. Applicable documents

The following documents form a part of this specification, and the equipment supplied must conform to the applicable code provisions:

a. City of Los Angeles Building Code, Plumbing and electrical sections
b. California Industrial Code

3. General description

This system shall include a) five stainless steel chambers, b) a separate vacuum pumping system for each, c) vacuum instrumentation, d) appurtenances necessary to complete the test system, as detailed below.

4. Detailed description. Refer to Figure 61 for relative positions of components.

a. Vacuum chambers

All metal parts which "see" high vacuum in this system, except those specifically excluded in this specification, shall be fabricated of type 304 stainless steel meeting ASTM Specification A-240. The vacuum chambers shall be structurally designed in accordance with good vacuum practice to avoid virtual leaks and traps for contamination. All welded joints shall be continuously welded on the vacuum side and skip welded on the outside for strength, and shall be made by certified welders. Welds must be sound as determined by a standard dye penetrant check, but need not be radiographed. Welds need not be ground flat. The interior of the vacuum chambers shall be polished to a #4 finish after fabrication.

All chambers shall have dished bottoms, and domed, flanged lids. Each lid shall be sealed to its chamber by a double O-ring seal with a pump-out fitting between the O-rings. The flange shall have 18 bolt holes, with clearances so that the lid will be usable in any bolt hole alignment position.

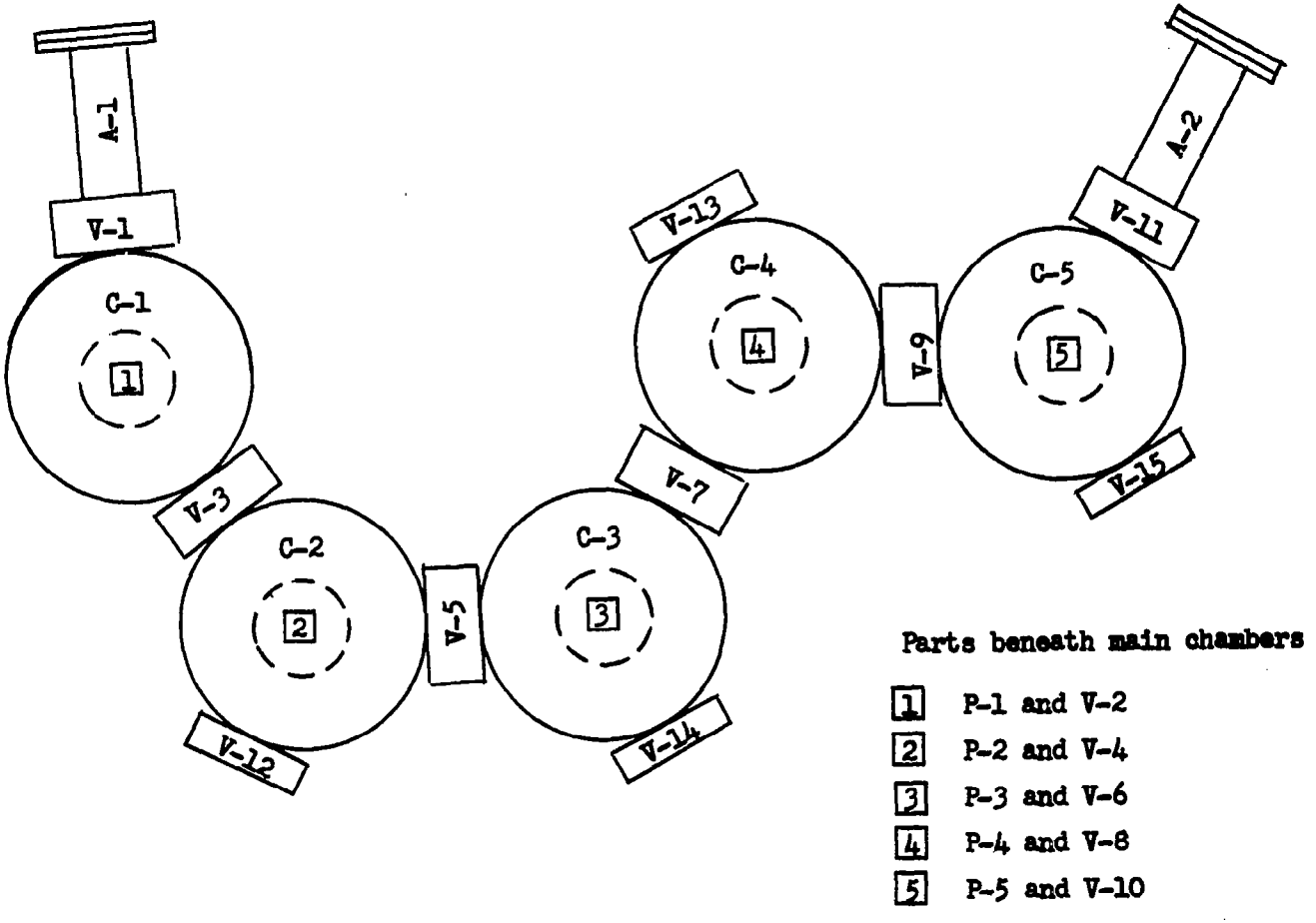

Figure 61. Relative Positions of Components of Environmental Test System.

Each chamber shall have a system of copper cooling coils soft-soldered to the exterior of the chamber with 50-50 lead-tin solder. Each cooling system shall be capable of maintaining the chamber wall at or below 40°C (120°F) under a total internal heat load of 3 kw.

The domed lid for each chamber shall have two 6" diameter viewing ports with centers on a diameter of the chamber. The glass shall be double O-ring sealed on the vacuum side with a pump-out between the rings. One lighting fixture sized to fit a viewport shall be provided for each lid.

The domed lid for each chamber shall have a flange to accept a RYE Controls manipulator, Model MLHT, and shall be provided with a cover for use in the acceptance tests. Each chamber shall have three four-inch ports or equivalent for the introduction of electrical leads and thermocouples. A total of eight 20-amp electrical feed-throughs and twenty thermocouple feed-throughs shall be provided in the cover plates of these ports in each chamber.

Each chamber shall have a circular floor plate with a 3/4" raised lip around the circumference, with the plate at the level of the lower weld.

Each chamber shall be provided with two ports in the side to accept RYE Controls manipulators, model MLHT, which ports shall be provided with covers. The centers of these ports shall be 12" above the floor plate, and opposite the entrance ports.

Each chamber shall have two hangers for storage racks extending around the inner circumference of the chamber, except where other equipment renders it impractical, one 9" above the floor plate level and one 16" above the floor plate level. These hangers shall consist of a stainless steel strip nominally 1/8" thick by 1" high, set out 1/4" from the chamber wall.

Specific details unique to individual chambers are as follows:

C-1: 24" nominal diameter, 22" from top flange to the weld between the dished bottom and the cylindrical portion. There shall be a 2" port on the side for introduction of potassium.

C-2: 24" nominal diameter, 18" from top flange to the weld between the domed bottom and the cylindrical portion. Ports shall be provided for an electron-beam welder and three rotary feed-throughs CVC Type SR-75. These rotary feed-throughs shall be provided and installed in place. There shall also be a glove port attached to a 6" stainless steel valve. The centerline of this port shall be 8" above the floor plate level.

C-3, C-4, and C-5: These three chambers are identical, 24" nominal diameter, 22" from top flange to the weld between domed bottom and cylindrical portion. Each shall have a glove port identical to that in C-2.

b. Antechambers. A-1 and A-2 are identical, nominally 15" long and 5" in internal diameter. The end plate is O-ring sealed, and fastened to the antechamber with bolts equipped with wing nuts, or equivalent fasteners.

c. Pumping systems. Pumping systems P-1, P-2, P-3, and P-4 (Figure 59) are identical and each consists of the following:

15 cfm mechanical pump, Welch #1397
6" diffusion pump, NRC HS6-1500 with cold cap, with DC-705 pump fluid
Water baffle, NRC HW-6, 0318-6
Liquid nitrogen trap, NRC HN-6, 0315-6

The mechanical pump shall be fitted with a vibration isolator in the suction line, and shall be mounted to minimize the transmission of vibration to the chambers. The liquid nitrogen trap shall have provision for automatic filling. An oil trap shall be provided between the mechanical pump and the diffusion pump. Each diffusion pump must have fail-safe devices with manual re-set for protection in case of water or power failure. An adequate roughing line shall be provided, by-passing the diffusion pump, baffles, and 6" valve, to permit rough pumping of the chamber.

Pumping system P-5 consists of the following:

15 cfm mechanical pump, Welch #1397
6" diffusion pump, CVC Model MHG-300A, with charge of triple distilled mercury.
Water baffle, NRC HW-6, 0318-6
Liquid nitrogen trap, NRC HN-6, 0315-6

Automatic liquid nitrogen fill, fail-safe devices, and roughing line shall be provided as for P-1, etc. A molecular sieve trap system shall be provided between the diffusion pump and the mechanical pump.

Pumping systems P-6 and P-7 consist of the following, for pumping the antechambers:

Mechanical pump, Welch #1405
Diffusion pump, NRC H-2-P, with DC 705 pumping fluid.
Water baffle, NRC EB2-02-WC
Liquid nitrogen trap, NRC 0314-C4

Pumping system P-8 consists of a Welch #1402 (5 cfm) mechanical pump. It is connected to a vacuum manifold $1\frac{1}{2}$" nominal diameter, which in turn is connected to all the pump-out fittings on manipulators, valves, etc.

d. Valves. V-2, V-4, V-6, V-8, and V-10, joining the 6" liquid nitrogen traps to the vacuum chambers and V-12, V-13, V-14, and V-15 on the four glove port attachments (a total of nine) shall be General Technology Corporation SVS-61 manually operated stainless steel valves.

V-1, V-3, V-5, V-7, V-9, and V-11, joining the vacuum chambers to each other and to the antechambers, shall be General Technology Corporation SVS-41, manually operated stainless steel valves.

e. Vacuum readout equipment. Twelve Bayard-Alpert gauges, NRC 553P, shall be installed using stainless steel fittings so that they see the test space in the various enclosures as follows: one each on A-1 and A-2, two each on C-1, C-2, C-3, C-4, and C-5.

Thirteen thermocouple gauges, NRC 521, shall be installed as follows: one each on C-1, C-2, C-3, C-4, C-5, one on the oil trap in each 6" pumping system, one on the high vacuum manifold for the antechambers, one on the roughing line of P-6, and one on the roughing line of P-7.

There shall be three vacuum gauge controls, NRC Model 763. These shall be connected to the Bayard-Alpert and thermocouple gauges through a switching apparatus.

f. High vacuum seals. All flanged joints sealing the high vacuum region shall be double O-ring sealed where practical, with a pump-out connection between the O-rings. All inner O-rings shall be Viton-A; outer O-rings may be neoprene.

g. Support Structure. The environmental test system shall be supported by a suitable welded angle-iron frame. Each leg shall be fitted with a leveling screw which has a total adjustable travel of $2\frac{1}{2}$ inches. All external surfaces and steel framing shall be protected with grey hammertone industrial finish.

5. Performance requirements

All performance requirements are with a clean, dry, empty chamber with all accessories installed, except manipulators.

a. Vacuum, C-1, C-2, C-3, and C-4

i. Ultimate pressure: 1×10^{-7} Torr.
ii. Pump down time: 1 atmosphere to 1×10^{-6} Torr within one hour.

b. Vacuum, C-5 (mercury diffusion pump system)

i. Ultimate pressure: 5×10^{-6} Torr.

c. Vacuum, A-1 and A-2 (antechambers)

i. Ultimate pressure: 1×10^{-6} Torr.

6. Performance demonstration

The supplier shall perform qualification tests at the manufacturing plant. Then the supplier shall install the system in the specified AI laboratory and demonstrate that the system meets all the performance requirements specified herein. This shall include at least the following:

a. Demonstration of pump down time and ultimate pressure.

b. Demonstration of system leak rate with a Veeco MS-9 or equal helium mass spectrometer to be less than 5×10^{-10} cc/sec.

7. Work responsibility

The supplier shall be responsible for the complete design, fabrication, assembly, delivery, erection on site, and the checkout and demonstration of performance within the requirements of the contract. The installation of the system shall meet the City of Los Angeles plumbing and electrical code where applicable and carry the city electrical seal of approval. Within 20 days after the award of the contract, installation drawings shall be submitted in triplicate showing all required utility and installation services not furnished by the vendor. Operating weights of each major component and operational and maintenance space requirements shall be shown. The supplier shall furnish 3 copies of drawings for review prior to initiating any fabrication. Upon specific approval of AI project management, the supplier may initiate fabrication of parts of the assembly. Three copies of final drawings will be furnished no later than 45 days after the award of the contract. On delivery of the system, the supplier shall furnish 3 copies of test certifications and verification of conformance to design requirements noted on the drawings, including materials and processes. The supplier shall provide three (3) copies of operating, maintenance, and spare parts manuals.

APPENDIX II

Analytical Procedures

Analytical procedures used to determine solute concentrations in potassium, and to measure the concentration of certain impurities in both the solvent potassium and the solute crucibles, are detailed in this Appendix.

Preparation of Potassium Samples for Colorimetric Analyses

The potassium samples submitted for the various metal analyses are all treated in the following manner.

The potassium sample as received is melted from the collector into specially cleaned glassware in a recirculating inert atmosphere glove box. The potassium is then reacted with water vapor in a helium atmosphere, acidified with hydrochloric and hydrofluoric acids and diluted to a known volume. The potassium remaining in the collector after the melting procedure is dissolved very slowly in water which is added by means of a hypodermic syringe. The collector

is then rinsed with HCl and the rinsings combined with the solution of the potassium that was left in the collector. The solution in the flask is then acidified with hydrofluoric acid and diluted to a known volume.

In general, two acid etches are made on the collector. The first etch is concentrated hydrofluoric acid and the second etch is a mixture of nitric and hydrofluoric acids. The etches are diluted to volume in separate flasks and analyzed separately.

Very early in the program all the etches and solutions of potassium samples were combined into one solution.

Preparation of Potassium Samples for Spectrographic Analysis

Potassium samples for spectrographic analysis are processed inside a re-circulating inert atmosphere glove box. The potassium is transferred from the original container into a platinum boat without coming into contact with any other material. The sample is then removed from the glove box and dissolved in water. Hydrochloric acid is added to the sample to convert it from the hydroxide to the chloride salt. The salts are then dried at 80°C for three hours in a vacuum oven.

Spectrographic Analysis of Potassium

10 mg of the chloride salt as prepared above is weighed into a tantalum boat using a teflon spatula, and loaded into an electrode. The electrode, containing the sample, is excited with a DC arc and a photograph of the spectrum is obtained on two 4" x 10" glass plates. These spectrographic plates are evaluated by visually comparing the densities of the specified analytical lines of the impurity elements with the densities of corresponding element lines on standard plates.

Determination of Iron in Potassium, Molybdenum, and Tantalum

Principle

Iron is reduced to the bivalent state with ascorbic acid and hydroxlamine hydrochloride. The iron II forms a red complex with bathophenanthroline, and is determined spectrophotometrically. Ammonium tartrate is added to complex the molybdenum and tantalum. Boric acid is present to complex the fluoride ion. The standard deviation in the 1 to 12 μg range is 0.7 μg Fe. Standard deviation in the range of 80 to 100 μg is 3.1 μg while in the range of 100 to 250 μg the standard deviation is 5.9 μg Fe. The method is adapted from that reported by Penner and Inman (61).

Reagents

1. Bathophenanthroline, 0.001 M.

2. Ammonium Tartrate, 25% (iron free).
3. Boric Acid, 5% (iron free).
4. Hydroxlamine hydrochloride, 10% (iron free).
5. Ascorbic Acid, 10%.
6. Thiourea, 5%.
7. Sulfuric Acid, 1:1.
8. Ammonium Hydroxide, 28% NH_3, Reagent Grade.
9. Iso-Amyl Alcohol, Reagent Grade.

Procedures

Samples containing 1 to 50 μg iron are measured into small beakers. Formic acid is added to destroy the NO_3^- ion. The sides of the beakers are washed down, and ammonium tartrate solution is added followed by heating, cooling, and the addition of boric acid. After a twenty minute waiting period 0.5 ml of 1:1 H_2SO_4, 3 ml of ascorbic acid and 2 ml of hydroxlamine hydrochloride are added and the sample is allowed to stand for ten minutes. The pH is adjusted to 5.5 with ammonium hydroxide and the sample is diluted to 25 ml in a graduated separatory funnel. Thiourea is added and the sample is allowed to stand for five minutes. Bathophenanthroline is added and after 15 minutes the iron complex is extracted into iso-amyl alcohol. The optical density of the iso-amyl alcohol extract is read against a reagent blank in a Beckman D.U. spectrophotometer at 536 mμ. The iron concentration is found from a calibration curve prepared at the same time as the sample.

Determination of Molybdenum in Potassium and Tantalum

Principle

Dithiol reacts with molybdenum in solution to give the green complex of molybdenum VI. Iron II added in the form of ferrous sulfate accelerates the reaction between dithiol and molybdenum at room temperatures. Citric acid complexes tungsten and prevents its reaction with dithiol and boric acid is present to complex the fluoride ion. The average standard deviation in the range of 1 to 50 μg is 0.5 μg Mo. The method is based on that published by Sandell (70).

Reagents

1. Dithiol (Toluene - 3, 4 dithiol), 0.2% in 0.25 N NaOH.
2. Sulfuric Acid, 1:3.
3. Boric Acid, 4%.
4. Citric Acid, 50%.
5. Ferrous Sulfate, 1 ml = 1 mg Fe.
6. Iso Amyl Acetate, Reagent Grade.
7. Molybdenum Standard, 1 ml = 2 μg Mo.
8. Phosphoric Acid, 85%.

Procedure

To a 125 ml separatory funnel add 15 ml boric acid reagent followed by a sample containing 1 to 25 μg molybdenum. Then four ml of 1:3 sulfuric acid, three drops of phosphoric acid, 1 ml of citric acid reagent, and 1 ml of ferrous sulfate solution are added. Dilute to 20 ml, add 2 ml of the dithiol solution, and allow to stand at room temperature for two hours. The molybdenum complex is extracted with two portions of iso-amyl acetate, exactly 15 ml and 10 ml respectively. The organic layer is drained into a 40 ml vial, capped and centrifuged. The optical density of the iso-amyl acetate extract is read against a reagent blank in a Beckman D.U. spectrophotometer at 670 mμ. A calibration curve is prepared at the same time as the samples.

Determination of Niobium in Potassium and Tantalum

Principle

In strong hydrochloric acid solutions niobium forms a yellow thiocyanate complex which is extracted with di-ethyl ether and can be determined spectrophotometrically. Tartaric acid is added to prevent hydrolysis of tantalum, and stannous chloride is added to reduce the iron. Boric acid is present to complex the fluoride ion. The method used is that of Bukhsh and Hume (16). The average standard deviation in the range of 20 to 70 μg Nb is 2.2 μg.

Reagents

1. Boric Acid, 4%.
2. Ammonium Thiocyanate, 23%.
3. Stannous Chloride - Tartaric Acid Reagent, 15% $SnCl_2$-1M Tartaric Acid.
4. Hydrochloric Acid - Tartaric Acid Reagent, 9M HCl - 1M Tartaric Acid.
5. Di-ethyl Ether, Reagent Grade.

Procedure

A sample containing 1 to 50 μg niobium is measured into a separatory funnel. The following reagents are added in rapid succession with mixing after each addition: 10 ml of boric acid, 5 ml of ammonium thiocyanate, 2 ml of stannous chloride-tartaric acid reagent, and 5 ml of hydrochloric acid-tartaric acid reagent. After five minutes the sample is extracted with di-ethyl ether. The layers are separated and the ether phase collected in a 25 ml volumetric flask. The ether extraction is repeated on the aqueous phase after additional ammonium thiocyanate and hydrochloric acid-tartaric acid reagents are added. The combined ether extracts are diluted to 25 ml. After standing for thirty minutes the optical density of the ether extract is read on a Beckman D.U. spectrophotometer at 385 mμ against a reagent blank. The concentration of niobium is read from a calibration curve prepared at the same time as the samples are run.

Determination of Tantalum in Potassium and Etch Solutions in the Absence of Molybdenum and Iron

Principle

Phenylfluorone forms a bright red complex with tantalum in slightly acid solution. Interference from some metals present as impurities is avoided by a preliminary extraction of tantalum with iso-butyl ketone from a HCl-HF medium. EDTA is added to complex co-extracted metals and boric acid is added to complex the fluoride ion. This is an adaptation of Luke's method (90).

Reagents

1. Tantalum Standard, 25 μg/ml.
2. Acetate Buffer Solution, pH 4.5, containing 5 g. gelatin per liter.
3. Hydrochloric Acid - Hydrofluoric Acid Solution, 20 ml HCl + 20 ml HF + 300 ml H_2O.
4. Phenylfluorone, 0.01% in methanol.
5. Hydrofluoric Acid, 1:99.
6. Methyl Isobutyl Ketone (MIBK), Reagent Grade.
7. Boric acid, 40 g per liter.
8. Ethylenediamine Tetra-acetic Acid, Disodium Salt (EDTA), 10%.

Procedure

A sample containing 10 to 125 μg Ta is measured into a 50 ml teflon beaker and evaporated to dryness in a water bath. After the sample has cooled, 5 ml of HCl-HF solution is added and the sample transferred to a separatory funnel. The beaker is rinsed with an additional portion of HCl-HF solution. The tantalum is extracted with 5 ml of the MIBK. The extraction is repeated and the combined MIBK extracts are transferred to teflon beakers and evaporated to dryness.

The organic material is then destroyed by the addition of 0.25 ml HNO_3 + 0.25 ml $HClO_4$ and evaporating to fumes of $HClO_4$. The evaporation with HNO_3 and $HClO_4$ is repeated, the sample taken to dryness, and the residue dissolved by adding 1 ml of HF (1:99). After the sample has cooled, 5 ml of EDTA solution, 10 ml of buffer solution, and 10 ml of phenylfluorone solution are added. After a thirty minute wait 5 ml of boric acid solution is added, the flask is diluted to volume with acetic acid (1:9), and the optical density is read against a reagent blank in a Beckman D.U. spectrophotometer at 530 mμ. A calibration curve is prepared simultaneously with the samples.

Determination of Tantalum in Potassium and Etch Solutions in the Presence of Molybdenum or Iron

Principle

Both molybdenum and iron form colored complexes with phenylfluorone, and therefore interfere with the determination of tantalum by the previously described method. When more than 1 mg of an interfering element is expected to be present in the portion taken for color development, a preliminary separation by solvent extraction is required. Under the proper conditions methylisobutyl ketone ("Hexone") will extract tantalum preferentially from aqueous solution. This extraction, as described by Kolthoff and Elving (50), is the basis for this method.

Reagents

1. HF Acid Mixture No. 1 - Carefully add 320 ml conc. H_2SO_4 to 150 ml H_2O and allow to cool. Weigh out 82 g NH_4F and dissolve in 340 ml conc. HF. When solutions have cooled, mix together and dilute to 1 liter in a polyethylene bottle.

2. HF Acid Mixture No. 2 - Carefully add 400 ml conc. H_2SO_4 to 75 cc H_2O and allow to cool. Weigh out 103 g NH_4F and dissolve in 425 ml of conc. HF. Mix solutions together and dilute to 1 liter in a polyethylene bottle.

3. Hexone (methylisobutyl ketone) - Distill reagent grade hexone and collect fraction boiling at 114-116°C. Equilibrate by shaking 900 ml hexone (distilled) with 100 ml HF Acid Mixture No. 1.

Procedure

Transfer an aliquot containing up to 50 mg Mo to a 100 ml teflon beaker and evaporate to dryness. Cool, add 0.5 ml conc. HNO_3 and 0.5 ml conc. $HClO_4$ and fume to near dryness. Cool, and 0.5 ml conc. HNO_3 and repeat the evaporation to dryness. Cool, add 50 ml of HF Acid Mixture No. 1. Carefully transfer the solution to a 200 ml polyethylene bottle without washing. Add 50 ml of Hexone reagent and tighten the cap of the bottle. Place the bottle on a mechanical shaker and shake for 15 minutes. Separate the top (organic) layer with polyethylene equipment and retain. Discard the aqueous layer, wash the bottle, and return the organic layer to the bottle. Add 50 ml of HF Acid Mixture No. 1 and replace the bottle on the shaker. Shake for 15 minutes and again remove the top layer, discard the aqueous layer, and return the organic layer to the bottle.

Add 25 ml of 5% H_2O_2, replace the cap and return the bottle to the shaker for 15 minutes. Remove the organic layer and discard. Transfer the aqueous layer to a 100 ml teflon beaker and place on a hot plate. The presence of a yellow color at this point indicates considerable Mo has accompanied Ta through the extraction. In this case, it is necessary to evaporate the solution to dryness, take up in 50 ml of HF Acid Mixture No. 1, and repeat the extraction cycle. If no appreciable yellow color is noticed, the solution is evaporated to dryness and the salts taken up in 1 ml of 1:99 HF, and diluted to a convenient volume. Color development is then carried out on a suitable aliquot as in the previous procedure.

Determination of Manganese in Iron

Principle

Manganese is oxidized to permanganate with potassium periodate. The analysis is performed in a phosphate medium to reduce the interference of high concentrations of iron. The permanganate ion serves as its own chromogenic agent. This is an ASTM standard method (4).

This procedure was used for the analysis of a sample of iron crucible material.

Preliminary tests showed the sample to contain less Mn than any standard iron available; therefore, the sample was used as the matrix material to verify the procedure and Mn was determined by the "Method of Additions."

Reagents

Manganese Standard: 1.00 mg Mn metal dissolved in sulfuric acid and diluted to 100 ml. Final concentration: 10 μg Mn/ml.

Acid Mixture: 250 ml conc. HNO_3, 125 ml 85% H_3PO_4, and 100 ml conc. H_2SO_4 diluted to 1000 ml with water.

Potassium Periodate: 10 g KIO_4 dissolved in 10 ml of the acid mixture and diluted to 100 ml with water.

Procedure

4.991 g of the iron sample was dissolved in 125 ml of the acid mixture plus 20 ml of 85% H_3PO_4. The solution was diluted to 200 ml with water. Nine 20 ml aliquots of the Fe sample (0.4991 g/aliquot) were pipetted into 50 ml volumetric flasks. Five of the aliquots were spiked with known quantities of the Mn standard. 5 ml of KIO_4 solution was added to each of the spiked aliquots as well as to two of the unspiked aliquots. Nothing was added to the remaining sample aliquots which were used as reference solutions.

All aliquots were heated to boiling, cooled, and diluted to 50 ml with water and the optical densities of the resultant solutions were measured against a reagent blank. Results are tabulated below. All aliquots contained 0.4991 g of iron sample.

μg Mn Added	Results O.D.	O.D. minus reference
0 (no KIO_4)	0.181	-
0 (no KIO_4)	0.180	-
0	0.181	0.0
0	0.181	0.0
3.0	0.217	0.036
4.0	0.230	0.049
5.0	0.245	0.064
8.0	0.277	0.096
10.	0.298	0.117

Thus, no Mn was detected in the sample and the procedure was verified with a maximum deviation of about 5% from the best straight line drawn through the points.

Determination of Oxygen in Potassium

Principle

Potassium is separated from potassium oxide by repeated extraction by mercury. Potassium oxide is insoluble in mercury and floats on the surface of the amalgam. The method is based on that of Pepkowitz and Judd (62).

Reagents

Standard HCl (app. 3N)
Standard NaOH (app. 3N)
Triple Distilled Mercury

Procedure

The complete amalgamation of the sample is performed inside a recirculating inert atmosphere glove box. The sample is removed from the sample container and placed inside the reaction vessel. Degassed mercury (40 ml) is added and heat is applied until the potassium melts. The reaction vessel is shaken for one minute and allowed to stand fifteen seconds. All but 1 ml of the amalgam is drained from the reaction vessel. Mercury (10 ml) is added to the reaction vessel and the shake, stand, and drain cycle is repeated a total of five times. From the last extraction, a portion of the amalgam is drained into a separate container to be analyzed for residual potassium. The exact potassium content of this portion of amalgam is determined by extracting 5 ml of the amalgam with 20 ml of 0.01N HCl and determining potassium in the aqueous phase by flame photometry. The remaining amalgam drainings are combined. The reaction vessel containing approximately 1 ml of mercury is washed with water containing phenolphthalein (to indicate complete removal of any oxide), acidified, and diluted to a known volume. Potassium content is determined by flame photometry. The contributions of the small quantity of residual potassium in the 1 ml mercury extract is subtracted from the total potassium content to obtain net potassium due to the oxide. Sample weight is determined by extracting the amalgam with the standard HCl and back titration with the standard NaOH.

Determination of Nitrogen in Potassium

Principle

Nessler reagent (K_2HgI_4) reacts with ammonia to form a reddish brown colloidal compound. The optical density of this compound is measured on a spectrophotometer. This method is adapted from that described by Boltz (12).

Reagents

H_2SO_4, 0.0002N.
Nessler Reagent.
Nitrogen Standard, 1 ml=1 μg Nitrogen.

Procedure

Purge a distillation flask with helium before placing sample in the flask, and introduce 1 gm sample of K. Leave purge on throughout entire analysis. Water is added dropwise to the distillation flask until the sample is dissolved and then 10 ml water is added in excess. Distill 8-10 ml of the solution

over into 10 ml of the H_2SO_4 reagent in the receiving flask. Transfer the distillate to a 25 ml volumetric flask, add 0.75 ml Nessler reagent, bring to volume, and let stand 15 minutes for color development. The optical densities of the standards and sample are read against a water blank in a Beckman Spectrophotometer at 430 m_μ.

Determination of Elemental Carbon in Potassium

Principle

The sample of potassium metal is dissolved in H_2O and acidified with 1:1 H_2SO_4. The resulting solution is evaporated to approximately one-third the original volume and the wet oxidation with Van Slyke reagent is performed on the slurry. The liberated CO_2 is quantitatively determined by gas chromatography. The method is described by Van Slyke and co-workers (81, 82).

Reagents

Van Slyke Reagent - (39.0 g CrO_3, 495 ml H_2SO_4 (15% SO_3), and 255 ml 85% H_3PO_4. The mixture is allowed to stand for two hours at 145°C ± 5°C and then cooled to room temperature prior to use.)

H_2SO_4 Solution - 100 ml H_2SO_4 (36N) are added to an equal volume of distilled, carbonate free H_2O.

Apparatus

Gas Chromatograph - Loenco Model 15B Gas Chromatograph.

Column - 2' x $\frac{1}{4}$" activated silica gel.

Oven Temperature - 90°C.

Carrier Gas - helium - 40 cc/min.

Filament Current - 100 milliamperes.

Oxidation Apparatus - This apparatus consists of a reaction vessel, a burette with a teflon stopcock for introduction of the Van Slyke reagent, and an analytical train containing a water trap and a MnO_2 trap (SO_2 adsorption). The train is directly connected to a gas sampling valve fitted with a glass wool packed-loop for CO_2 condensation.

Procedure

A sample of the potassium metal (~1 g) is transferred from a tared glass weighing bottle into a reaction flask which has been purged with argon. Exactly 10.0 ml of H_2O is slowly added to reaction flask containing the potassium metal. After complete dissolution of the potassium has been effected, 5.0 ml of the H_2SO_4 solution is added and the resulting aqueous

K_2SO_4 is evaporated down to approximately 5 ml. The salt "slurry" is allowed to cool to room temperature. The reaction flask is then fitted onto the oxidation apparatus and the system is purged with helium for ~10 min. 10.0 ml of Van Slyke reagent is introduced into the reaction flask and the mixture is heated to boiling for 30 min. The resulting CO_2 is condensed on the glass wool-packed loop which has been cooled with liquid nitrogen. The flask containing the liquid nitrogen is replaced with one containing H_2O at ~100°C. The CO_2 expands into the gas chromatograph for a direct readout on a strip chart recorder.

Calibration

The calibration of the apparatus is carried out by acidification of high purity $BaCO_3$ and oxidation of reagent grade potassium acid phthalate.

APPENDIX III

Procedures for the Measurement of the Surface Area Using the Double Layer Capacitance Technique

The double layer capacitance (DLC) of a surface in contact with an aqueous electrolyte originates from the fact that on any such surface adsorption of charged ions occurs. The nature, charge, and extent of adsorption of the ions is a function of the potential of this surface, among other factors. The capacitance measurement either at constant current or voltage then measures the effective capacitance of a condenser formed by the surface, the distribution of the ions on the surface of the samples, and the ions very close to the surface.

For many metal surfaces in contact with aqueous electrolyte solutions, the DLC is relatively constant over a potential region just anodic to the region of H_2 gas evolution. In this region the surface of the metal is presumably covered by a layer of adsorbed H^+ ions or H atoms. This region is one in which no oxidation of the metal surface occurs. Measurements of the DLC for purposes of surface area determination are best carried out at the cathodic portion of this "flat" region. This region is determined by measuring the DLC *vs* the potential of the sample and examining the results. From this, the best value of applied potential for use in the measurements is identified. Once this is determined, measurements of DLC are made on a specimen of known surface area. (In the present case, these are electro polished surfaces of known geometric area of an assumed surface roughness of 1.10 ± 0.05.) The DLC is then measured for samples of any shape and size and their true surface areas determined by a simple calculation.

A procedure was designed to measure the double layer capacitance of single crystal samples of Nb, Ta, and Mo, and ultra pure polycrystalline Fe. The procedure used and the data obtained from these samples were then used to measure the surface areas of the crucibles used in the alkali metal solubility study.

Experimental

The experimental steps involved in measuring the true surface area of the metal samples were:

1. Mount the samples in metallurgical resin and measure the apparent physical area.

2. Mechanically polish.
3. Electropolish to maximum smoothness.
4. Examine under a microscope to check the surface condition.
5. Measure the double layer capacity.
6. Calculate the capacity per cm^2 assuming a roughness of 1.1.

Most of these steps required experimental work to perfect the techniques. Therefore, it is useful to describe the complete procedure and indicate the trouble spots.

After the standard specimens were mounted, they were mechanically polished on a metallurgical wheel starting with 180 mesh SiC and decreasing to 600 mesh SiC grit. They were then polished with .5 μ Al_2O_3 (Linde) to a mirror-bright, nearly scratch-free, surface. Iron samples were additionally polished with a dry micro-cloth.

The refractory metals were electropolished in a solution of 4.5% H_2SO_4 and 1.25% HF in methanol (U.S. Patent 3,033,769, R. F. Cortes), at a voltage of 20 volts and a current density of 3 amps/sq. cm. Iron samples were polished in an electrolyte consisting of 300 ml H_2SO_4, 600 ml H_3PO_4, 150 ml H_2O, and 35 ml of a saturated solution of dextrose. The voltage was 8.5 to 9 volts and the current 20 to 22 amps. With the electrolyte flowing over the specimen at 60-70°C, five to twelve minutes were required to achieve a good polish on the iron. Microscopic examination at 600X showed all samples to be essentially free of etch-pits and scratches after electropolishing.

To measure the double layer capacity, the equipment and circuitry of Hackerman (56, 89) were duplicated exactly. A signal generator applies a square wave across the sample electrode and a non-polarizable platinized platinum electrode through a 15,000 ohm current-limiting resistor. The shape of the square wave is altered by the capacitance in the cell and this is observed on an oscilloscope. a d.c. potential is applied across the same two electrodes and its effect on the voltage across the cell is measured with reference to a standard calomel electrode. The change in shape of the square wave due to this d.c. potential is observed on the scope. Since capacity $C = (dt/de)(E/R)$, knowing the constant current factor (E/R), the value of (dt/de) observed on the oscilloscope allows the total capacity to be calculated.

It was found that degassing of the solution was not critical and the procedure described by Hackerman was therefore modified. Pure argon was passed through the solution but this was done for two hours prior to measurement. Hackerman passed argon through his solution for 16 hours before testing. The test solution used as 1M Na_2SO_4.

The voltage curves for all the metals were run from highly cathodic, just below hydrogen evolution, to just anodic where dissolution of the metal or oxide formation begins with respect to the standard calomel electrode. From these curves, the voltage range where the capacitance is constant with voltage was obtained so that for subsequent samples, the full curves did not need to be run. This useful voltage range was found to be -0.2 to -0.5 volts vs a standard calomel electrode (SCE) for tantalum and niobium, -0.1 to -0.3 volts vs SCE for molybdenum, and 0 to -1.5 volts vs SCE for iron.

After the above procedures were established with both single crystal and polycrystal specimens of the metals of interest, the crucibles used in the solubility determinations were measured. The results of the DLC measurements on the standard specimens, on solubility crucibles, and on platinum as a reference, are shown in Tables XV, XVI, XVII, and XVIII of this report.

REFERENCES

Literature Cited

1. R. M. Adams and A. Glassner, "Reactor Development Program Progress Report," ANL-6885 (1964).

2. R. M. Adams and A. Glassner, "Reactor Development Program Progress Report," ANL-6923 (1964).

3. N. W. H. Addink, "Quantitative Spectrochemical Analysis by Means of the Constant-Temperature Direct-Current Carbon Arc," Spectrochem. Acta 5, 495 (1953).

4. ASTM Methods of Chemical Analysis, p. 168, American Society for Testing Materials, Philadelphia (1960).

5. C. V. Banks, et al., "Determination of Oxygen in Yttrium and Yttrium Fluoride by the Inert Gas Fusion Method," Anal. Chem., 32, 1613, (1960).

6. N. M. Beskorovaynyy and Yu. I. Yakovlev, "Study of Corrosion of Iron and Chromium Steels in Liquid Lithium," Metallurgy and Metallography of Pure Metals (Translation) Gordon and Breach, N.Y. (1962).

7. F. L. Bett, "Compatibility Between Solid and Liquid Metals," Proc. Austr. Atom. Energy Symp. (1958) Section I.

8. F. L. Bett and A. Draycott, "The Compatibility of Beryllium with Liquid Sodium and NaK in Dynamic Systems," A/Conf. 15/P/1091 (1958).

9. M. Blander, North American Aviation Science Center, Thousand Oaks, Calif. private communication (1964).

10. S. S. Blecherman, et al., "Solubility Studies in Alkali Metals," CONF-650411-4 (1965).

11. A. D. Bogard, "The Solubility of Iron in Sodium Metal, Sodium-Sodium Oxide, and Sodium-Sodium Oxide-Sodium Hydroxide," NRL Report 4131 (1953).

12. D. F. Boltz, Colorimetric Determination of Nonmetals, Vol. VIII, Interscience Publishers, Inc., N.Y., (1958), p. 92.

13. R. N. Boos, et al., "Isotope Dilution - Static Combination Method for Organic Carbon in Submilligram Specimens," Anal. Chem. 28, 390 (1956).

14. J. L. Brandt and C. N. Cochran, "Gas Content of Solid Aluminum by Solid Extraction and Vacuum Fusion," J. Metals, 8, 1672 (1956).

15. L. A. Bromley, R. K. Edwards and R. L. McKisson, "Sodium Pump for Purification of Inert Atmospheres," Rev. Sci. Inst. 23, 342, (1952).

16. M. N. Bukhsh and D. N. Hume, "Colorimetric Determination of Niobium in the Presence of Tantalum," Anal. Chem. 27, 116 (1955).

17. Yu. F. Bychkov, et al., "Determination of Solubility of Metals in Lithium," Met. i Metalloved. Christykh Metal, Sbornik Nauch. Rabot (1960) (2), 178 CA:55:15281c (1961).

18. Yu. F. Bychkov, et al., "Determination of the Solubility of Metals in Lithium," Soviet J. Atomic Energy 7 (6), 987 (1961).

19. Y. F. Bychkov, et al., "Determining Solubility of Metals in Lithium," Metallurgy and Metallography of Pure Metals, Translation by B. Chalmers, Gordon and Breach Publ., N.Y. (1962).

20. Chemical and Metallurgical Services, UKAEA, (Springfields) "The Gasometric Determination of Carbon in Niobium Metal," United Kingdom Atomic Energy Authority, PG Report 239(S), (1963).

21. W. A. Dupraw, et al., "Determination of Oxygen in Potassium," Anal. Chem. 36, 430 (1964).

22. R. Dyck and T. J. Veleker, "Spectrographic Analysis of Molybdenum Metal Powder," Anal. Chem., 31, 1640 (1959).

23. F. M. Evens, "A New Technique for the Determination of Oxygen and Nitrogen in Steel," Dissertation Abstracts, 23, 3099 (1963).

24. C. T. Ewing, et al., "High Temperature Properties of Sodium and Potassium," Ninth Progress Report, NRL-5964 (1963).

25. H. M. Finniston, "Corrosion in Liquid Metal," Proc. Austr. Atom. Energy Symp. (1958) p. 189.

26. D. E. Fornwalt and M. K. Healy, "A Method for the Spectrographic Determination of Trace Impurities in Niobium," Applied Spectroscopy, 13, 38 (1959).

27. W. B. Fortune and M. G. Mellon, "Determination of Iron with O-phenanthroline. A Spectrophotometric Study," Ind. Eng. Chem., Anal. Ed. 10, 60 (1938).

28. R. E. Fryxell, "Determination of Very Small Amounts of Carbon in Metals," Anal. Chem., 30, 273 (1958).

29. W. S. Ginell and R. J. Teitel, "Solubility of Transition Metals in Molten Potassium," Paper presented at AEC-NASA Liquid Metals Information Meeting, April 21-23 (1965) Gatlinburg, Tenn.

30. J. A. Grand, et al., "The Solubility of Tantalum and Cobalt in Sodium by Activation Analysis," J. Phys. Chem. 63 [7], 1192 (1959).

31. J. G. Gratton, "Solubility of Carbon in Sodium at Elevated Temperature," KAPL-1807 (1957).

32. P. Greenberg, "Spectrophotometric Determination of Tungsten in Tantalum, Titanium, and Zirconium Using Dithiol," Anal. Chem., 29, 896 (1957).

33. C. B. Griffith and M. W. Mallett, "Determination of Hydrogen in Wrought Aluminum Alloys," Anal. Chem., 25, 1085 (1953).

34. J. C. Guyon, et al., "Spectrophotometric Determination of Niobium as Reduced Molybdoniobic Acid," Anal. Chem., 34, 640 (1962).

35. R. E. Heffelfinger, et al., "Analysis of High-Purity Iron," Anal. Chem., 30, 112 (1958).

36. J. Herrington, "Determination of Microgram Amounts of Carbon in Sodium" United Kingdom Atomic Energy Authority, AWRE-O-62/62 (1962).

37. G. W. Horsley, "Mass Transport and Corrosion of Iron-Based Alloys in Liquid Metals," J. Nuclear Energy: Pt. B, Reactor Technology 1, 84 (1959).

38. C. B. Jackson, Ed., Liquid Metals Handbook, Sodium-NaK Supplement, TID-5277 (1955).

39. R. J. Jawcrowski, et al., "The Determination of Oxygen in Lithium," Anal. Chem., 35, 1275 (1963).

40. D. S. Jesseman, et al., "Preliminary Investigation of Metallic Elements in Molten Lithium," NEPA-1465 (1950).

41. R. V. Jury, "Spectrographic Analysis of High Purity Lithium Compounds," United Kingdom Atomic Energy Authority, AERE-C/R-1871 (1957).

42. Y. Kakita and H. Goto, "Spectrophotometric Determination of Tantalum in Iron, Steel, and Niobium Metal," Anal. Chem., 34, 618 (1962).

43. G. J. Kamin, et al., "Inert Gas Fusion Determination of Oxygen in Vanadium, Niobium, and Tantalum," Anal. Chem., 35, 1053 (1963).

44. K. J. Kelly, "Solubility Studies in Alkali Metals," Paper presented at AEC-NASA Liquid Metals Information Meeting, April 21-22 (1965) Gatlinburg, Tenn.

45. K. J. Kelly, "Liquid Metal Corrosion Research," NASA-AEC Liquid Metals Corrosion Meeting, Dec. 7-8 (1960), Wash. D. C., NASA-TN-D-769, p. 27 (1961).

46. P. L. Kirk, Quantitative Ultramicroanalysis, John Wiley and Sons, N.Y. (1950).

47. R. F. Koenig, "Corrosion of Zirconium and Its Alloys in Liquid Metals," KAPL-982 (1953).

48. H. Kohji, Trans. Japan Inst. Metals, 3, 137 (1962).

49. I. M. Kolthoff, et al., Treatise on Analytical Chemistry, Part 2, Vol. 1, p. 378, Interscience Encyclopedia, Inc., N.Y., (1963).

50. I. M. Kolthoff, et al., Treatise on Analytical Chemistry, Part 2, Vol. 6, p. 267, Interscience Publishers, N.Y., (1964).

51. T. A. Kovacina and R. R. Miller, "The Solubility of Columbium-1% Zirconium in Sodium by Activation Analysis," NRL-6051 (1964).

52. H. W. Leavenworth and R. E. Cleary, "Solubility of Ni, Cr, Fe, Ti, and Mo in Liquid Lithium," Acta. Met. 9, 519 (1961); (PWAC-356).

53. R. A. Lindberg, National Aeronautics and Space Administration, Lewis Research Center, Cleveland, Ohio; personal communication, Oct. (1965).

54. R. N. Lyon, Ed., Liquid Metals Handbook, Second Edition, NAVEXOS P-733 (Rev.), U.S. Government Printing Office, Washington 25, D.C. (1952).

55. B. Minushkin, "Solution Rates and Equilibrium Solubility of Nickel and Iron in Liquid Lithium," NDA 2141-1 (1961).

56. J. J. McMullen and N. Hackerman, "Capacities of Solid Metal-Solution Interfaces," J. Electrochem. Soc., 106, 341 (1959).

57. J. A. Norris, "Spectrographic Determination of Trace Elements in Metals," Symposium on Spectrochemical Analysis for Trace Elements, ASTM Special Technical Publication No. 221, p. 23, (1957) (See other ASTM Methods, e.g., E-2 SM9-9 (1957).

58. T. L. O'Connor and H. H. Uhlig, "Absolute Areas of Some Metallic Surfaces," J. Phys. Chem., 61, 402 (1957).

59. L. E. Owen and J. Y. Ellenberg, "Spectrochemical Analysis of Lithium," Anal. Chem., 23, 1823 (1951).

60. R. A. Pasternak, "High Temperature Oxidation and Nitridation of Niobium in Ultrahigh Vacuum," SRIA-132, Nov. (1964).

61. Elsie M. Penner and W. R. Inman, "Extraction and Determination of Iron as the Bathophenanthroline Complex in High-Purity Niobium, Tantalum, Molybdenum and Tungsten Metals," Talanta, 9, 1027 (1962).

62. L. P. Pepkowitz and W. C. Judd, "Determination of Sodium Monoxide in Sodium," Anal. Chem., 22, 1283 (19650).

63. L. P. Pepkowitz, et al., "Determination of Sodium Monoxide in Sodium, An Addendum," Anal. Chem., 26, 246 (1954).

64. L. P. Pepkowitz, and W. P. Moak, "Precision Determination of Low Concentrations of Carbon in Metals," Anal. Chem., 26, 1022 (1954).

65. L. P. Pepkowitz and J. T. Porter, "The Determination of Carbon in Sodium," KAPL-1444 (1955).

66. L. P. Pepkowitz and E. R. Proud, "Determination of Hydrogen," Anal. Chem., 21, 1000 (1949).

67. S. J. Rodgers, et al., "Iron and Nickel Concentrations in Sodium," MSA-TR-27 (1954).

68. J. J. Sand, "Solubility of Iron in Liquid Lithium," AD 209470, Div. 4, CMCC-HEF-166 (1958).

69. M. Sittig, Sodium, Its Manufacture, Properties and Uses, p. 356, Reinhold Publishing Co., N.Y., (1956).

70. E. B. Sandell, Colorimetric Metal Analysis, 3rd Ed., p. 649, Interscience Publishers, N.Y., (1959).

71. W. G. Smiley, "Determination of Oxygen in Metals Without High Vacuum by Capillary Trap Method," Anal. Chem., 27, 1098 (1955).

72. F. D. Snell and C. T. Snell, Colorimetric Methods of Analysis, 3rd Ed., Vol. II, p. 478, D. Van Nostrand Co., N.Y., (1955).

73. F. D. Snell and C. T. Snell, Colorimetric Methods of Analysis, 3rd Ed., Vol. II, p. 757, D. Van Nostrand Co., (1955).

74. F. D. Snell and C. T. Snell, Colorimetric Methods of Analysis, 3rd Ed., Vol. II, p. 660, D. Van Nostrand Co., (1955).

75. D. A. Stevenson and J. Wulff, "Investigation of Phenomena Related to Liquid Metal Corrosion," NYO-2160 (1958).

76. D. R. Stull and G. C. Sinke, Thermodynamic Properties of the Elements, Advances in Chemistry Series, #18, American Chemical Society, Wash. D. C., (1956).

77. J. H. Swisher, "Solubility of Iron, Nickel, and Cobalt in Liquid Potassium and Effect of Oxygen Gettering Agents on Iron Solubility," NASA-TN-D-2734 (1965).

78. F. Tepper and J. Greer, "Factors Affecting the Compatibility of Liquid Cesium with Containment Metals," AFML-TR-64-327 (1964). AD-608385.

79. T. Tepper and J. Greer, "Factors Affecting the Compatibility of Liquid Cesium with Containment Metals," ASD-TDR-63-824, Pt I, (1963).

80. F. Twyman, Metal Spectroscopy, C. Griffin, London, (1951) p. 467.

81. D. D. Van Slyke, et al., "Manometric Carbon Determination," J. Biol. Chem. 136, 509 (1940).

82. D. D. Van Slyke, et al., "Reagents for the Van Slyke-Folch Wet Carbon Combustion," J. Biol. Chem., 191, 299 (1951).

83. R. C. Vogel, Ed., Argonne National Laboratory Chemical Engineering Division Research Highlights, May, 1964, to April, 1965, ANL-7020 (1965).

84. D. I. Walter, "Determination of Oxygen in Titanium," NRL 3577 (1949).

85. C. H. Ward, et al., "Titrimetric Determination of Nitrogen in Sodium," LA-2892 (1963).

86. S. Weisberger, et al., "Universal Spectrographic Method for the Analysis of Iron and Steel," Applied Spectroscopy, 9, 19 (1955).

87. P. F. Young and R. W. Arabian, "Determination of Temperature Coefficient of Solubility of Various Metals in Rubidium and the Corrosive Effects of Rubidium on Various Alloys at Temperatures from 1000° to 2000°F," AGN 8063 (1962). Also summarized in "NASA-AEC Liquid Metals Corrosion Meeting Oct. 2-3 (1963), Vol. I," p. 167, NASA-SP-41 (1964).

88. R. K. Young and D. W. Cleaves, "Determination of Hydrogen in Titanium Metals by Hot Extraction," Anal. Chem., 28, 372 (1956).

89. R. J. Brodd and N. Hackerman, "Polarization Capacity of Solid Electrodes and True Surface Area Values," J. Electrochem. Soc., 104, 704 (1957).

90. C. L. Luke, "Photometric Determination of Tantalum with Phenylfluorone," Anal. Chem. 31, 904 (1959).

91. W. S. Ginell and R. J. Teitel, "Determination of the Solubility of Several Transition Metals in Molten Potassium," Paper presented at the American Nuclear Society Meeting, November (1965) in Washington, D. C..

92. E. Steele, from a paper given at the NASA-AEC Round Robin Conference on the Analysis of Oxygen in Alkali Metals, September 22-23 (1965), Cleveland, Ohio.

SUPPLEMENTARY REFERENCES

R. M. Adams and A. Glassner, "Argonne National Laboratory Reactor Development Program, Report for January, 1964," ANL-6840 (1964).

C. C. Addison and D. H. Kerridge, "The Solubility of Metals in Liquid Metals," A.E.R.E. M/R 2299 (1957).

G. R. Argue, "Double Layer Capacitance Measurements on Ta, Mo, and Nb to Determine Surface Areas," AI-TDR-9773 (1964).

K. Q. Bagley and K. R. Montgomery, "The Solubility of Nickel in Lithium," Report No. IGR-TN/C-250, Culcheth Labs, Culcheth, Lancs., England (1955).

E. F. Batutis, et al., "The Influence of Oxygen on the Corrosion of Armco Iron and Type 347 Stainless Steel in 1000°F Sodium," NP-5433 (1954).

R. A. Baus, et al., "The Solubility of Structural Materials in Sodium," Proc. Int. Conf. on Peaceful Uses of Atomic Energy 9 (1956) UN, N.Y..

S. S. Blecherman, et al., "The Solubility of Molybdenum in Lithium and Potassium," TIM-850 (1965).

C. F. Bonilla and G. Shulman, "The Vapor Pressure of Rubidium," CU-2660-18 (1965); BNL 928, #344 (1965).

H. I. Bowers and W. E. Ferguson, "Structural Materials in LASL Liquid Sodium Systems," (LASL) BNL 844, #155 p. 40 (1963).

E. G. Brush, "Evaluation of the Behavior of Aluminum in Sodium," KAPL-M-EGB-16 (1954).

E. G. Bunzel and E. J. Kohlmeyer, "On the Thermal Behavior of Sodium Compounds, Especially of Sodium Oxide and Sodium Sulfide and Their Reactions with Metals," Z. anorg. u. allgem. Chem. 254, 1 (1947).

G. W. Burdi, "Snap Technology Handbook Volume I, Liquid Metals," NAA-SR-8617 (1964).

W. T. Chandler and N. J. Hoffman, "The Role of Oxygen on Attack of Refractory Metals by Alkali Metals," Paper given at National Refractory Metals Symposium, Los Angeles, Calif. Dec. 9-10 (1963).

W. T. Chandler and N. J. Hoffmam, "Effects of Liquid and Vapor Cesium on Container Materials, Final Report," ASD-TDR-62-965 (1962).

Helen Chick, Compiler, "Bibliography on Corrosion by Liquid Metals (1957-September 1962)," LAMS-2779 (1962).

K. T. Claxton, "Review of Solubility Data for the Liquid Sodium-Oxygen System," AERE-R-4897 (1965).

J. A. DeMastry and N. M. Griesenauer, "Refractory Metals in Lithium at Elevated Temperatures," Paper presented at AEC-NASA Liquid Metal Information Meeting, April 21-22 (1965) Gatlinburg, Tenn.

J. R. DiStefano and E. E. Hoffman, "Corrosion Mechanisms in Refractory Metal-Alkali Metal Systems," ORNL-3424 (1963).

P. G. Drugas and L. R. Kelman, "Equipment and Procedures for Studying the Equilibrium Solubility of Iron in NaK," ANL-5359 (1953).

R. P. Dudek and K. M. Ferguson, "The Corrosion Testing of Various Materials in Na," BW-7020 (1957).

W. A. Dupraw, et al., "Determination of Oxygen in Potassium," Anal. Chem., 36, [2], 430 (1964).

D. Dutina, "Current State of Art on Alkali Metal Analysis," Paper presented at AEC-NASA Liquid Metals Information Meeting, April 21-22 (1965) Gatlinburg, Tenn.

R. L. Eichelberger, "Recent Information on Moderator Sheath Corrosion in Liquid Sodium," BNL-489, p. 168 (1957).

L. F. Epstein, "Static and Dynamic Corrosion and Mass Transfer in Liquid Metal Systems," Chemical Engineering Progress Symposium Series No. 20 Vol. 53, 67 (1957).

C. T. Ewing, et al., "High Temperature Properties of Sodium and Potassium, Progress Report No. 12," NRL-6094, AD-602243 (1963).

C. R. Fisher and P. Y. Achener, "Alkali Metals Evaluation Program, Quarterly Progress Report, Oct. 1 - Dec. 31, 1964," AGN-8131 (1965).

A. Haire and L. Hays, "Energy Conversion Systems Reference Handbook - Heat Exchangers," WADD-TR-60-699, Vol. VII (1960); AD 256881 (1960).

J. M. Hochman and C. F. Bonilla, "The Saturated Liquid and Vapor Density of Cesium to 3000°F, and the Critical Point of Cesium," CU-2660-11 (1965); BNL-928, #344 (1965).

E. E. Hoffman, "Boiling Alkali Metal and Related Studies, Purification of Potassium Metal," NASA-TN-D-769, p. 15 (1961).

E. E. Hoffman and D. H. Jansen, "Lithium Symposium - Analytical Procedures and High Temperature Corrosion - Reading List," ORNL CF-57-10-6 (Rev. January 20, 1958) (1958).

G. W. Horsley, "The Corrosion of Iron by Oxygen-Contaminated Sodium," A.E.R.E. M/R 1441 (1954).

D. S. Jesseman, et al., "Solubilities of Metallic Elements in Molten Lithium," U.S. Dept. Comm.; Office of Tech. Serv. PB Report 160, 750 (1961).

L. R. Kelman, et al., "Resistance of Materials to Attack by Liquid Metals," ANL-4417 (1950).

L. R. Kelman, "Effect of Sodium-Potassium Alloy on Various Materials at Elevated Temperatures," CT-3726 (1946).

T. A. Kovacina, et al., "High Temperature Properties of Sodium and Potassium," NRL-5904 (1963).

T. A. Kovacina and R. R. Miller, "The Solubility of Nickel in Sodium by a Tracer Technique," Nucl. Sci and Eng., 10, [2], 163 (1961).

A. W. Lemmon, Jr., "Engineering Properties of Potassium, Eighth Quarterly Report," BMI-EPP-QPR 62/8 (1962).

A. W. Lemmon, Jr., "Engineering Properties of Potassium, Seventh Quarterly Report," BMI-EPP-QPR 62/7 (1962).

A. P. Litman, "The Effect of Oxygen on the Corrosion of Niobium by Liquid Potassium," (Thesis), ORNL-3751 (1965).

M. Makanski, "Thermodynamic Properties of Sodium," J. Chem. and Eng. Data, 5, [4], 441 (1960).

W. D. Manly, "Fundamentals of Liquid Metal Corrosion," ORNL-2055 (1956); Corrosion 12, 336t, (1956).

R. L. McKisson, "Analysis of the Freezing Point Depression Technique of Determining Impurity Content of Alkali Metal," AI-TDR-9404 (1964).

B. Minushkin, "Purification and Analysis of Oxygen in Sodium by Electrochemical Methods," Paper presented at the AEC-NASA Liquid Metals Information Meeting, April 21-22 (1965) Gatlinburg, Tenn.

NASA-AEC Liquid Metals Corrosion Meeting, Dec 14-15 (1961), Brookhaven National Laboratory, (TID-7626 (pt 1) (1962).

Oak Ridge National Laboratory, "Proceedings of the 1963 High-Temperature Liquid Metal Heat Transfer Technology Meeting," ORNL 3605 (1963).

R. S. Reynolds, "Final Report - Liquid Metal Technology Review of Work from March 1949 to May 1954," NP-5614 (1954).

S. J. Rodgers and J. W. Mausteller, "Solubility of Na_2O in NaK, T.R. #47," NP-5898 (1956).

A. J. Romano, "The Corrosion of Refractory Metals and Their Alloys by Sodium Liquid and Vapor at Temperature up to 1260°C," Paper presented at 1965 Annual Meeting, ANS, Gatlinburg, Tenn. June 21-25 (1965).

L. Rosenblum, "Liquid Metals Research Program; Purification of Alkali Metals," NASA-TN-D 769, p. 65 (1961).

O. N. Salmon and T. J. Cashman, "Solubility of Sodium Monoxide in Liquid Sodium," KAPL-1653 (1956).

J. P. Stone, et al., "High Temperature Properties of Sodium, Potassium, and Cesium, Fourteenth Progress Report," NRL 6128 (1964).

J. P. Stone, et al., "High Temperature Properties of Sodium, Potassium, and Cesium, Thirteenth Progress Report," NRL 6213 (1965); BNL-928, #354 (1965).

S. W. Strauss, et al., "The Atomic Size Effect and Alloying Behavior in Liquid Metals," Acta Met. 6, 604 (1958).

P. L. Studt, et al., "Bibliography on Liquid Metals Technology of Hg, K, Na, and NaK," NP-14434 (1963); AGC-2550 (1963); NASA-CR-59028 (1963).

R. J. Teitel, "High Temperature Centrifuge for Niobium and Tantalum Solubility in Potassium," Paper given at the ANS 1965 Annual Meeting, June 21-25 (1965) Gatlinburg, Tenn.

F. Tepper, "Solubility of Refractory Metals and Carbon in Cesium," Paper presented at AEC-NASA Liquid Metals Information Meeting, April 21-22 (1965) Gatlinburg, Tenn.

C. R. Tipton, Jr., (Ed.), Reactor Handbook, Vol. I, Materials, Interscience Publishers, Inc. N. Y. (1960).

W. D. Weathorford, et al., "Properties of Inorganic Energy-Conversion and Heat-Transfer Fluids for Space Applications," WADD-TR-61-96 (1961).

C. E. Weber and L. F. Epstein, "Problems in the Use of Molten Sodium as a Heat Transfer Fluid," J. Metallurgy and Ceramics, 3, 85 (1949); TID-67, p. 85 (1949) (Secret).

C. E. Weber and L. F. Epstein, "Problems in the Use of Molten Sodium as a Heat Transfer Fluid, Part II," J. Metallurgy and Ceramics, 6, 36 (1951); TID-70, p. 36 (1951) (Secret).

J. R. Weeks and D. H. Gurinsky, "Solid Metal-Liquid Metal Reactions in Bismuth and Sodium," Liquid Metals and Solidification ASM (1958).

R. N. Weltman, "Comments on 'In-House Liquid Metals Investigation' at NASA-LRC," BNL-892, #261, p. 26 (1964).

J. L. White, "A Thermodynamic Analysis of Solubility in Liquid Metal Systems," NRL-5555 (1960).

D. D. Williams, "The Solubility of Impurities in Liquid Sodium," NRL-Memo-424 (1955).

D. D. Williams, "Solubility of Oxygen in Potassium Metal and Sodium-Potassium Alloys," NRL-3894 (1951).

G. R. Zellars, Compiler, "Analysis of Oxygen in Potassium, NASA Round-Robin Meeting Held June 4, 1964," NASA-TM X-1085 (1965).